Construction of C^1 Polygonal Splines over Quadrilateral Partitions

Ming-Jun Lai * James Lanterman†

July 23, 2021

Abstract

In this paper we construct smooth bivariate spline functions over a polygonal partition, e.g. a convex quadrilateral partition by using vertex spline techniques. Vertex splines, introduced in [10] are smooth piecewise polynomial functions supported over a collection of triangles sharing a vertex. In this paper, we extend the concept of vertex splines to the partition of polygons and describe how to construct C^1 vertex polygonal splines over a collection of quadrilaterals. We begin with our construction of C^1 vertex splines over a collection of parallelograms, although they may not be axis-orientated. Then the construction is generalized to the setting of general quadrilaterals. We will use various monomials of Wachspress GBC functions of degrees 5 and 7 to explain how to construct C^1 vertex splines together with additional special splines called edge and face splines. With these splines at hand, we construct quasi-interpolatory formulas, whose approximation properties will be shown. Numerical interpolation and approximation results will be presented. Finally, three applications of these splines are explained: the first one is to form smooth locally supported GBC functions, the second one is to construct smooth suitcase corners, and the third one to construct C^1 surfaces over quadrilateral partitions with extra-ordinary points(EP). Several examples will be demonstrated to show the convenience of using these splines.

1 Introduction

Recently, there have been efforts to use finite element-like functions over polygonal partitions to numerically solve partial differential equations (see [14], and the references therein). Some efforts were made based on virtual finite elements over polygons (see [2], [3], [4]). Several researchers used discontinuous Galerkin methods and a weak Galerkin method over polygons for numerical solutions of PDEs (see [36], [30]).

Other attempts have been made to use continuous generalized barycentric coordinates (GBCs) defined on polygons for numerical solution of partial differential equations (see [33], [28], [14], [25]). In the interest of numerically solving PDEs of higher order, we should consider construction of smooth elements over polygonal or polyhedral partitions. Such a construction has not been well-studied in the literature to the best of the authors' knowledge. A group led by G. Sangalli has actively worked on the isogeometric analysis of biharmonic equations over unstructured quadrilaterals. See [18] and [19] as well as the literature therein.

The work in this paper creates a related framework, showing that similar results can be achieved using GBC-based construction. Since GBCs are defined over n-gons for arbitrary n, this construction

*mjlai@uga.edu. Department of Mathematics, University of Georgia, Athens, GA 30602. This research is partially supported by the National Science Foundation under the grant #DMS 1521537.

†jmlanter@uga.edu. Department of Mathematics, University of Georgia, Athens, GA 30602.

opens a door toward a larger theory to extend the results to partitions of polygons with arbitrary number of edges.

Another motivation for smooth polygonal splines can be found in geometric design, where tensor-product B-spline surfaces have been widely standardized to represent functions and surfaces in research and industries such as aircraft and car body design. However, they are not flexible enough for some geometric modeling, such as a suitcase corner, because the B-spline surface is formed by the union of many collections of exactly four quadrilateral B-spline patches. A standard task in geometric design is to construct a C^1 surface to blend tensor-product B-spline patches over quadrilateral meshes which meet at several vertices of a valence other than 4, called extraordinary points (EPs). While this task can be solved by recursive subdivision (e.g. [9]), a blending surface with a finite small number of patches is often preferable. Bi-quintic spline surfaces have been constructed by manually adjusting coefficients of 6 types (see [17]) or by solving a minimization for several different types of functionals (see [23] and [22]). It can be difficult and costly to solve these minimizations over, say, the surface of an entire airplane; it can be desirable to have a concrete construction instead. Another approach to construct C^1 Bézier surfaces over quadrilateral partitions is summarized in a recent monograph [5]. C^1 functional surfaces over a mix of triangles and quadrilaterals were constructed in [16]. A family of C^1 quadrilateral finite elements is recently available in [19] which generalizes the construction by Brenner and Sung [8] based on C^0 polynomial elements of tensor-product degree $p = 6$. It is a global method minimizing the thin-plate energy when constructing smooth surfaces. The construction in this paper is a local approach which may be more convenient for surface designers.

Approximation theory on multivariate splines has been studied for many years. In particular, the theory of spline functions over triangulations has been fully studied (see [26]), and many applications, including numerical solution of PDE and scattered data fitting, have been thoroughly explored (see [1]). Recently, a construction of locally supported spline functions over polygonal partitions was carried out in [14]. Generalized barycentric coordinates (GBCs) defined on polygons (see [13]) can be pieced together to form continuous vertex spline functions which are supported over the collection of all polygons sharing a common vertex. The locally supported spline functions are continuous, but this construction cannot ensure even C^1 smoothness (see [14] for details). It is natural to extend the construction and explore how to construct smoother locally-supported spline functions. Recall in [10], the concept of vertex splines (smooth spline functions supported over a cell of triangles sharing a vertex) was first introduced. Some C^1 quintic vertex splines were constructed (see [24] for a detailed construction). Although vertex splines over a collection of parallelograms were considered in [24], no concrete construction was carried out. In fact, construction of smooth vertex splines over polygonal partitions has not been well-studied since then.

While our over-arching goal is to describe a method to build such splines over more arbitrary partitions of quadrilaterals (and even polygons with more edges), one of the purposes of this paper is to describe a construction of C^1 splines over a collection of convex quadrilaterals. We shall begin our construction over a specialized quadrilateral partition to motivate our construction over a general convex quadrilateral. See two collections of parallelograms as in Figure 1. The left figure indicates a situation where 6 tensor product B-spline surfaces are pieced together. In order to make them C^1 joined, one can replace the corresponding 6 subsurfaces by the patch generated by our scheme described in this paper. Similarly, the right figure in Figure 1 shows the case that 5 tensor product B-spline surfaces are joined at a point. One can use our C^1 vertex splines to replace these 5 B-spline surface patches and form a C^1 surface over the partition. In the end of the paper, we will present an example of a construction of smooth suitcase corners where three B-spline surface patches are jointed at a point.

We utilize Wachspress GBCs in our construction. It happens that, in this special setting of parallelograms, the spline functions which we will construct using these GBCs are in fact bi-quintic

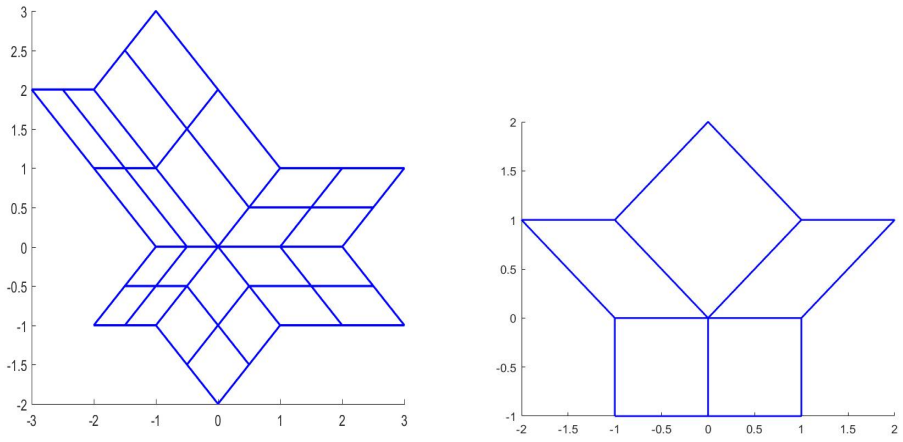

Figure 1: Two parallelogram partitions

polynomials, so we could use the theory of bi-quintic B-splines to explain our construction. However, over more general quadrilaterals, the GBCs will actually be rational functions, and this will be necessary to successfully construct the splines we seek in that context. For this reason, we first explain our construction around GBCs even in the setting of parallelograms, in order to provide meaningful connections to the more general construction of smooth polygonal splines over quadrilaterals.

Our construction is based on monomials of Wachspress coordinates of degree 5 and degree 7. They can be used to form vertex splines satisfying various interpolatory conditions at a vertex, and can be used in a natural and convenient way to reproduce polynomials. If we suppose that $\mathcal{P}$ is a collection of parallelograms, then at each vertex $v \in \mathcal{P}$ we shall construct C^1 vertex splines $\psi_v, \psi_{x,v}, \psi_{y,v}, \psi_{x^2,v}, \psi_{xy,v}$, and $\psi_{y^2,v}$ such that they are supported over Ω_v, the union of all parallelograms in $\mathcal{P}$ which share the common vertex v, and satisfy some interpolatory conditions. For example, ψ_v is a C^1 function over Ω, supported only in Ω_v, and satisfies

$$\psi_v(w) = \delta_{v,w}, \nabla\psi_v(w) = 0, \nabla^2\psi_v(w) = 0 \tag{1}$$

for all vertices w of $\mathcal{P}$. Similarly, $\psi_{x,v}$ is a C^1 function over Ω which is supported over Ω_v satisfying

$$\psi_{x,v}(w) = 0, \nabla\psi_{x,v}(w) = (\delta_{v,w}, 0), \nabla^2\psi_{x,v}(w) = 0 \tag{2}$$

for all vertices w of $\mathcal{P}$. The remaining functions are defined similarly. See their figures in the next sections. We will build an analogous construction over a more general quadrilateral partition using monomials of Wachspress coordinates of power 7. This construction will be given in the section after the next. Our construction is assisted by using MATHEMATICA. In particular, the simplification of the complicated terms takes a long time and is highly error-prone by hand. The reader who is interested in more detail or clarity in the intermediate steps of the calculations in the body of the paper can refer to [27], which lists a great deal more detail over much longer calculations. In addition, we use MATLAB for numerical implementation of the long and very complicated formulae for further verification of the polynomial reproduction and numerical approximation of functions. Adopting MATHEMATICA and MATLAB enables us to verify all computation so that we can be sure of the correctness of the derived results. Without MATHEMATICA, the computation described in this paper is horrendous, and extremely frustrating to perform without making an error - on more than one occasion, an entire chalkboard has been filled by only a single step of some of these calculations.

However, once the formulae for these functions have been obtained and verified, they can simply be implemented in software to construct C^1 surfaces, as demonstrated near the end of this paper. The authors are willing to share their MATHEMATICA and MATLAB codes with the interested reader upon request. Our MATLAB code is stable and efficient to use. All graphics shown in this paper can be generated within an hour.

Let $S^1(\mathcal{P}) = \{\sum_{v\in\mathcal{P}} \sum_{\alpha+\beta\le 2} c_{\alpha,\beta,v}\psi_{x^\alpha y^\beta,v}, c_{\alpha,\beta,v} \in \mathbb{R}\}$ be the C^1 vertex spline space over the partition $\mathcal{P}$. It is clear that $\mathcal{P}$ can be uniformly refined; see uniform refinement schemes in [26]. Hence, we let $\mathcal{P}_k$ be the uniform refinement of $\mathcal{P}_{k-1}$ starting with a partition $\mathcal{P}_1$ of parallelograms/quadrilaterals of Ω. We shall study the approximation properties of $S^1(\mathcal{P}_k)$ by showing that $f - Q_k(f) \to 0$ for some $Q_k(f) \in S^1(\mathcal{P}_k)$ as $k \to \infty$. In addition, we shall construct special splines called edge splines and face splines in order to be able to reproduce polynomials of higher degree. An edge spline is a C^1 function supported over the union of two quadrilaterals sharing a common edge. A face spline is a C^1 function supported only on one quadrilateral.

The paper is organized as follows. We first recall Wachspress' generalized barycentric coordinates, and then introduce monomials of Wachspress coordinates in §2. We begin the construction of various vertex, edge, and face splines using degree 5 monomials of Wachspress GBC functions which are locally supported in $\mathcal{P}$ based on parallelograms in §3, and a similar vertex spline construction based on degree 7 monomials of Wachspress coordinates quadrilaterals supported over more general quadrilateral partitions in §4. We explain two constructions of quasi-interpolatory operators, one based on the vertex splines without edge and face splines, and another based on all the splines we constructed. Results of numerical approximation using these quasi-interpolatory splines will be demonstrated in §5. Finally, in §6, we point out that our vertex splines have applicable properties which emulate GBCs, i.e. they form locally supported GBC-like functions. We use these functions to form C^1 spline surfaces modeling a suitcase corner; a few smooth suitcase corners will be shown, showing that they are certainly useful for surface construction. An example of a smooth bunny surface will be presented. Finally, we conclude the paper with a few remarks and open problems.

2 Preliminary on Wachspress Coordinates

Given a partition $\mathcal{P}$ of parallelograms or general quadrilaterals over a polygonal domain Ω, let V be the set of all vertices in $\mathcal{P}$. For a vertex $v \in V$, denote by Ω_v the union of the parallelograms/quadrilaterals in $\mathcal{P}$ which contain v. Our construction uses Wachspress generalized barycentric coordinates (see [37]), so for convenience, let us briefly introduce the associated notation.

Let $P_n = \langle v_1, \ldots, v_n\rangle$ be a convex polygon. We use the definition given in [13]: Any functions ϕ_i, $i = 1, \ldots, n$, will be called generalized barycentric coordinates (GBCs) of P_n if, for all $\mathbf{x} \in P_n$, $\phi_i(\mathbf{x}) \ge 0$ and

$$\sum_{i=1}^{n} \phi_i(\mathbf{x}) = 1, \qquad \text{and} \qquad \sum_{i=1}^{n} \phi_i(\mathbf{x}) v_i = \mathbf{x}. \tag{3}$$

When $n = 3$, P_n is a triangle, and the coordinates ϕ_1, ϕ_2, ϕ_3 can be uniquely determined by (3), and are the usual barycentric coordinates. For $n > 3$, the coordinates ϕ_i are not uniquely determined by (3) alone, but they share a basic property that they are piecewise linear on the boundary of P_d:

$$\begin{gathered}\phi_i(\mathbf{v}_j) = \delta_{ij}, \text{ and} \\ \phi_i((1-\mu)\mathbf{v}_j + \mu\mathbf{v}_{j+1}) = (1-\mu)\phi_i(\mathbf{v}_j) + \mu\phi_i(\mathbf{v}_{j+1}) \text{ for } \mu \in [0,1].\end{gathered} \tag{4}$$

Wachspress (rational) coordinates are the most commonly used GBCs. For any $\mathbf{x} \in P_n$, let $A_i(\mathbf{x})$ be

the signed area of the triangle $\langle \mathbf{x}, v_i, v_{i+1} \rangle$, and $C_i = A_i(v_{i-1})$. Then define the functions

$$w_i(\mathbf{x}) = C_i \prod_{j=1}^{n-2} A_{i+j}(\mathbf{x}),\ i = 1, ..., n \ \text{ and } \ W(\mathbf{x}) = \sum_{i=1}^{n} w_i(\mathbf{x}),$$

where the functions A_i are indexed cyclically (i.e. $A_{n+1} = A_1$).

Then the functions $\phi_i = w_i/W$, $i = 1, ..., n$ are the Wachspress GBCs, which are rational functions. See [13] for several other representations of these coordinates.

First, however, we will note an interesting property of Wachspress coordinates on parallelograms. While Wachspress coordinates are generally defined as rational functions, we can actually say the following:

Lemma 1 *Wachspress coordinates on parallelograms are quadratic polynomials. In fact, they are tensor products of two linear polynomials.*

Proof. Let $P = \langle v_1, v_2, v_3, v_4 \rangle$ be a parallelogram. Since P is a parallelogram, then each subtriangle of its vertices has the same area; that is, there is a constant C such that $C_i = C$ for all $i = 1, 2, 3, 4$. Then we can simplify the expression of ϕ_i by

$$\phi_i = \frac{A_{i+1}A_{i+2}}{\sum_{j=1}^{4} A_{j+1}A_{j+2}}$$

Now, the functions A_j are linear polynomials, and notice that, where $\mathbf{e}_j$ is the edge of P joining the vertices v_j and v_{j+1}, $A_j|_{\mathbf{e}_j} = 0$. Moreover, since P is a parallelogram, it is easy to see that the functions A_j are constant along the edge opposite $\mathbf{e}_j$, $\mathbf{e}_{j+2}$, and in fact $A_j|_{\mathbf{e}_{j+2}} = C$. This implies, then, that $A_j = C - A_{j+2}$. Then we can simplify the sum in the denominator of ϕ_i by

$$\sum_{j=1}^{4} A_{j+1}A_{j+2} = C^2,$$

so we have

$$\phi_i = \frac{A_{i+1}A_{i+2}}{C^2},$$

which is a quadratic polynomial. □

Next we introduce monomials of Wachspress GBC coordinates. That is, for any indices $\mathbf{j} = (j_1, \cdots, j_n) \in \mathbb{Z}^n$ with $|\mathbf{j}| = j_1 + \cdots + j_n$, we define

$$M^{\mathbf{j}}(\mathbf{x}) = \phi_1^{j_1} \cdots \phi_n^{j_n}, \mathbf{j} \in \mathbb{Z}_+^n. \tag{5}$$

We shall first use the space of all functions which are linear combinations of $M^{\mathbf{j}}, |\mathbf{j}| = 5$. For convenience, let $L_k = \{\sum_{|\mathbf{j}|=k} c_{\mathbf{j}} M_{\mathbf{j}}, c_{\mathbf{j}} \in \mathbb{R}\}$ for $k = 1, 2, 3, ...$ be the space of polynomials of Wachspress coordinate functions of degree k. We mainly use $k = 5$ and $k = 7$ in the rest of the paper. One reason that we do not use the monomials of even degree because we want our construction to be applied to any vertex in $\mathcal{P}$ in the same fashion without overlap. Indeed, if one uses degree d, there are $d + 1$ terms of monomials which are not zero on any edge e of parallelogram P. By using the same order of derivatives at each vertex of edge e, $d + 1$ should be even and hence, d should be odd. We are not able to use degree 4 or smaller in order to have a vertex spline over quadrilateral partitions which are as general as a partition of parallelograms. See [27] for an overview of analogous degree 3 and 4 constructions; [5] explains the underlying phenomenon.

3 Construction of Various Vertex Splines over Parallelograms

Since we are using only partitions of parallelograms in this section, by Lemma 1, whatever function ψ_v we build, it will actually be a piecewise polynomial. This means we will, in fact, be constructing a subspace of usual bivariate splines. Similar spaces have been constructed over parallelograms in related works (cf. [5], [22], [19]); however, we will not simply use the well-established methods such as tensor-product B-splines to describe the results in this section. Instead, we will use polynomials of Wachspress GBCs in order to motivate our construction over more general quadrilaterals. Moreover, this novel basis will be designed to be well-suited for ease-of-use in manipulating a smooth surface easily after implementation, while maintaining certain constraints like smoothness and value properties at points of interest, and has the advantage of a closed-form which allows for one-time implementation in terms of the underlying partition. Let us show the monomial terms of Wachspress GBCs together with a bubble function $B = \phi_i\phi_{i+2} = \phi_{i+1}\phi_{i-1}$ in Figure 2 which are divided into a few blocks associated with the four corners. Hence, there are 36 coefficients associated with these terms which require us to determine for each kind of vertex splines.

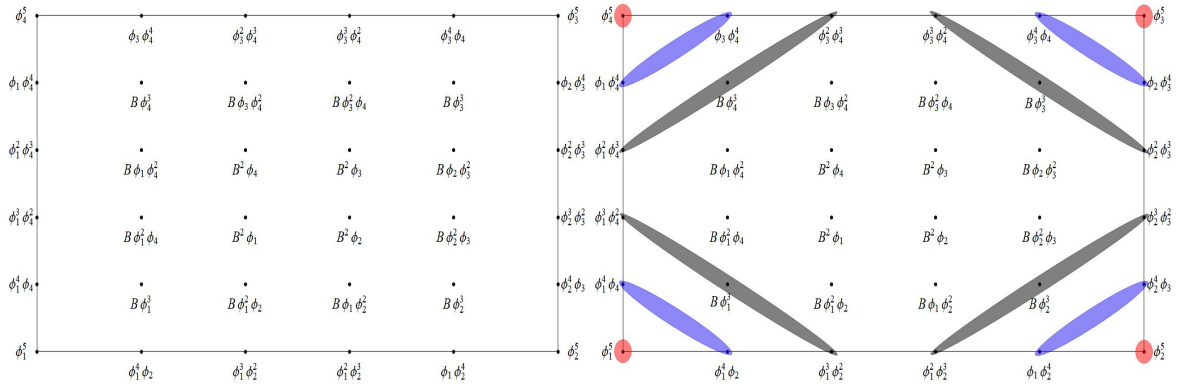

Figure 2: Monomial terms with bubble function B and groups of these terms associated with four vertex splines at corners

We shall describe various polygonal splines in the following subsections. These splines satisfy some interpolatory conditions which can be used to approximate unknown functions or reconstruct smooth surfaces. We construct three types of splines: one is supported over the union Ω_v of all parallelograms which share a common vertex v (involving coefficients at all kinds of domain points, but especially focusing on those seen in the right graph of Figure 2), another is supported over two parallelograms sharing a common edge (focused on coefficients seen in the left graph of Figure 3), and finally another which is completely supported over a single parallelogram (focused on coefficients seen in the right graph of Figure 3).

3.1 Nodal Basis Functions ψ_v

Our first goal is to construct a function ψ_v satisfying the following properties:

Property 1. $\psi_v(w) = \delta_{v,w}$ for $w \in V$; Property 2. supp $(\psi_v) \subseteq \Omega_v$;

Property 3. $\psi_v \in C^1(\Omega)$; Property 4. $\sum \psi_v = 1$, and

Property 5. ψ_v is piecewise-defined, with a non-zero piece for each parallelogram in Ω_v.

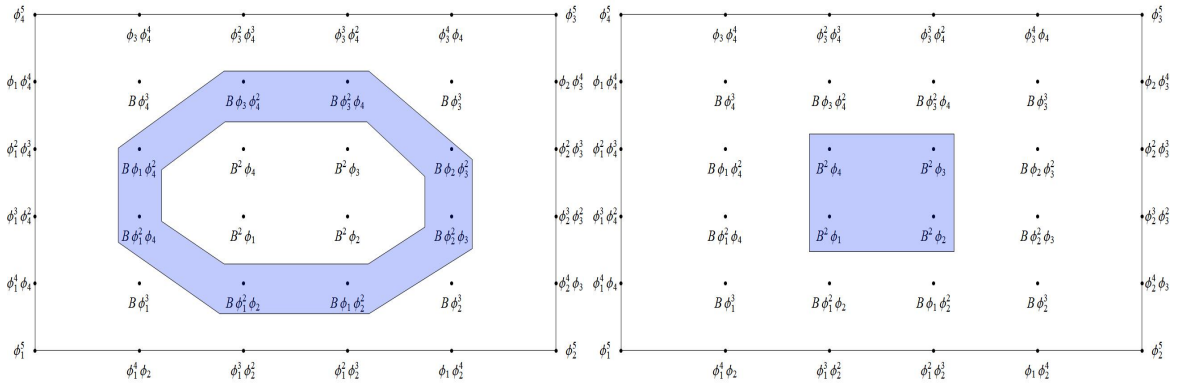

Figure 3: Two groups of the monomials with bubble function B associated with edge splines and face splines

In addition, we shall prescribe two more conditions later when needed.

We choose a parallelogram P_1 in Ω_v, and let P_1 have vertices v_1, v_2, v_3, v_4. Then $v = v_i$ for some $i = 1, 2, 3, 4$. We denote the edge connecting vertices v_i and v_{i+1} by $\mathbf{e}_i$. We first construct a function ψ_i on P_1, and we will do so in a way that an analogous construction on another parallelogram $P_2 \in \Omega_v$ will join C^1-smoothly at v and over a shared edge. Considering Properties 2 & 3 from above, we know that we will desire that $\psi_i|_{\mathbf{e}_{i+1}} = \psi_i|_{\mathbf{e}_{i+2}} = 0$, in order to have continuity of ψ_v over all of Ω, particularly at the boundary of Ω_v. Moreover, we will also need $\nabla\psi_i|_{\mathbf{e}_{i+1}} = \nabla\psi_i|_{\mathbf{e}_{i+2}} = 0$ in order to satisfy Property 3 at the boundary of Ω_v. Since $\phi_i|_{\mathbf{e}_{i+1}} = \phi_i|_{\mathbf{e}_{i+2}} = 0$, we will simply require that ϕ_i^2 divides ψ_i, so we have $\psi_i = \phi_i^2 Q_i$ for some degree-3 polynomial of Wachspress coordinates Q_i.

Since $\sum_{j=1}^{4} \phi_j = 1$, we can express any degree d polynomial of Wachspress coordinates by a linear combination of monomials of the form $\phi_i^j \phi_{i+1}^k \phi_{i+2}^l \phi_{i-1}^m$ where $j+k+l+m = d$ for non-negative integer powers j, k, l, m. However, not all of these terms are linearly independent; in fact, it is easy to see that, in the case of parallelograms,

$$\phi_i \phi_{i+2} = \frac{1}{C^4} \prod_{j=1}^{4} A_j = \phi_{i-1}\phi_{i+1}.$$

With this in mind, we can create a list of linearly independent degree-3 monomials of Wachspress coordinates, and we arrange them strategically to form the following template for ψ_i:

$$\begin{aligned}\psi_i = {} & \phi_i^2(J_0\phi_i^3 + \phi_i^2(J_1\phi_{i+1} + J_2\phi_{i-1}) + \phi_i(J_3\phi_{i+1}^2 + J_4\phi_{i-1}^2) + J_5\phi_{i+1}^3 + J_6\phi_{i-1}^3 \\ & + \phi_{i+2}(K_0\phi_i^2 + \phi_i(K_1\phi_{i+1} + K_2\phi_{i-1}) + K_3\phi_{i+1}^2 + K_4\phi_{i-1}^2) \\ & + \phi_{i+2}^2(S_0\phi_i + S_1\phi_{i+1} + S_2\phi_{i-1} + S_3\phi_{i+2}))\end{aligned} \tag{6}$$

for some constants J_m, K_d, S_p; $m = 0, ..., 6, n = 0, ..., 4, p = 0, 1, 2, 3$ to be determined below.

The arrangement of (6) is done very intentionally. All terms which have value on the edges $\mathbf{e}_i$ and $\mathbf{e}_{i-1}$, and therefore affect the value and gradient of ψ_v on these edges, are given a coefficient J_m for some m. We often call these the *edge terms*. The terms which do not affect the value of ψ_v on these edges, but do affect the gradient, are given a coefficient of K_n for some n. We call these *smoothness terms*. Finally, the remaining terms, which affect neither the value nor gradient on the edges, are given a coefficient of S_p for some p, and are called *combinatorial terms*.

The edge term coefficients are the easiest to determine. Property 1 above easily gives us that $J_0 = 1$, since the only term in ψ_i which is valued at any vertex is $J_0\phi_i^5$, which is valued J_0 at v_i. More edge term coefficients can be found by considering the gradient at the vertex v_i. Since $\phi_j(v_i) = \delta_{i,j}$, we can quickly take the gradient of ψ_i at v_i to retrieve

$$\nabla\psi_i|_{v_i} = 5\nabla\phi_i|_{v_i} + J_1\nabla\phi_{i+1}|_{v_i} + J_2\nabla\phi_{i-1}|_{v_i} + K_0\nabla\phi_{i+2}|_{v_i}. \tag{7}$$

Since $\phi_{i+2}|_{\mathbf{e}_i} = \phi_{i+2}|_{\mathbf{e}_{i-1}} = 0$, $\nabla\phi_{i+2}|_{v_i} = 0$. The other gradients, however, will be nonzero at v_i. Letting $\mathbf{n}_j$ be the outward unit normal to the edge-directional unit vector $\tilde{\mathbf{e}}_j = \dfrac{v_{j+1} - v_j}{|\mathbf{e}_j|}$, we have

$$\begin{aligned}\nabla\phi_i &= \frac{1}{C^2}\left(\nabla A_{i+1}A_{i+2} + A_{i+1}\nabla A_{i+2}\right)\\ \Rightarrow \nabla\phi_i|_{v_i} &= \frac{-1}{2C^2}\left(C|\mathbf{e}_{i+1}|\mathbf{n}_{i+1} + C|\mathbf{e}_{i+2}|\mathbf{n}_{i+2}\right) = \frac{1}{2C}\left(|\mathbf{e}_i|\mathbf{n}_i + |\mathbf{e}_{i-1}|\mathbf{n}_{i-1}\right).\end{aligned}$$

Similarly we can determine that

$$\begin{aligned}\nabla\phi_{i+1} &= \frac{1}{C^2}\left(\nabla A_{i+2}A_{i-1} + A_{i+2}\nabla A_{i-1}\right) \text{ that is, } \nabla\phi_{i+1}|_{v_i} = \frac{-1}{2C}|\mathbf{e}_{i-1}|\mathbf{n}_{i-1}\\ \nabla\phi_{i-1} &= \frac{1}{C^2}\left(\nabla A_iA_{i+1} + A_i\nabla A_{i+1}\right) \text{ that is, } \nabla\phi_{i-1}|_{v_i} = \frac{-1}{2C}|\mathbf{e}_i|\mathbf{n}_i.\end{aligned}$$

Then (7) yields

$$\nabla\psi_i|_{v_i} = (5 - J_1)|\mathbf{e}_{i-1}|\mathbf{n}_{i-1} + (5 - J_2)|\mathbf{e}_i|\mathbf{n}_i.$$

Consider that the function we build in another parallelogram in Ω_v should share the same gradient at v. However, clearly the gradient we have computed here depends not only on the values of J_1 and J_2, but on the length and direction of the edges of P_1. We wish to avoid any further geometric restrictions, and so the only reasonable ways to make the gradients match would either be to choose values of J_1 and J_2 which depend on the surrounding parallelograms rather than just on P_1, or to simply let the gradient at v be 0. We will take the latter route, and add a new property to our list:

- Property 6. $\nabla\psi_v|_v = 0$.

Hence we choose $J_1 = J_2 = 5$.

Now the remaining coefficients can be determined by considering Property 4 above. Within P_1, this property can be translated to mean that $\sum_{i=1}^{4}\psi_i = 1$. Let us focus only on edge $\mathbf{e_i}$ for now. Since $\psi_{i+2}|_{\mathbf{e}_i} = \psi_{i-1}|_{\mathbf{e}_i} = 0$, we only need that $\psi_i|_{\mathbf{e}_i} + \psi_{i+1}|_{\mathbf{e}_i} = 1$. Considering the edge terms from each of these, along with the fact that $\phi_{i-1}|_{\mathbf{e}_i} = \phi_{i+2}|_{\mathbf{e}_i} = 0$, we can write

$$\psi_i|_{\mathbf{e}_i} + \psi_{i+1}|_{\mathbf{e}_i} = \phi_i^5 + 5\phi_i^4\phi_{i+1} + (J_{3,i} + J_{5,i+1})\phi_i^3\phi_{i+1}^2 + (J_{5,i} + J_{3,i+1})\phi_i^2\phi_{i+1}^3 + 5\phi_i\phi_{i+1}^4 + \phi_{i+1}^5.$$

We'll want $(1 - (\psi_i + \psi_{i+1}))|_{\mathbf{e}_i} = 0$. Subtracting the sum from the constant 1 is not difficult when you consider that $\phi_i|_{\mathbf{e}_i} + \phi_{i+1}|_{\mathbf{e}_i} = 1$, so in particular $(\phi_i + \phi_{i+1})^5|_{\mathbf{e}_i} = 1$. Then we can see that

$$(1 - (\psi_i + \psi_{i+1}))|_{\mathbf{e}_i} = (10 - (J_{3,i} + J_{5,i+1}))\phi_i^3\phi_{i+1}^2 + (10 - (J_{5,i} + J_{3,i+1}))\phi_i^2\phi_{i+1}^3, \tag{8}$$

and we need this to be 0. Of course, (8) is not enough to determine the values of J_3 and J_5 uniquely, but thinking ahead, there is another useful requirement we can impose. Even if we were to have some

completed functions ψ_v for each vertex, then every function in the linear span of the ψ_v will have gradient 0 at every vertex, and so if we wished to contain even linear polynomials in this span, we will need functions which can adjust the gradient at the vertices. Not only is this possible, but we can also even adjust the Hessian at the vertices nicely, as we will show later. With this in mind, it will also be helpful to add a seventh property to our list:

- Property 7. $\nabla^2 \psi_v|_{w \in V} = 0$.

Now, let us consider $\frac{\partial^2 \psi_i}{\partial \tilde{\mathbf{e}}_i^2}|_{v_{i+1}}$. Combining the facts that $\phi_{i-1}|_{\mathbf{e}_i} = \phi_{i+2}|_{\mathbf{e}_i} = 0$, $\phi_i|_{v_{i+1}} = 0$, and ϕ_i and ϕ_{i+1} are linear on $\mathbf{e}_i$, then this computation is fairly easy:

$$\frac{\partial^2 \psi_i}{\partial \tilde{\mathbf{e}}_i^2}|_{v_{i+1}} = 2J_5 \left(\frac{\partial \phi_i}{\partial \tilde{\mathbf{e}}_i} \right)^2 |_{v_{i+1}} = \frac{2J_5}{|\mathbf{e}_i|^2},$$

which is 0 if and only if J_5 is 0. Going back to (8) and replacing J_5 by 0 implies, then, that $J_3 = 10$; a similar computation shows that these coefficients will also force $\frac{\partial^2 \psi_i}{\partial \tilde{\mathbf{e}}_i^2}|_{v_i} = 0$.

A nearly identical analysis on e_{i-1} yields $J_4 = 10$ and $J_6 = 0$, forcing $\frac{\partial^2 \psi_i}{\partial \tilde{\mathbf{e}}_{i-1}^2}|_{v_{i-1}} = 0$, and we finally have all the edge term coefficients.

Computing the smoothness term coefficients is a bit more complicated. K_0 will be the easiest, and can be determined using Property 7. Consider $\frac{\partial^2 \psi_i}{\partial \tilde{\mathbf{e}}_i \partial \tilde{\mathbf{e}}_{i-1}}|_{v_i}$:

$$\begin{aligned}
\frac{\partial^2 \psi_i}{\partial \tilde{\mathbf{e}}_i \partial \tilde{\mathbf{e}}_{i-1}}|_{v_i} &= 20 \frac{\partial \phi_i}{\partial \tilde{\mathbf{e}}_i} \frac{\partial \phi_i}{\partial \tilde{\mathbf{e}}_{i-1}} + 5 \frac{\partial^2 \phi_i}{\partial \tilde{\mathbf{e}}_i \partial \tilde{\mathbf{e}}_{i-1}} + 20 \frac{\partial \phi_i}{\partial \tilde{\mathbf{e}}_i} \frac{\partial \phi_{i-1}}{\partial \tilde{\mathbf{e}}_{i-1}} + 20 \frac{\partial \phi_i}{\partial \tilde{\mathbf{e}}_{i-1}} \frac{\partial \phi_{i+1}}{\partial \tilde{\mathbf{e}}_i} \\
&\quad + 5 \left(\frac{\partial^2 \phi_{i+1}}{\partial \tilde{\mathbf{e}}_i \partial \tilde{\mathbf{e}}_{i-1}} + \frac{\partial^2 \phi_{i-1}}{\partial \tilde{\mathbf{e}}_i \partial \tilde{\mathbf{e}}_{i-1}} \right) + K_0 \frac{\partial^2 \phi_{i+2}}{\partial \tilde{\mathbf{e}}_i \partial \tilde{\mathbf{e}}_{i-1}} \\
&= \frac{-20 - 5 + 20 + 20 + 10 - K_0}{|\mathbf{e}_i||\mathbf{e}_{i-1}|} = \frac{25 - K_0}{|\mathbf{e}_i||\mathbf{e}_{i-1}|}
\end{aligned}$$

Since we desire that $\nabla^2 \psi_i|_{v_i} = 0$, then we must set $K_0 = 25$. One can check that the mixed edge-direction derivatives are conveniently already 0 at the other vertices, so we have satisfied Property 7 at all vertices now.

The remaining smoothness term coefficients will be determined by Property 3. Since Wachspress coordinates are smooth on the interior of the polygon over which they are defined, we need only worry about C^1 smoothness at the shared edges and vertices between parallelograms. Since we have fully controlled the gradient at all the vertices, we need only worry about the shared edges between adjacent parallelograms.

Choose a parallelogram $P_2 \in \Omega_v$ which is adjacent to P_1. Without loss of generality, assume that $v = v_{i,P_1} = v_{i,P_2}$ and $v_{i+1,P_1} = v_{i-1,P_2}$, so that $\mathbf{e}_{i,P_1} = \mathbf{e}_{i-1,P_2}$ and $\tilde{\mathbf{e}}_{i,P_1} = -\tilde{\mathbf{e}}_{i-1,P_2}$. See Figure 4.

Now consider ψ_{i,P_1} and ψ_{i,P_2} on the shared edge. Since Wachspress coordinates are linear polynomials on edges, both ψ_{i,P_1} and ψ_{i,P_2} are degree-5 polynomials on the shared edge, and are in fact the same polynomial. To enforce C^1-smoothness, then, we can take the derivative of both functions on this edge in the outward normal direction, and require that $\frac{\partial \psi_{i,P_1}}{\partial \mathbf{n}_{i,P_1}}|_{\mathbf{e}_{i,P_1}} + \frac{\partial \psi_{i,P_2}}{\partial \mathbf{n}_{i-1,P_2}}|_{\mathbf{e}_{i-1,P_2}} = 0$. First we compute the outward normal derivatives of the Wachspress coordinates. Where θ_j is the interior

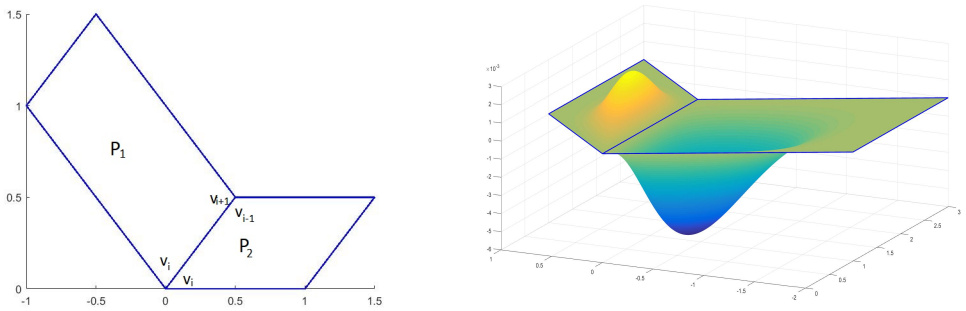

Figure 4: Two adjacent parallelograms sharing an edge and an edge spline to be discussed later

angle of the parallelogram at vertex v_j, we retrieve the following:

$$\frac{\partial \phi_i}{\partial \mathbf{n}_i}|_{\mathbf{e}_i} = \frac{1}{2C}\left(|\mathbf{e}_i|\phi_i - |\mathbf{e}_{i-1}|\cos(\theta_i)\right),$$
$$\frac{\partial \phi_{i+1}}{\partial \mathbf{n}_i}|_{\mathbf{e}_i} = \frac{1}{2C}\left(|\mathbf{e}_i|\phi_{i+1} + |\mathbf{e}_{i-1}|\cos(\theta_i)\right),$$
$$\frac{\partial \phi_{i-1}}{\partial \mathbf{n}_i}|_{\mathbf{e}_i} = -\frac{|\mathbf{e}_i|}{2C}\phi_i, \text{ and } \frac{\partial \phi_{i+2}}{\partial \mathbf{n}_i}|_{\mathbf{e}_i} = -\frac{|\mathbf{e}_i|}{2C}\phi_{i+1}.$$

Now we compute the directional derivatives of ψ_i:

$$\begin{aligned}\frac{\partial \psi_i}{\partial \mathbf{n}_i}|_{\mathbf{e}_i} &= \frac{\partial \phi_i}{\partial \mathbf{n}_i}(30\phi_i^2\phi_{i+1}^2) + \frac{\partial \phi_{i-1}}{\partial \mathbf{n}_i}(-20\phi_i^3\phi_{i+1}) + \frac{\partial \phi_{i+2}}{\partial \mathbf{n}_i}(20\phi_i^4 + (K_1-20)\phi_i^3\phi_{i+1} + K_3\phi_i^2\phi_{i+1}^2)\\ &= \phi_i^3\phi_{i+1}^2\left((50-K_1)\frac{|\mathbf{e}_i|}{2C} - 30\frac{|\mathbf{e}_{i-1}|\cos(\theta_i)}{2C}\right) + \phi_i^2\phi_{i+1}^3\left(-K_3\frac{|\mathbf{e}_i|}{2C} - 30\frac{|\mathbf{e}_{i-1}|\cos(\theta_i)}{2C}\right);\\ \frac{\partial \psi_i}{\partial \mathbf{n}_{i-1}}|_{\mathbf{e}_{i-1}} &= \frac{\partial \phi_i}{\partial \mathbf{n}_{i-1}}(30\phi_i^2\phi_{i-1}^2) + \frac{\partial \phi_{i+1}}{\partial \mathbf{n}_{i-1}}(-20\phi_i^3\phi_{i-1}) + \frac{\partial \phi_{i+2}}{\partial \mathbf{n}_{i-1}}(20\phi_i^4 + (K_2-20)\phi_i^3\phi_{i-1} + K_4\phi_i^2\phi_{i-1}^2)\\ &= \phi_i^3\phi_{i-1}^2\left((50-K_2)\frac{|\mathbf{e}_{i-1}|}{2C} - 30\frac{|\mathbf{e}_i|\cos(\theta_i)}{2C}\right) + \phi_i^2\phi_{i-1}^3\left(-K_4\frac{|\mathbf{e}_{i-1}|}{2C} - 30\frac{|\mathbf{e}_i|\cos(\theta_i)}{2C}\right).\end{aligned}$$

Then, since $\phi_{i,P_1}|_{\mathbf{e}_{i,P_1}} = \phi_{i,P_2}|_{\mathbf{e}_{i-1,P_2}}$ and $\phi_{i+1,P_1}|_{\mathbf{e}_{i,P_1}} = \phi_{i-1,P_2}|_{\mathbf{e}_{i-1,P_2}}$, we have

$$\begin{aligned}&\frac{\partial \psi_{i,P_1}}{\partial \mathbf{n}_{i,P_1}}|_{\mathbf{e}_{i,P_1}} + \frac{\partial \psi_{i,P_2}}{\partial \mathbf{n}_{i-1,P_2}}|_{\mathbf{e}_{i-1,P_2}}\\ =&\phi_{i,P_1}^3\phi_{i+1,P_1}^2\left((50-K_{1,P_1})\frac{|\mathbf{e}_{i,P_1}|}{2C_{P_1}} - 30\frac{|\mathbf{e}_{i-1,P_1}|\cos(\theta_{i,P_1})}{2C_{P_1}} + (50-K_{2,P_2})\frac{|\mathbf{e}_{i-1,P_2}|}{2C_{P_2}} - 30\frac{|\mathbf{e}_{i,P_2}|\cos(\theta_{i,P_2})}{2C_{P_2}}\right)\\ &- \phi_{i,P_1}^2\phi_{i+1,P_1}^3\left(K_{3,P_1}\frac{|\mathbf{e}_{i,P_1}|}{2C_{P_1}} + 30\frac{|\mathbf{e}_{i-1,P_1}|\cos(\theta_{i,P_1})}{2C_{P_1}} + K_{4,P_2}\frac{|\mathbf{e}_{i-1,P_2}|}{2C_{P_2}} + 30\frac{|\mathbf{e}_{i,P_2}|\cos(\theta_{i,P_2})}{2C_{P_2}}\right).\end{aligned}$$

Of course, we have more than enough degrees of freedom to make this sum evaluate to 0, but we still desire that the coefficients of a function associated with one parallelogram be independent of the geometry of other parallelograms. Then we ought to set

$$K_1 = 50 - 30\frac{|\mathbf{e}_{i-1}|}{|\mathbf{e}_i|}\cos(\theta_i), \qquad K_2 = 50 - 30\frac{|\mathbf{e}_i|}{|\mathbf{e}_{i-1}|}\cos(\theta_i),$$
$$K_3 = -30\frac{|\mathbf{e}_{i-1}|}{|\mathbf{e}_i|}\cos(\theta_i), \qquad K_4 = -30\frac{|\mathbf{e}_i|}{|\mathbf{e}_{i-1}|}\cos(\theta_i).$$

Now we are almost finished. As things stand, we have (after a little simplification)

$$\psi_i = \phi_i^2\Bigg(\phi_i^3 + 5\phi_i^2(\phi_{i+1}+\phi_{i-1}) + 10\phi_i(\phi_{i+1}^2+\phi_{i-1}^2) \\ + \phi_{i+2}\left(25\phi_i^2 + \phi_i\left(\left(50 - 30\frac{|\mathbf{e}_{i-1}|}{|\mathbf{e}_i|}\cos(\theta_i)\right)\phi_{i+1} + \left(50 - 30\frac{|\mathbf{e}_i|}{|\mathbf{e}_{i-1}|}\cos(\theta_i)\right)\phi_{i-1}\right)\right. \\ \left. -30\cos(\theta_i)\left(\frac{|\mathbf{e}_{i-1}|}{|\mathbf{e}_i|}\phi_{i+1}^2 + \frac{|\mathbf{e}_i|}{|\mathbf{e}_{i-1}|}\phi_{i-1}^2\right)\right) + \phi_{i+2}^2(S_0\phi_i + S_1\phi_{i+1} + S_2\phi_{i-1} + S_3\phi_{i+2})\Bigg).$$

Now we consider the combinatorial coefficients, which can be determined by Property 4. Since $\sum_{j=1}^{4}\phi_j = 1$, $\left(\sum_{j=1}^{4}\phi_j\right)^5 = 1$, which helps us compare. If we compute $1 - \sum_{j=1}^{4}\psi_i$, and recall $B = \phi_i\phi_{i+2} = \phi_{i+1}\phi_{i-1}$, then we find that

$$1 - \sum_{j=1}^{4}\psi_i = -B^2\sum_{j=1}^{4}(S_{0,j} + S_{1,j-1} + S_{2,j+1} + S_{3,j+2} - 100).$$

While we have very much freedom, we choose to force $S_1 = S_2 = S_3 = 0$, and we will stick to this choice for the functions we'll build later in the paper as well. Hence we have $S_0 = 100$. We have now completed our construction with an explicit formula for ψ_i:

$$\psi_i = \phi_i^2\Bigg(\phi_i^3 + 5\phi_i^2(\phi_{i+1}+\phi_{i-1}) + 10\phi_i(\phi_{i+1}^2+\phi_{i-1}^2) \\ + \phi_{i+2}\left(25\phi_i^2 + \phi_i\left(\left(50 - 30\frac{|\mathbf{e}_{i-1}|}{|\mathbf{e}_i|}\cos(\theta_i)\right)\phi_{i+1} + \left(50 - 30\frac{|\mathbf{e}_i|}{|\mathbf{e}_{i-1}|}\cos(\theta_i)\right)\phi_{i-1}\right)\right. \\ \left. -30\cos(\theta_i)\left(\frac{|\mathbf{e}_{i-1}|}{|\mathbf{e}_i|}\phi_{i+1}^2 + \frac{|\mathbf{e}_i|}{|\mathbf{e}_{i-1}|}\phi_{i-1}^2\right)\right) + 100\phi_{i+2}^2\phi_i\Bigg). \tag{9}$$

The discussion of this subsection serves as a proof of the following theorem:

Theorem 1 *Let $\mathcal{P}$ be a parallelogram partition of Ω with set of vertices V. Then for a vertex $v \in V$, the function*

$$\psi_v(\mathbf{x}) := \begin{cases} \psi_{i,P}(\mathbf{x}), & x \in P, v_i = v, P \in \Omega_v \\ 0 & x \notin \Omega_v \end{cases}$$

is a piecewise polynomial function in $C^1(\Omega)$ with the following properties:

(1) $\psi_v(w) = \delta_{v,w}$ for $w \in V$; (2) $\nabla\psi_v|_w = 0$ for $w \in V$; (3) $\nabla^2\psi_v|_w = 0$ for $w \in V$; (4) $\sum_{v\in V}\psi_v = 1$.

Using the cell Ω_v of parallelograms shown on the right graph of Figure 1 with v being the interior vertex of the union of all parallelograms in Ω_v, the function ψ_v is plotted in Figure 5.

3.2 Gradient Interpolation Functions $\psi_{x,v}$ and $\psi_{y,v}$

By an analogous construction to the previous subsection, we can construct functions $\psi_{x,v}, \psi_{y,v}$ in $C^1(\Omega)$ which have the following properties:

Property 1. $\psi_{x,v}|_{w\in V} = \psi_{y,v}|_{w\in V} = 0$; Property 2. $\nabla\psi_{x,v}|_{w\in V} = \langle\delta_{v,w}, 0\rangle$ and $\nabla\psi_{y,v}|_{w\in V} = \langle 0, \delta_{v,w}\rangle$;

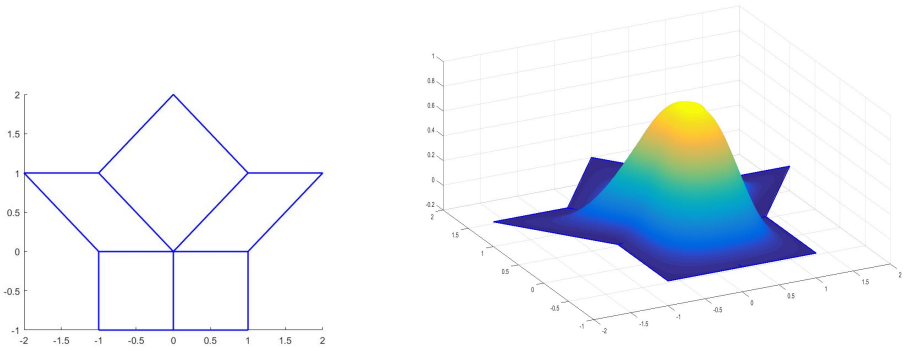

Figure 5: The plot of ψ_v over the cell Ω_v shown on the right graph of Figure 1

Property 3. $\nabla^2\psi_{x,v}|_{w\in V} = \nabla^2\psi_{y,v}|_{w\in V} = 0$; Property 4. $\text{supp}(\psi_{x,v})$, $\text{supp}(\psi_{y,v}) \subseteq \Omega_v$; and

Property 5. $\sum_{v\in V} v_x\psi_v + \psi_{x,v} = x$ and $\sum_{v\in V} v_y\psi_v + \psi_{y,v} = y$.

Reusing the notation of the same arbitrary parallelogram P_1 and beginning with the same template (6) as in the previous subsection, one can follow the same steps (but instead aiming to satisfy the 5 properties above) to reach the following solution for the function $\psi_{x,i}$:
writing $\langle e_{i,x}, e_{i,y}\rangle := (v_{i+1,x} - v_{i,x}, v_{i+1,y} - v_{i,y})$ as a vector representation of the edges,

$$\begin{aligned}\psi_{x,i} =&\phi_i^2\Bigg(\phi_i^2(e_{i,x}\phi_{i+1} - e_{i-1,x}\phi_{i-1}) + 4\phi_i(e_{i,x}\phi_{i+1}^2 - e_{i-1,x}\phi_{i-1}^2)\\
&+\phi_{i+2}\Bigg(5\left(e_{i,x} - e_{i-1,x}\right)\phi_i^2 + \phi_i\left(\left(\left(20 - 18\frac{|\mathbf{e}_{i-1}|}{|\mathbf{e}_i|}\cos(\theta_i)\right)e_{i,x} - 10e_{i-1,x}\right)\phi_{i+1}\right.\\
&\left.-\left(\left(20 - 18\frac{|\mathbf{e}_i|}{|\mathbf{e}_{i-1}|}\cos(\theta_i)\right)e_{i-1,x} - 10e_{i,x}\right)\phi_{i-1}\right)\\
&-12\frac{|\mathbf{e}_{i-1}|}{|\mathbf{e}_i|}\cos(\theta_i)e_{i,x}\phi_{i+1}^2 + 12\frac{|\mathbf{e}_i|}{|\mathbf{e}_{i-1}|}\cos(\theta_i)e_{i-1,x}\phi_{i-1}^2\Bigg) + 40\left(e_{i,x} - e_{i-1,x}\right)\phi_i\phi_{i+2}^2\Bigg).\end{aligned} \tag{10}$$

Theorem 2 *Let $\mathcal{P}$ be a parallelogram partition of Ω with set of vertices V. Then for a vertex $v \in V$, the function*

$$\psi_{x,v}(\mathbf{x}) := \begin{cases} \psi_{x,i,P}(\mathbf{x}), & x \in P, v_i = v, P \in \Omega_v \\ 0 & x \notin \Omega_v \end{cases}$$

is a piecewise polynomial function in $C^1(\Omega)$ with the following properties:

Property 1. $\psi_{x,v}(w) = 0$ for $w \in V$; Property 2. $\nabla\psi_{x,v}|_w = \langle\delta_{v,w}, 0\rangle$ for $w \in V$;

Property 3. $\nabla^2\psi_{x,v}|_w = 0$ for $w \in V$; Property 4. $\sum_{v\in V} v_x\psi_v + \psi_{x,v} = x$.

Proof. First restrict to a single parallelogram $P_1 \in \Omega_v$, and refer to the definition of the function $\psi_{x,i}$ over P_1 in (10). Notice that $\psi_{x,i}$ is a degree-5 polynomial of Wachspress coordinates, and every term is uniformly of degree exactly 5. The only Wachspress monomial of degree 5 which is valued at v_i is ϕ_i^5, but this monomial is not present in the definition of $\psi_{x,i}$; therefore it is clear to see that $\psi_{x,i}(v_i) = 0$.

Notice also that $\psi_{x,i}$ has a factor of ϕ_i^2, and $\phi_i|_{v_j} = 0$ for $i \neq j$, so $\psi_{x,i}|_{v_j} = 0$ for $i \neq j$. This proves that $\psi_{x,i}$ satisfies Property 1 on P_1, and therefore $\psi_{x,v}$ satisfies the property over all of Ω.

Due to the factor of ϕ_i^2, we can see that $\psi_{x,i}$ is doubly zero at all vertices other than v_i, so clearly $\nabla\psi_{x,i}|_{v_j} = 0$ for $i \neq j$. To satisfy Property 2, we must also show that $\nabla\psi_{x,i}|_{v_i} = \langle 1, 0\rangle$. We'll do so by taking the directional derivatives along the edges joined at v_i.

$$\begin{aligned}
\left.\frac{\partial\psi_{x,i}}{\partial\tilde{\mathbf{e}}_i}\right|_{v_i} &= \left.\phi_i^2\left(\phi_i^2\left(e_{i,x}\frac{\partial\phi_{i+1}}{\partial\tilde{\mathbf{e}}_i} - e_{i-1,x}\frac{\partial\phi_{i-1}}{\partial\tilde{\mathbf{e}}_i}\right) + 0\right)\right|_{v_i} \\
&= 1\left(1\left(e_{i,x}\frac{1}{|\mathbf{e}_i|} - e_{i-1,x}(0)\right) + 0\right) \\
&= \frac{e_{i,x}}{|\mathbf{e}_i|}
\end{aligned}$$

Similarly, $\left.\frac{\partial\psi_{x,i}}{\partial\tilde{\mathbf{e}}_{i-1}}\right|_{v_i} = \frac{e_{i-1,x}}{|\mathbf{e}_{i-1}|}$.

For any unit vector $\mathbf{d} = \langle \mathbf{d_x}, \mathbf{d_y}\rangle$, we can write $\mathbf{d} = \alpha\tilde{\mathbf{e}}_\mathbf{i} + \beta\tilde{\mathbf{e}}_{\mathbf{i-1}}$ for some real values α and β. Then since we know the Wachspress coordinates are smooth on P_1, and therefore $\psi_{x,i}$ is smooth on P_1, we can write

$$\begin{aligned}
\left.\frac{\partial\psi_{x,i}}{\partial\mathbf{d}}\right|_{v_i} &= \alpha\left.\frac{\partial\psi_{x,i}}{\partial\tilde{\mathbf{e}}_i}\right|_{v_i} + \beta\left.\alpha\frac{\partial\psi_{x,i}}{\partial\tilde{\mathbf{e}}_{i-1}}\right|_{v_i} \\
&= \alpha\frac{e_{i,x}}{|\mathbf{e}_i|} + \beta\frac{e_{i-1,x}}{|\mathbf{e}_{i-1}|} \\
&= \mathbf{d_x} \\
\Rightarrow \nabla\psi_{x,i}|_{v_i} &= \langle 1, 0\rangle
\end{aligned}$$

This shows that $\psi_{x,i}$ satisfies Property 2 on P_1, and therefore $\psi_{x,v}$ satisfies the property over all of Ω.

Using the same reasoning, we'll prove that $\psi_{x,i}$ satisfies Property 3 on P_1 by showing that

$$\left.\frac{\partial^2\psi_{x,i}}{\partial\tilde{\mathbf{e}}_j^2}\right|_{v_j} = \left.\frac{\partial^2\psi_{x,i}}{\partial\tilde{\mathbf{e}}_{j-1}^2}\right|_{v_j} = \left.\frac{\partial^2\psi_{x,i}}{\partial\tilde{\mathbf{e}}_j\partial\tilde{\mathbf{e}}_{j-1}}\right|_{v_j} = 0$$

for all vertices v_j.

Let's start at v_{i+2}. Since $\phi_i|_{\mathbf{e}_{i+1}} = \phi_i|_{\mathbf{e}_{i+2}} = 0$, and ϕ_i^2 is a factor of $\psi_{x,i}$, clearly $\left.\frac{\partial^2\psi_{x,i}}{\partial\tilde{\mathbf{e}}_{i+1}^2}\right|_{v_{i+2}} = \left.\frac{\partial^2\psi_{x,i}}{\partial\tilde{\mathbf{e}}_{i+2}^2}\right|_{v_{i+2}} = 0$. The mixed-directional derivative is less obvious, but a fairly easy calculation. If we write $\psi_{x,i} = \phi_i^2 Q$ for the appropriate degree-3 Wachspress polynomial Q,we see that

$$\begin{aligned}
\left.\frac{\partial^2\psi_{x,i}}{\partial\tilde{\mathbf{e}}_{i+1}\partial\tilde{\mathbf{e}}_{i+2}}\right|_{v_{i+2}} &= \left.\frac{\partial}{\partial\tilde{\mathbf{e}}_{i+1}}\left(2\phi_i\frac{\partial\phi_i}{\partial\tilde{\mathbf{e}}_{i+2}}Q + \phi_i^2\frac{\partial Q}{\partial\tilde{\mathbf{e}}_{i+2}}\right)\right|_{v_{i+2}} \\
&= \left(2\frac{\partial\phi_i}{\partial\tilde{\mathbf{e}}_{i+1}}\frac{\partial\phi_i}{\partial\tilde{\mathbf{e}}_{i+2}}Q + 2\phi_i\frac{\partial^2\phi_i}{\partial\tilde{\mathbf{e}}_{i+1}\partial\tilde{\mathbf{e}}_{i+2}}Q\right. \\
&\quad \left.+2\phi_i\frac{\partial\phi_i}{\partial\tilde{\mathbf{e}}_{i+2}}\frac{\partial Q}{\partial\tilde{\mathbf{e}}_{i+1}} + 2\phi_i\frac{\partial\phi_i}{\partial\tilde{\mathbf{e}}_{i+1}}\frac{\partial Q}{\partial\tilde{\mathbf{e}}_{i+2}} + \phi_i^2\frac{\partial^2 Q}{\partial\tilde{\mathbf{e}}_{i+1}\partial\tilde{\mathbf{e}}_{i+2}}\right)\Bigg|_{v_{i+2}} \\
&= 2(0)(0)Q + 2(0)\frac{\partial^2\phi_i}{\partial\tilde{\mathbf{e}}_{i+1}\partial\tilde{\mathbf{e}}_{i+2}}Q + 2(0)(0)\frac{\partial Q}{\partial\tilde{\mathbf{e}}_{i+1}} + 2(0)(0)\frac{\partial Q}{\partial\tilde{\mathbf{e}}_{i+2}} + (0)^2\frac{\partial^2 Q}{\partial\tilde{\mathbf{e}}_{i+1}\partial\tilde{\mathbf{e}}_{i+2}} \\
&= 0,
\end{aligned}$$

so now we have that $\nabla^2\psi_{x,i}|_{v_{i+2}} = 0$.

Now focus on v_{i+1}. Since $\phi_i|_{\mathbf{e}_{i+1}} = 0$, then it should be easy to see that $\left.\dfrac{\partial^2\psi_{x,i}}{\partial\tilde{\mathbf{e}}_{i+1}^2}\right|_{v_{i+1}} = 0$.

Using the same definition for Q as before, first note that $Q|_{v_{i+1}} = 0$, and let us compute the following:

$$\begin{aligned}
\left.\frac{\partial^2\psi_{x,i}}{\partial\tilde{\mathbf{e}}_i^2}\right|_{v_{i+1}} &= \left.\frac{\partial}{\partial\tilde{\mathbf{e}}_i}\left(2\phi_i\frac{\partial\phi_i}{\partial\tilde{\mathbf{e}}_i}Q + \phi_i^2\frac{\partial Q}{\partial\tilde{\mathbf{e}}_i}\right)\right|_{v_{i+1}} \\
&= \left.\left(2\left(\frac{\partial\phi_i}{\partial\tilde{\mathbf{e}}_i}\right)^2 Q + 2\phi_i\frac{\partial^2\phi_i}{\partial\tilde{\mathbf{e}}_i^2}Q + 4\phi_i\frac{\partial\phi_i}{\partial\tilde{\mathbf{e}}_i}\frac{\partial Q}{\partial\tilde{\mathbf{e}}_i} + \phi_i^2\frac{\partial^2 Q}{\partial\tilde{\mathbf{e}}_i^2}\right)\right|_{v_{i+1}} \\
&= 2\left(\frac{\partial\phi_i}{\partial\tilde{\mathbf{e}}_i}\right)^2(0) + 2(0)(0)(0) + 4(0)\frac{\partial\phi_i}{\partial\tilde{\mathbf{e}}_i}\frac{\partial Q}{\partial\tilde{\mathbf{e}}_i} + (0)^2\frac{\partial^2 Q}{\partial\tilde{\mathbf{e}}_i^2} \\
&= 0.
\end{aligned}$$

Finally, we need to take the mixed-direction derivative:

$$\begin{aligned}
\left.\frac{\partial^2\psi_{x,i}}{\partial\tilde{\mathbf{e}}_{i-1}\partial\tilde{\mathbf{e}}_i}\right|_{v_{i+1}} &= \left.\frac{\partial}{\partial\tilde{\mathbf{e}}_{i-1}}\left(2\phi_i\frac{\partial\phi_i}{\partial\tilde{\mathbf{e}}_i}Q + \phi_i^2\frac{\partial Q}{\partial\tilde{\mathbf{e}}_i}\right)\right|_{v_{i+1}} \\
&= \left.\left(2\frac{\partial\phi_i}{\partial\tilde{\mathbf{e}}_{i-1}}\frac{\partial\phi_i}{\partial\tilde{\mathbf{e}}_i}Q + 2\phi_i\frac{\partial^2\phi_i}{\partial\tilde{\mathbf{e}}_{i-1}\partial\tilde{\mathbf{e}}_i}Q + 2\phi_i\frac{\partial\phi_i}{\partial\tilde{\mathbf{e}}_i}\frac{\partial Q}{\partial\tilde{\mathbf{e}}_{i-1}} + 2\phi_i\frac{\partial\phi_i}{\partial\tilde{\mathbf{e}}_{i-1}}\frac{\partial Q}{\partial\tilde{\mathbf{e}}_i} + \phi_i^2\frac{\partial^2 Q}{\partial\tilde{\mathbf{e}}_{i-1}\partial\tilde{\mathbf{e}}_i}\right)\right|_{v_{i+1}} \\
&= 2\frac{\partial\phi_i}{\partial\tilde{\mathbf{e}}_{i-1}}\frac{\partial\phi_i}{\partial\tilde{\mathbf{e}}_i}(0) + 2(0)\frac{\partial^2\phi_i}{\partial\tilde{\mathbf{e}}_{i-1}\partial\tilde{\mathbf{e}}_i}(0) + 2(0)\frac{\partial\phi_i}{\partial\tilde{\mathbf{e}}_i}\frac{\partial Q}{\partial\tilde{\mathbf{e}}_{i-1}} + 2(0)\frac{\partial\phi_i}{\partial\tilde{\mathbf{e}}_{i-1}}\frac{\partial Q}{\partial\tilde{\mathbf{e}}_i} + (0)^2\frac{\partial^2 Q}{\partial\tilde{\mathbf{e}}_{i-1}\partial\tilde{\mathbf{e}}_i} \\
&= 0,
\end{aligned}$$

so now we see that $\nabla^2\psi_{x,i}|_{v_{i+1}} = 0$. A similar calculation shows that $\nabla^2\psi_{x,i}|_{v_{i-1}} = 0$.

Finally focus on v_i. Noting that $Q|_{v_i} = 0$, we have

$$\begin{aligned}
\left.\frac{\partial^2\psi_{x,i}}{\partial\tilde{\mathbf{e}}_i^2}\right|_{v_i} &= \left.\frac{\partial}{\partial\tilde{\mathbf{e}}_i}\left(2\phi_i\frac{\partial\phi_i}{\partial\tilde{\mathbf{e}}_i}Q + \phi_i^2\frac{\partial Q}{\partial\tilde{\mathbf{e}}_i}\right)\right|_{v_i} \\
&= \left.\left(2\left(\frac{\partial\phi_i}{\partial\tilde{\mathbf{e}}_i}\right)^2 Q + 2\phi_i\frac{\partial^2\phi_i}{\partial\tilde{\mathbf{e}}_i^2}Q + 4\phi_i\frac{\partial\phi_i}{\partial\tilde{\mathbf{e}}_i}\frac{\partial Q}{\partial\tilde{\mathbf{e}}_i} + \phi_i^2\frac{\partial^2 Q}{\partial\tilde{\mathbf{e}}_i^2}\right)\right|_{v_i} \\
&= 2\left(\frac{-1}{|\mathbf{e}_i|}\right)^2(0) + 2(1)(0)(0) + 4(1)\left(\frac{-1}{|\mathbf{e}_i|}\right)\left.\frac{\partial Q}{\partial\tilde{\mathbf{e}}_i}\right|_{v_i} + (1)^2\left.\frac{\partial^2 Q}{\partial\tilde{\mathbf{e}}_i^2}\right|_{v_i} \\
&= \left.\frac{\partial^2 Q}{\partial\tilde{\mathbf{e}}_i^2}\right|_{v_i} - \frac{4}{|\mathbf{e}_i|}\left.\frac{\partial Q}{\partial\tilde{\mathbf{e}}_i}\right|_{v_i}. \qquad (11)
\end{aligned}$$

This time, we're going to need to actually consider the derivatives of Q. First we write

$$Q = \phi_i^2(e_{i,x}\phi_{i+1} - e_{i-1,x}\phi_{i-1}) + 4\phi_i(e_{i,x}\phi_{i+1}^2 - e_{i-1,x}\phi_{i-1}^2) + \phi_{i+2}R$$

for the appropriate degree-2 polynomial of Wachspress coordinates R.

$$\begin{aligned}
\left.\frac{\partial Q}{\partial \tilde{\mathbf{e}}_i}\right|_{v_i} &= \left(2\phi_i\frac{\partial \phi_i}{\partial \tilde{\mathbf{e}}_i}(e_{i,x}\phi_{i+1} - e_{i-1,x}\phi_{i-1}) + \phi_i^2\left(e_{i,x}\frac{\partial \phi_{i+1}}{\partial \tilde{\mathbf{e}}_i} - e_{i-1,x}\frac{\partial \phi_{i-1}}{\partial \tilde{\mathbf{e}}_i}\right)\right. \\
&\quad + 4\frac{\partial \phi_i}{\partial \tilde{\mathbf{e}}_i}(e_{i,x}\phi_{i+1}^2 - e_{i-1,x}\phi_{i-1}^2) + 8\phi_i\left(e_{i,x}\phi_{i+1}\frac{\partial \phi_{i+1}}{\partial \tilde{\mathbf{e}}_i} - e_{i-1,x}\phi_{i-1}\frac{\partial \phi_{i-1}}{\partial \tilde{\mathbf{e}}_i}\right) \\
&\quad \left. + \frac{\partial \phi_{i+2}}{\partial \tilde{\mathbf{e}}_i}R + \phi_{i+2}\frac{\partial R}{\partial \tilde{\mathbf{e}}_i}\right)\Bigg|_{v_i} \\
&= 2(1)\left(\frac{-1}{|\mathbf{e}_i|}\right)(0) + (1)^2\left(e_{i,x}\frac{1}{|\mathbf{e}_i|} - 0\right) \\
&\quad + 4\left(\frac{-1}{|\mathbf{e}_i|}\right)(0) + 8(1)(0) \\
&\quad + 0R + 0R \\
&= \frac{e_{i,x}}{|\mathbf{e}_i|};
\end{aligned}$$

$$\begin{aligned}
\left.\frac{\partial^2 Q}{\partial \tilde{\mathbf{e}}_i^2}\right|_{v_i} &= \left(2\left(\frac{\partial \phi_i}{\partial \tilde{\mathbf{e}}_i}\right)^2(e_{i,x}\phi_{i+1} - e_{i-1,x}\phi_{i-1}) + 2\phi_i\frac{\partial^2 \phi_i}{\partial \tilde{\mathbf{e}}_i^2}(e_{i,x}\phi_{i+1} - e_{i-1,x}\phi_{i-1})\right. \\
&\quad + 4\phi_i\frac{\partial \phi_i}{\partial \tilde{\mathbf{e}}_i}\left(e_{i,x}\frac{\partial \phi_{i+1}}{\partial \tilde{\mathbf{e}}_i} - e_{i-1,x}\frac{\partial \phi_{i-1}}{\partial \tilde{\mathbf{e}}_i}\right) + \phi_i^2\left(e_{i,x}\frac{\partial^2 \phi_{i+1}}{\partial \tilde{\mathbf{e}}_i^2} - e_{i-1,x}\frac{\partial^2 \phi_{i-1}}{\partial \tilde{\mathbf{e}}_i^2}\right) \\
&\quad + 4\frac{\partial^2 \phi_i}{\partial \tilde{\mathbf{e}}_i^2}(e_{i,x}\phi_{i+1}^2 - e_{i-1,x}\phi_{i-1}^2) + 16\frac{\partial \phi_i}{\partial \tilde{\mathbf{e}}_i}\left(e_{i,x}\phi_{i+1}\frac{\partial \phi_{i+1}}{\partial \tilde{\mathbf{e}}_i} - e_{i-1,x}\phi_{i-1}\frac{\partial \phi_{i-1}}{\partial \tilde{\mathbf{e}}_i}\right) \\
&\quad + 8\phi_i\left(e_{i,x}\left(\frac{\partial \phi_{i+1}}{\partial \tilde{\mathbf{e}}_i}\right)^2 + e_{i,x}\phi_{i+1}\frac{\partial^2 \phi_{i+1}}{\partial \tilde{\mathbf{e}}_i^2} - e_{i-1,x}\left(\frac{\partial \phi_{i-1}}{\partial \tilde{\mathbf{e}}_i}\right)^2 - e_{i-1,x}\phi_{i-1}\frac{\partial^2 \phi_{i-1}}{\partial \tilde{\mathbf{e}}_i^2}\right) \\
&\quad \left. + \frac{\partial^2 \phi_{i+2}}{\partial \tilde{\mathbf{e}}_i}R + 2\frac{\partial \phi_{i+2}}{\partial \tilde{\mathbf{e}}_i} + \phi_{i+2}\frac{\partial^2 R}{\partial \tilde{\mathbf{e}}_i}\right)\Bigg|_{v_i} \\
&= 2\left(\frac{-1}{|\mathbf{e}_i|}\right)^2(0) + 2(1)(0)(0) + 4(1)\left(\frac{-1}{|\mathbf{e}_i|}\right)\left(\frac{e_{i,x}}{|\mathbf{e}_i|} - 0\right) + (1)^2(0) + 4(0)(0) + 16\left(\frac{-1}{|\mathbf{e}_i|}\right)(0) \\
&\quad + 8(1)\left(e_{i,x}\left(\frac{1}{|\mathbf{e}_i|}\right)^2 + 0 - 0 - 0\right) + 0 + 0 + 0 \\
&= \frac{4e_{i,x}}{|\mathbf{e}_i|^2}.
\end{aligned}$$

Then we see that (11) resolves to 0, as desired.

A similar calculation shows that $\left.\frac{\partial^2 \psi_{x,i}}{\partial \tilde{\mathbf{e}}_{i-1}^2}\right|_{v_i} = 0$, leaving us to check the mixed-direction derivative:

$$\begin{aligned}
\left.\frac{\partial^2 \psi_{x,i}}{\partial \tilde{\mathbf{e}}_{i-1}\partial \tilde{\mathbf{e}}_i}\right|_{v_i} &= \left.\frac{\partial}{\partial \tilde{\mathbf{e}}_{i-1}}\left(2\phi_i\frac{\partial \phi_i}{\partial \tilde{\mathbf{e}}_i} + \phi_i^2\frac{\partial Q}{\partial \tilde{\mathbf{e}}_i}\right)\right|_{v_i} \\
&= \left(2\frac{\partial \phi_i}{\partial \tilde{\mathbf{e}}_{i-1}}\frac{\partial \phi_i}{\partial \tilde{\mathbf{e}}_i}Q + 2\phi_i\frac{\partial^2 \phi_i}{\partial \tilde{\mathbf{e}}_{i-1}\partial \tilde{\mathbf{e}}_i}Q + 2\phi_i\frac{\partial \phi_i}{\partial \tilde{\mathbf{e}}_i}\frac{\partial Q}{\partial \tilde{\mathbf{e}}_{i-1}} + 2\phi_i\frac{\partial \phi_i}{\partial \tilde{\mathbf{e}}_{i-1}}\frac{\partial Q}{\partial \tilde{\mathbf{e}}_i} + \phi_i^2\frac{\partial^2 Q}{\partial \tilde{\mathbf{e}}_{i-1}\partial \tilde{\mathbf{e}}_i}\right)\Bigg|_{v_i} \\
&= \frac{-2e_{i-1,x}}{|\mathbf{e}_i||\mathbf{e}_{i-1}|} + \frac{2e_{i,x}}{|\mathbf{e}_{i-1}||\mathbf{e}_i|} + \left(\frac{\partial^2 Q}{\partial \tilde{\mathbf{e}}_{i-1}\partial \tilde{\mathbf{e}}_i}\right)\Bigg|_{v_i} \qquad (12)
\end{aligned}$$

We need to know the mixed-direction derivative of Q:

$$\begin{aligned}
\left.\frac{\partial^2 Q}{\partial\tilde{\mathbf{e}}_{i-1}\partial\tilde{\mathbf{e}}_i}\right|_{v_i} &= \frac{\partial}{\partial\tilde{\mathbf{e}}_{i-1}}\left(2\phi_i\frac{\partial\phi_i}{\partial\tilde{\mathbf{e}}_i}(e_{i,x}\phi_{i+1}-e_{i-1,x}\phi_{i-1})+\phi_i^2\left(e_{i,x}\frac{\partial\phi_{i+1}}{\partial\tilde{\mathbf{e}}_i}-e_{i-1,x}\frac{\partial\phi_{i-1}}{\partial\tilde{\mathbf{e}}_i}\right)\right.\\
&\quad+4\frac{\partial\phi_i}{\partial\tilde{\mathbf{e}}_i}(e_{i,x}\phi_{i+1}^2-e_{i-1,x}\phi_{i-1}^2)+8\phi_i\left(e_{i,x}\phi_{i+1}\frac{\partial\phi_{i+1}}{\partial\tilde{\mathbf{e}}_i}-e_{i-1,x}\phi_{i-1}\frac{\partial\phi_{i-1}}{\partial\tilde{\mathbf{e}}_i}\right)\\
&\quad\left.+\frac{\partial\phi_{i+2}}{\partial\tilde{\mathbf{e}}_i}R+\phi_{i+2}\frac{\partial R}{\partial\tilde{\mathbf{e}}_i}\right)\Bigg|_{v_i}\\
&=\left(2\frac{\partial\phi_i}{\partial\tilde{\mathbf{e}}_{i-1}}\frac{\partial\phi_i}{\partial\tilde{\mathbf{e}}_i}(e_{i,x}\phi_{i+1}-e_{i-1,x}\phi_{i-1})+2\phi_i\frac{\partial^2\phi_i}{\partial\tilde{\mathbf{e}}_{i-1}\partial\tilde{\mathbf{e}}_i}(e_{i,x}\phi_{i+1}-e_{i-1,x}\phi_{i-1})\right.\\
&\quad+2\phi_i\frac{\partial\phi_i}{\partial\tilde{\mathbf{e}}_i}\left(e_{i,x}\frac{\partial\phi_{i+1}}{\partial\tilde{\mathbf{e}}_{i-1}}-e_{i-1,x}\frac{\partial\phi_{i-1}}{\partial\tilde{\mathbf{e}}_{i-1}}\right)+2\phi_i\frac{\partial\phi_i}{\partial\tilde{\mathbf{e}}_{i-1}}\left(e_{i,x}\frac{\partial\phi_{i+1}}{\partial\tilde{\mathbf{e}}_i}-e_{i-1,x}\frac{\partial\phi_{i-1}}{\partial\tilde{\mathbf{e}}_i}\right)\\
&\quad+\phi_i^2\left(e_{i,x}\frac{\partial^2\phi_{i+1}}{\partial\tilde{\mathbf{e}}_{i-1}\partial\tilde{\mathbf{e}}_i}-e_{i-1,x}\frac{\partial^2\phi_{i-1}}{\partial\tilde{\mathbf{e}}_{i-1}\partial\tilde{\mathbf{e}}_i}\right)+4\frac{\partial^2\phi_i}{\partial\tilde{\mathbf{e}}_{i-1}\partial\tilde{\mathbf{e}}_i}(e_{i,x}\phi_{i+1}^2-e_{i-1,x}\phi_{i-1}^2)\\
&\quad+8\frac{\partial\phi_i}{\partial\tilde{\mathbf{e}}_i}\left(e_{i,x}\phi_{i+1}\frac{\partial\phi_{i+1}}{\partial\tilde{\mathbf{e}}_{i-1}}-e_{i-1,x}\phi_{i-1}\frac{\partial\phi_{i-1}}{\partial\tilde{\mathbf{e}}_{i-1}}\right)\\
&\quad+8\frac{\partial\phi_i}{\partial\tilde{\mathbf{e}}_{i-1}}\left(e_{i,x}\phi_{i+1}\frac{\partial\phi_{i+1}}{\partial\tilde{\mathbf{e}}_i}-e_{i-1,x}\phi_{i-1}\frac{\partial\phi_{i-1}}{\partial\tilde{\mathbf{e}}_i}\right)\\
&\quad+8\phi_i\left(e_{i,x}\frac{\partial\phi_{i+1}}{\partial\tilde{\mathbf{e}}_{i-1}}\frac{\partial\phi_{i+1}}{\partial\tilde{\mathbf{e}}_i}+e_{i,x}\phi_{i+1}\frac{\partial^2\phi_{i+1}}{\partial\tilde{\mathbf{e}}_{i-1}\partial\tilde{\mathbf{e}}_i}\right.\\
&\qquad\left.-e_{i-1,x}\frac{\partial\phi_{i-1}}{\partial\tilde{\mathbf{e}}_{i-1}}\frac{\partial\phi_{i-1}}{\partial\tilde{\mathbf{e}}_i}-e_{i-1,x}\phi_{i-1}\frac{\partial^2\phi_{i-1}}{\partial\tilde{\mathbf{e}}_{i-1}\partial\tilde{\mathbf{e}}_i}\right)\\
&\quad\left.+\frac{\partial^2\phi_{i+2}}{\partial\tilde{\mathbf{e}}_{i-1}\partial\tilde{\mathbf{e}}_i}R+\frac{\partial\phi_{i+2}}{\partial\tilde{\mathbf{e}}_i}\frac{\partial R}{\partial\tilde{\mathbf{e}}_{i-1}}+\frac{\partial\phi_{i+2}}{\partial\tilde{\mathbf{e}}_{i-1}}\frac{\partial R}{\partial\tilde{\mathbf{e}}_i}+\phi_{i+2}\frac{\partial^2 R}{\partial\tilde{\mathbf{e}}_{i-1}\partial\tilde{\mathbf{e}}_i}\right)\Bigg|_{v_i}\\
&=0+0+2(1)\left(\frac{-1}{|\mathbf{e}_i|}\right)\left(0-e_{i-1,x}\frac{-1}{|\mathbf{e}_{i-1}|}\right)+2(1)\frac{1}{|\mathbf{e}_{i-1}|}\left(e_{i,x}\frac{1}{|\mathbf{e}_i|}-0\right)\\
&\quad+(1)^2\left(e_{i,x}\frac{1}{|\mathbf{e}_{i-1}||\mathbf{e}_i|}-e_{i-1,x}\frac{1}{|\mathbf{e}_{i-1}||\mathbf{e}_i|}\right)+0+0+0+0\\
&\quad+\frac{-1}{|\mathbf{e}_{i-1}||\mathbf{e}_i|}R|_{v_i}+0+0+0\\
&=-3\frac{e_{i-1,x}}{|\mathbf{e}_{i-1}||\mathbf{e}_i|}+3\frac{e_{i,x}}{|\mathbf{e}_{i-1}||\mathbf{e}_i|}-\frac{1}{|\mathbf{e}_{i-1}||\mathbf{e}_i|}(5(e_{i,x}-e_{i-1,x}))\\
&=2\frac{e_{i-1,x}}{|\mathbf{e}_{i-1}||\mathbf{e}_i|}-2\frac{e_{i,x}}{|\mathbf{e}_{i-1}||\mathbf{e}_i|}.
\end{aligned}$$

Substituting this back into (12) yields 0 as desired, finally showing that $\psi_{x,i}$ satisfies Property 3 at all vertices in P_1, and therefore $\psi_{x,v}$ satisfies Property 3 across all of Ω.

Property 4 can and should be proven using a computational aid, like Mathematica. One should begin by noting that, over P_1,

$$x=\left(\sum_{i=1}^4 v_{i,x}\phi_i\right)\left(\sum_{i=1}^4\phi_i\right)^4. \tag{13}$$

The difference

$$x-\sum_{i=1}^4 v_{i,x}\psi_i+\psi_{x,i}$$

where x is replaced by the expansion of (13) provides an expression of uniformly degree-5 monomials of Wachspress coordinates, which can be termwise resolved to 0 by using the following facts:

$$\tilde{\mathbf{e}}_{i-1} = \begin{pmatrix} -\cos(\theta_i) & \sin(\theta_i) \\ -\sin(\theta_i) & -\cos(\theta_i) \end{pmatrix} \tilde{\mathbf{e}}_i, \text{ and}$$
$$\tilde{\mathbf{e}}_i = \begin{pmatrix} -\cos(\theta_i) & -\sin(\theta_i) \\ \sin(\theta_i) & -\cos(\theta_i) \end{pmatrix} \tilde{\mathbf{e}}_{i-1}. \tag{14}$$

While we've addressed all 4 properties listed in the theorem, we have yet to show that $\psi_{x,v} \in C^1(\Omega)$. It is sufficient to show that $\psi_{x,v} \in C^1(\Omega_v)$, since we know that $\psi_{x,v} = 0 \in \Omega \ / \Omega_v$ and $\nabla\psi_{x,v}|_{\partial\Omega_v} = 0$, so $\psi_{x,v}$ is differentiable outside of Ω_v up to its boundary. To show that $\psi_{x,v}$ is differentiable in Ω_v, we choose a second quadrilateral in Ω_v, say P_2; without loss of generality, suppose that $v = v_{i,P_1} = v_{i,P_2}$. Then if $P_2 \cap P_1$ is only v, we know that $\psi_{x,v}$ is in $C^1(P_1 \cup P_2)$ trivially, since $\psi_{x,v}$ is smooth on the interior of P_1 and P_2, and $\nabla\psi_{x,i,P_1}|_{v_{i,P_1}} = \nabla\psi_{x,i,P_2}|_{v_{i,P_2}} = \langle 1, 0\rangle$.

Suppose instead that P_1 and P_2 share an edge - then since $v = v_{i,P_1} = v_{i,P_2}$, they must share the edge $\mathbf{e}_{i,P_1} = \mathbf{e}_{i-1,P_2}$, so that $v_{i+1,P_1} = v_{i-1,P_2}$. We need to show that the functions ψ_{x,i,P_1} and ψ_{x,i,P_2} join smoothly over the shared edge.

It is simple to show that the join along the edge is C^0 :

$$\psi_{x,i,P_1}|_{\mathbf{e}_{i,P_1}} = e_{i,x,P_1}\phi_{i,P_1}^3\phi_{i+1,P_1}\left(\phi_{i,P_1} + 4\phi_{i+1,P_1}\right);$$
$$\psi_{x,i,P_2}|_{\mathbf{e}_{i-1,P_2}} = -e_{i-1,x,P_2}\phi_{i,P_2}^3\phi_{i-1,P_2}\left(\phi_{i,P_2} + 4\phi_{i-1,P_2}\right).$$

Considering that $\mathbf{e}_{i,P_1} = \mathbf{e}_{i-1,P_2}$, $e_{i,x,P_1} = -e_{i-1,x,P_2}$, $\phi_{i,P_1}|_{\mathbf{e}_{i,P_1}} = \phi_{i,P_2}|_{\mathbf{e}_{i-1,P_2}}$, and $\phi_{i+1,P_1}|_{\mathbf{e}_{i,P_1}} = \phi_{i-1,P_2}|_{\mathbf{e}_{i-1,P_2}}$, the two expressions above are clearly equivalent.

To show C^1 smoothness across the shared edge, we'll show that $\left.\dfrac{\partial\psi_{x,i,P_1}}{\partial\mathbf{n}_{i,P_1}}\right|_{\mathbf{e}_{i,P_1}} = \left.\dfrac{\partial\psi_{x,i,P_2}}{\partial\mathbf{n}_{i-1,P_2}}\right|_{\mathbf{e}_{i-1,P_2}}$, considering that $\mathbf{n}_{i,P_1} = -\mathbf{n}_{i-1,P_2}$.

Dropping consideration for which polygon we are in, let's refer to a generic $\psi_{x,i}$ and take the relevant outward-normal derivatives on the edge $\mathbf{e}_i$. It will benefit us to go on and consider the

derivative of the component we denoted Q earlier:

$$\begin{aligned}
\left.\frac{\partial Q}{\partial \mathbf{n}_i}\right|_{\mathbf{e}_i} &= \left(2\phi_i \frac{\partial \phi_i}{\partial \mathbf{n}_i}(e_{i,x}\phi_{i+1} - e_{i-1,x}\phi_{i-1}) + \phi_i^2\left(e_{i,x}\frac{\partial \phi_{i+1}}{\partial \mathbf{n}_i} - e_{i-1,x}\frac{\partial \phi_{i-1}}{\partial \mathbf{n}_i}\right)\right. \\
&\quad + 4\frac{\partial \phi_i}{\partial \mathbf{n}_i}(e_{i,x}\phi_{i+1}^2 - e_{i-1,x}\phi_{i-1}) + 8\phi_i\left(e_{i,x}\phi_{i+1}\frac{\partial \phi_{i+1}}{\partial \mathbf{n}_i} - e_{i-1,x}\phi_{i-1}\frac{\partial \phi_{i-1}}{\partial \mathbf{n}_i}\right) \\
&\quad \left. + \frac{\partial \phi_{i+2}}{\partial \mathbf{n}_i}R + \phi_{i+2}\frac{\partial R}{\partial \mathbf{n}_i}\right)\Bigg|_{\mathbf{e}_i} \\
&= 2\phi_i\left(\left(\frac{|\mathbf{e}_i|}{2C} - \frac{|\mathbf{e}_{i-1}|\cos(\theta_i)}{2C}\right)\phi_i - \frac{|\mathbf{e}_{i-1}|\cos(\theta_i)}{2C}\phi_{i+1}\right)(e_{i,x}\phi_{i+1}) \\
&\quad + \phi_i^2\left(e_{i,x}\left(\left(\frac{|\mathbf{e}_i|}{2C} + \frac{|\mathbf{e}_{i-1}|\cos(\theta_i)}{2C}\right)\phi_{i+1} + \frac{|\mathbf{e}_{i-1}|\cos(\theta_i)}{2C}\phi_i\right) - e_{i-1,x}\left(-\frac{|\mathbf{e}_i|}{2C}\phi_i\right)\right) \\
&\quad + 4\left(\left(\frac{|\mathbf{e}_i|}{2C} - \frac{|\mathbf{e}_{i-1}|\cos(\theta_i)}{2C}\right)\phi_i - \frac{|\mathbf{e}_{i-1}|\cos(\theta_i)}{2C}\phi_{i+1}\right)(e_{i,x}\phi_{i+1}^2) \\
&\quad + 8\phi_i e_{i,x}\phi_{i+1}\left(\left(\frac{|\mathbf{e}_i|}{2C} + \frac{|\mathbf{e}_{i-1}|\cos(\theta_i)}{2C}\right)\phi_{i+1} + \frac{|\mathbf{e}_{i-1}|\cos(\theta_i)}{2C}\phi_i\right) \\
&\quad + \left(-\frac{|\mathbf{e}_i|}{2C}\phi_{i+1}\right)(R|_{\mathbf{e}_i}) \\
&= \phi_i^3\left(e_{i,x}\frac{|\mathbf{e}_{i-1}|\cos(\theta_i)}{2C} + e_{i-1,x}\frac{|\mathbf{e}_i|}{2C}\right) + \phi_i^2\phi_{i+1}\left(3e_{i,x}\frac{|\mathbf{e}_i|}{2C} + 7e_{i,x}\frac{|\mathbf{e}_{i-1}|\cos(\theta_i)}{2C}\right) \\
&\quad + 2e_{i,x}\phi_i\phi_{i+1}^2\left(2\frac{|\mathbf{e}_i|}{2C} - 3\frac{|\mathbf{e}_{i-1}|\cos(\theta_i)}{2C}\right) - 4e_{i,x}\left(\phi_{i+1}^3\frac{|\mathbf{e}_{i-1}|\cos(\theta_i)}{2C}\right) \\
&\quad - \frac{|\mathbf{e}_i|}{2C}\phi_{i+1}\left(5(e_{i,x} - e_{i-1,x})\phi_i^2 + \phi_i\phi_{i+1}\left(\left(20 - 18\frac{|\mathbf{e}_{i-1}|}{|\mathbf{e}_i|}\cos(\theta_i)\right)e_{i,x} - 10e_{i-1,x}\right)\right. \\
&\qquad \left. -12\frac{|\mathbf{e}_{i-1}|}{|\mathbf{e}_i|}\cos(\theta_i)e_{i,x}\phi_{i+1}^2\right) \\
&= \phi_i^3\left(e_{i,x}\frac{|\mathbf{e}_{i-1}|\cos(\theta_i)}{2C} + e_{i-1,x}\frac{|\mathbf{e}_i|}{2C}\right) + \phi_i^2\phi_{i+1}\left((5e_{i-1,x} - 2e_{i,x})\frac{|\mathbf{e}_i|}{2C} + 7e_{i,x}\frac{|\mathbf{e}_{i-1}|\cos(\theta_i)}{2C}\right) \\
&\quad + \phi_i\phi_{i+1}^2\left((10e_{i-1,x} - 8e_{i,x})\frac{|\mathbf{e}_i|}{2C} + 20e_{i,x}\frac{|\mathbf{e}_{i-1}|\cos(\theta_i)}{2C}\right) + \phi_{i+1}^3\left(8e_{i,x}\frac{|\mathbf{e}_{i-1}|\cos(\theta_i)}{2C}\right).
\end{aligned}$$

Now we use this result to compute the derivative of $\psi_{x,v}$:

$$\begin{aligned}
\left.\frac{\partial \psi_{x,i}}{\partial \mathbf{n}_i}\right|_{\mathbf{e}_i} &= \left.\left(2\phi_i \frac{\partial \phi_i}{\partial \mathbf{n}_i} Q + \phi_i^2 \frac{\partial Q}{\partial \mathbf{n}_i}\right)\right|_{\mathbf{e}_i} \\
&= 2\phi_i \left(\left(\frac{|\mathbf{e}_i|}{2C} - \frac{|\mathbf{e}_{i-1}|\cos(\theta_i)}{2C}\right)\phi_i - \frac{|\mathbf{e}_{i-1}|\cos(\theta_i)}{2C}\phi_{i+1}\right)\left(\phi_i^2(e_{i,x}\phi_{i+1}) + 4\phi_i(e_{i,x}\phi_{i+1}^2)\right) \\
&\quad + \phi_i^2\left(\left.\frac{\partial Q}{\partial \mathbf{n}_i}\right|_{\mathbf{e}_i}\right) \\
&= 2e_{i,x}\phi_i^2\phi_{i+1}\left(\phi_i^2\left(\frac{|\mathbf{e}_i|}{2C} - \frac{|\mathbf{e}_{i-1}|\cos(\theta_i)}{2C}\right) + \phi_i\phi_{i+1}\left(4\frac{|\mathbf{e}_i|}{2C} - 5\frac{|\mathbf{e}_{i-1}|\cos(\theta_i)}{2C}\right)\right. \\
&\qquad \left. -4\phi_{i+1}^2\left(\frac{|\mathbf{e}_{i-1}|\cos(\theta_i)}{2C}\right)\right) \\
&\quad + \phi_i^2\left(\phi_i^3\left(e_{i,x}\frac{|\mathbf{e}_{i-1}|\cos(\theta_i)}{2C} + e_{i-1,x}\frac{|\mathbf{e}_i|}{2C}\right)\right. \\
&\qquad + \phi_i^2\phi_{i+1}\left((5e_{i-1,x} - 2e_{i,x})\frac{|\mathbf{e}_i|}{2C} + 7e_{i,x}\frac{|\mathbf{e}_{i-1}|\cos(\theta_i)}{2C}\right) \\
&\qquad + \phi_i\phi_{i+1}^2\left((10e_{i-1,x} - 8e_{i,x})\frac{|\mathbf{e}_i|}{2C} + 20e_{i,x}\frac{|\mathbf{e}_{i-1}|\cos(\theta_i)}{2C}\right) \\
&\qquad \left. +\phi_{i+1}^3\left(8e_{i,x}\frac{|\mathbf{e}_{i-1}|\cos(\theta_i)}{2C}\right)\right) \\
&= \phi_i^5\left(e_{i,x}\frac{|\mathbf{e}_{i-1}|\cos(\theta_i)}{2C} + e_{i-1,x}\frac{|\mathbf{e}_i|}{2C}\right) \\
&+ \phi_i^4\phi_{i+1}\left(5e_{i-1,x}\frac{|\mathbf{e}_i|}{2C} + 5e_{i,x}\frac{|\mathbf{e}_{i-1}|\cos(\theta_i)}{2C}\right) \\
&+ \phi_i^3\phi_{i+1}^2\left(10e_{i-1,x}\frac{|\mathbf{e}_i|}{2C} + 10e_{i,x}\frac{|\mathbf{e}_{i-1}|\cos(\theta_i)}{2C}\right) \\
&= \left(e_{i,x}\frac{|\mathbf{e}_{i-1}|\cos(\theta_i)}{2C} + e_{i-1,x}\frac{|\mathbf{e}_i|}{2C}\right)(\phi_i^5 + 5\phi_i^4\phi_{i+1} + 10\phi_i^3\phi_{i+1}^2).
\end{aligned}$$

Similar calculations along $\mathbf{e}_{i-1}$ will show that

$$\left.\frac{\partial \psi_{x,i}}{\partial \mathbf{n}_{i-1}}\right|_{\mathbf{e}_{i-1}} = \left(-e_{i-1,x}\frac{|\mathbf{e}_i|\cos(\theta_i)}{2C} - e_{i,x}\frac{|\mathbf{e}_{i-1}|}{2C}\right)(\phi_i^5 + 5\phi_i^4\phi_{i-1} + 10\phi_i^3\phi_{i-1}^2).$$

Considering that $2C = |\mathbf{e}_i||\mathbf{e}_{i-1}|\sin(\theta_i)$ and the identities from (14), we can express these two derivatives in a form which is much more convenient for this particular calculation:

$$\begin{aligned}
\left.\frac{\partial \psi_{x,i}}{\partial \mathbf{n}_i}\right|_{\mathbf{e}_i} &= \left(\frac{e_{i,y}}{|\mathbf{e}_i|}\right)(\phi_i^5 + 5\phi_i^4\phi_{i+1} + 10\phi_i^3\phi_{i+1}^2), \\
\left.\frac{\partial \psi_{x,i}}{\partial \mathbf{n}_{i-1}}\right|_{\mathbf{e}_{i-1}} &= \left(\frac{e_{i-1,y}}{|\mathbf{e}_{i-1}|}\right)(\phi_i^5 + 5\phi_i^4\phi_{i-1} + 10\phi_i^3\phi_{i-1}^2).
\end{aligned}$$

Considering that $\mathbf{e}_{i,P_1} = \mathbf{e}_{i-1,P_2}$, $\phi_{i,P_1}|_{\mathbf{e}_{i,P_1}} = \phi_{i,P_2}|_{\mathbf{e}_{i-1,P_2}}$, and $\phi_{i+1,P_1}|_{\mathbf{e}_{i,P_1}} = \phi_{i-1,P_2}|_{\mathbf{e}_{i-1,P_2}}$, then it is immediately clear that

$$\left.\frac{\partial \psi_{x,i,P_1}}{\partial \mathbf{n}_{i,P_1}}\right|_{\mathbf{e}_{i,P_1}} + \left.\frac{\partial \psi_{x,i,P_2}}{\partial \mathbf{n}_{i-1,P_2}}\right|_{\mathbf{e}_{i-1,P_2}} = 0,$$

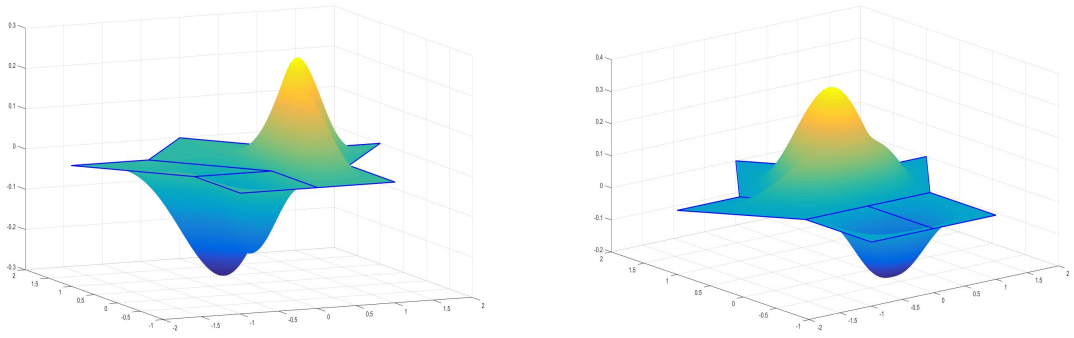

Figure 6: The plot of $\psi_{x,v}$ and $\psi_{y,v}$ over the partition shown on the right of Figure 1

which proves that $\psi_{x,v}$ is C^1 over the edges in Ω_v, the last remaining property we needed in order to prove that $\psi_{x,v} \in C^1(\Omega)$. This concludes the proof. □

Simply replacing x with y will yield $\psi_{y,i}$. We present their graphs and contour plots in Figure 6.

3.3 Hessian Interpolation Functions $\psi_{x^2,v}$, $\psi_{y^2,v}$, and $\psi_{xy,v}$

Next we extend our construction to build functions $\psi_{x^2,v}$, $\psi_{y^2,v}$, and $\psi_{xy,v} \in C^1(\Omega)$ that satisfy the following properties:

1. $\psi_{x^2,v}|_{w\in V} = \psi_{y^2,v}|_{w\in V} = \psi_{xy,v}|_{w\in V} = 0$
2. $\nabla\psi_{x^2,v}|_{w\in V} = \nabla\psi_{y^2,v}|_{w\in V} = \nabla\psi_{xy,v}|_{w\in V} = 0$
3. $\nabla^2\psi_{x^2,v}|_{w\in V} = \begin{bmatrix} \delta_{v,w} & 0 \\ 0 & 0 \end{bmatrix}$, $\nabla^2\psi_{y^2,v}|_{w\in V} = \begin{bmatrix} 0 & 0 \\ 0 & \delta_{v,w} \end{bmatrix}$, and $\nabla^2\psi_{xy,v}|_{w\in V} = \begin{bmatrix} 0 & \delta_{v,w} \\ \delta_{v,w} & 0 \end{bmatrix}$;
4. $\text{supp}(\psi_{x^2,v})$, $\text{supp}(\psi_{y^2,v})$, $\text{supp}(\psi_{xy,v}) \subseteq \Omega_v$;
5. $\sum_{v\in V} v_x^2\psi_v + 2v_x\psi_{x,v} + 2\psi_{x^2,v} = x^2$, $\sum_{v\in V} v_y^2\psi_v + 2v_y\psi_{y,v} + 2\psi_{y^2,v} = y^2$, and $\sum_{v\in V} v_xv_y\psi_v + v_y\psi_{x,v} + v_x\psi_{y,v} + \psi_{xy,v} = xy$.

For brevity, we shall suppress the computations as we did in the prior subsection.

$$\begin{aligned}
\psi_{x^2,i} = \frac{1}{2}\phi_i^2\Bigg(&\phi_i(e_{i,x}^2\phi_{i+1}^2 + e_{i-1,x}^2\phi_{i-1}^2) \quad + \phi_{i+2}\Bigg(- 2e_{i,x}e_{i-1,x}\phi_i^2 \\
&+ \phi_i\left(\left(5e_{i,x}^2\left(1 - \frac{|\mathbf{e}_{i-1}|}{|\mathbf{e}_i|}\cos(\theta_i)\right) - 4e_{i,x}e_{i-1,x}\right)\phi_{i+1}\right. \\
&\left. + \left(5e_{i-1,x}^2\left(1 - \frac{|\mathbf{e}_i|}{|\mathbf{e}_{i-1}|}\cos(\theta_i)\right) - 4e_{i,x}e_{i-1,x}\right)\phi_{i-1}\right) \\
&+ \left(e_{i,x}^2\frac{|\mathbf{e}_{i-1}|}{|\mathbf{e}_i|}\cos(\theta_i) + 4e_{i,x}e_{i-1,x}\right)\phi_{i+1}^2 + \left(e_{i-1,x}^2\frac{|\mathbf{e}_i|}{|\mathbf{e}_{i-1}|}\cos(\theta_i)\right. \\
&\left. + \ 4e_{i,x}e_{i-1,x}\right)\phi_{i-1}^2) + (10(e_{i,x}^2 + e_{i-1,x}^2) - 32e_{i,x}e_{i-1,x})\phi_i\phi_{i+2}^2\Bigg)
\end{aligned} \tag{15}$$

and

$$\psi_{xy,i} = \phi_i^2\Bigg(\phi_i(e_{i,x}e_{i,y}\phi_{i+1}^2 + e_{i-1,x}e_{i-1,y}\phi_{i-1}^2) + \phi_{i+2}\Bigg(- (e_{i,x}e_{i-1,y} + e_{i,y}e_{i-1,x})\phi_i^2$$
$$+ \phi_i\left(\left(5e_{i,x}e_{i,y}\left(1 - \frac{|\mathbf{e}_{i-1}|}{|\mathbf{e}_i|}\cos(\theta_i)\right) - 2(e_{i,x}e_{i-1,y} + e_{i,y}e_{i-1,x})\right)\phi_{i+1}\right.$$
$$\left. + \left(5e_{i-1,x}e_{i-1,y}\left(1 - \frac{|\mathbf{e}_i|}{|\mathbf{e}_{i-1}|}\cos(\theta_i)\right) - 2(e_{i,x}e_{i-1,y} + e_{i,y}e_{i-1,x})\right)\phi_{i-1}\right)$$
$$+ \left(e_{i,x}e_{i,y}\frac{|\mathbf{e}_{i-1}|}{|\mathbf{e}_i|}\cos(\theta_i) + 2(e_{i,x}e_{i-1,y} + e_{i,y}e_{i-1,x})\right)\phi_{i+1}^2$$
$$+ \left(e_{i-1,x}e_{i-1,y}\frac{|\mathbf{e}_i|}{|\mathbf{e}_{i-1}|}\cos(\theta_i) + 2(e_{i,x}e_{i-1,y} + e_{i,y}e_{i-1,x})\right)\phi_{i-1}^2\Bigg)$$
$$+ (10(e_{i,x}e_{i,y} + e_{i-1,x}e_{i-1,y}) - 16(e_{i,x}e_{i-1,y} + e_{i,y}e_{i-1,x}))\phi_i\phi_{i+2}^2\Bigg), \tag{16}$$

where replacing x with y in the expression of $\psi_{x^2,i}$ will yield $\psi_{y^2,i}$. Again, details can be found in [27], but the steps are again nearly identical to those shown in the construction of the functions ψ_v. Let us show their graphs and contour plots.

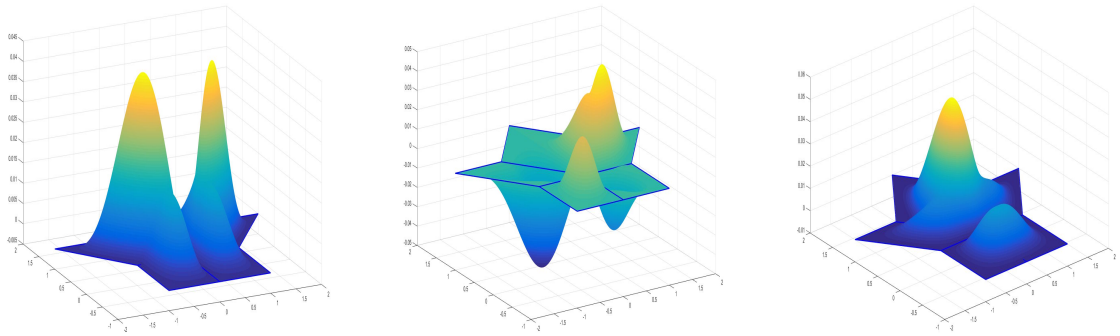

Figure 7: The plot of $\psi_{x^2,v}, \psi_{xy,v}, \psi_{y^2,v}$ over the partition shown on the right of Figure 1

3.4 A Quasi-Interpolatory Vertex Spline Operator

Let us explore how to use these vertex splines to construct a quasi-interpolatory operator. Given a function f that we wish to interpolate, we let $S_I(f)$ be the interpolatory function which satisfies

$$S_I(f)(v) = f(v),\ D_xS_I(f)(v) = f_x(v),\ D_yS_I(f)(v) = f_y(v),\ D_{xx}S_I(f)(v) = f_{xx}(v),$$
$$D_{xy}S_I(f)(v) = f_{xy}(v),\ D_{yy}S_I(f)(v) = f_{yy}(v), \tag{17}$$

for all vertex $v \in \mathcal{P}$. In fact, based on the previous subsections, S_I is given by

$$S_I(f) = \sum_{v\in\mathcal{P}} f(v)\psi_v + f_x(v)\psi_{x,v} + f_y(v)\psi_{y,v} + f_{xx}(v)\psi_{x^2,v} + f_{xy}(v)\psi_{xy,v} + f_{yy}(v)\psi_{y^2,v}. \tag{18}$$

We summarize the discussion above to conclude the following

Theorem 3 *Suppose that $f \in C^2(\Omega)$ and $\mathcal{P}$ be a partition of polynomial domain Ω consisting of parallelograms. Define $S_I(f)$ as in (18). Then $S_I(f)$ reproduces all polynomial functions of degree 2. That is, if $f \in \Pi_2$, the space of all quadratic polynomials, then $S_I(f) = f$.*

However, S_I is not sufficient to span all degree 5 polynomials. For example, it can be shown that

$$S_I(x^3) = \sum_{v \in \mathcal{P}} v_x^3 \psi_v + 3v_x^2 \psi_{x,v} + 6v_x \psi_{x^2,v} \neq x^3.$$

Within a single parallelogram P, we can express x^3 as a degree 5 Wachspress function by

$$x^3 = \left(\sum_{j=1}^{4} v_{j,x} \phi_j \right)^3 \left(\sum_{j=1}^{4} \phi_j \right)^2.$$

We can expand this expression and subtract $S_I(x^3)$, yielding a nonzero difference:

$$\begin{aligned} x^3\big|_P - S_I(x^3) =& B \sum_{j=1}^{4} 9\phi_j^2 \left(\phi_{j+1} e_{j,x}^2 \left(e_{j-1,x} + \frac{|e_{j-1}|}{|e_j|} \cos(\theta_j) e_{j,x} \right) \right. \\ & \left. - \phi_{j-1} e_{j-1,x}^2 \left(e_{j,x} + \frac{|e_j|}{|e_{j-1}|} \cos(\theta_j) e_{j-1,x} \right) \right) \\ & - 12B\phi_j (e_{j,x} - e_{j-1,x}) e_{j,x} e_{j-1,x}. \end{aligned} \tag{19}$$

Given the factor B, we see that there is no difference in value on the edges, but since only a single factor of B is present on the whole, we can see there is some difference in gradient on the edges. Since the values on the edges match, so must the derivatives in the directions of the edges. Next we will attempt to control the outward normal derivatives on each edge.

3.5 Edge Splines

We will construct *edge splines* over $\mathcal{P}$, which are supported on Ω_e, the union of two paralellograms sharing the edge e. While the vertex splines were built with the aim of controlling value, gradient, and Hessian at the vertices of a parallelogram P, edge splines will be built to control outward normal derivatives on the edges of P.

Let us focus on edge $\mathbf{e}_i$ of P. We must use degree 5 Wachspress monomials which do not affect values, gradients, or Hessians at the vertices, but do affect the outward normal derivative on $\mathbf{e}_i$. There are exactly two distinct such monomials: $\phi_i^2 \phi_{i+1}$ and $\phi_i \phi_{i+1}^2$. This gives us two degrees of freedom. We can control the outward normal derivative at two points on $\mathbf{e}_i$. We chose the points on $\mathbf{e}_i$ at which each monomial is maximized: $e_{i,i} := \frac{3}{5} v_i + \frac{2}{5} v_{i+1}$ and $e_{i,i+1} := \frac{2}{5} v_i + \frac{3}{5} v_{i+1}$, respectively.

Since these functions will be built with the intention of augmenting $S_I(f)$, we should first consider the outward normal derivative of $S_I(f)$ at points $e_{i,i}$ and $e_{i,i+1}$:

$$\begin{aligned} \left. \frac{\partial S_I(f)}{\partial \mathbf{n}_i} \right|_{e_{i,i}} &= 5^{-5} \mathbf{n}_i \left(\left(992 \nabla f^\top \big|_{v_{i+1}} + 2133 \nabla f^\top \big|_{v_i} \right) + 6 \left(39 \nabla^2 f \big|_{v_i} + 4 \nabla^2 f \big|_{v_{i+1}} \right) \mathbf{e}_i^\top \right); \\ \left. \frac{\partial S_I(f)}{\partial \mathbf{n}_i} \right|_{e_{i,i+1}} &= 5^{-5} \mathbf{n}_i \left(\left(992 \nabla f^\top \big|_{v_i} + 2133 \nabla f^\top \big|_{v_{i+1}} \right) - 6 \left(39 \nabla^2 f \big|_{v_{i+1}} + 4 \nabla^2 f \big|_{v_i} \right) \mathbf{e}_i^\top \right). \end{aligned}$$

For each interior edge, we can define two edge splines $\psi_{\mathbf{e}_i,1}$ and $\psi_{\mathbf{e}_i,2}$, each of which is supported over two parallelograms sharing edge $\mathbf{e}_i$ as follows:

$$\psi_{\mathbf{e}_i,1}^P = \phi_i^3 \phi_{i+1} \phi_{i+2} = B \phi_i^2 \phi_{i+1}, \text{ and } \psi_{\mathbf{e}_i,2}^P = \phi_i^2 \phi_{i+1}^2 \phi_{i+2} = B \phi_i \phi_{i+1}^2. \tag{20}$$

Denote by R the parallelogram which shares edge $\mathbf{e}_i$ with P, and without loss of generality assume that this edge is $\mathbf{e}_{i-1}$ with respect to R, so that $v_i^P = v_i^R$ and $v_{i+1}^P = v_{i-1}^R$. Define the functions

$$\psi_e(f)(\mathbf{x}) = \begin{cases} \psi_{e,i}^P(f)(\mathbf{x}), & x \in P, \\ \psi_{e,i-1}^R(f)(\mathbf{x}), & x \in R, \end{cases}$$
$$\psi_{e,i}^P(f) = B_P \phi_i^P \phi_{i+1}^P (K_{1,i}^P(f)\phi_i^P + K_{3,i}^P(f)\phi_{i+1}^P); \psi_{e,i-1}^R(f) = B_R \phi_i^R \phi_{i-1}^R (K_{2,i}^R(f)\phi_i^R + K_{4,i}^R(f)\phi_{i-1}^R)$$

for constants $K_{1,i}^P(f)$, $K_{2,i}^R(f)$, $K_{3,i}^P(f)$, and $K_{4,i}^R(f)$ which depend on the function f, where B_P and B_R are the bubble functions with respect to P and R. To determine these constants, we shall compute the normal derivative of $\psi_{e,i}^P(f)$ at the points $e_{i,i}^P$ and $e_{i,i+1}^P$:

$$\left.\frac{\partial \psi_{e,i}^P(f)}{\partial \mathbf{n}_i^P}\right|_{e_{i,i}^P} = -\frac{18|\mathbf{e}_i^P|}{5^5 C_P}(3K_{1,i}^P(f) + 2K_{3,i}^P(f)); \left.\frac{\partial \psi_{e,i}^P(f)}{\partial \mathbf{n}_i^P}\right|_{e_{i,i+1}^P} = -\frac{18|\mathbf{e}_i^P|}{5^5 C_P}(2K_{1,i}^P(f) + 3K_{3,i}^P(f)). \quad (21)$$

Our goal is to ensure the following:

$$\left.\frac{\partial \psi_{e,i}^P(f)}{\partial \mathbf{n}_i^P}\right|_{e_{i,i}^P} = \left(\frac{\partial f}{\partial \mathbf{n}_i^P} - \frac{\partial S_I(f)}{\partial \mathbf{n}_i^P}\right)\Big|_{e_{i,i}^P}, \text{ and } \left.\frac{\partial \psi_{e,i}^P(f)}{\partial \mathbf{n}_i^P}\right|_{e_{i,i+1}^P} = \left(\frac{\partial f}{\partial \mathbf{n}_i^P} - \frac{\partial S_I(f)}{\partial \mathbf{n}_i^P}\right)\Big|_{e_{i,i+1}^P}.$$

By (21) we require that

$$3K_{1,i}^P(f) + 2K_{3,i}^P(f) = \frac{5^5 C_P}{18|\mathbf{e}_i^P|}\left(\frac{\partial S_I(f)}{\partial \mathbf{n}_i^P} - \frac{\partial f}{\partial \mathbf{n}_i^P}\right)\Big|_{e_{i,i}^P} \text{ and}$$
$$2K_{1,i}^P(f) + 3K_{3,i}^P(f) = \frac{5^5 C_P}{18|\mathbf{e}_i^P|}\left(\frac{\partial S_I(f)}{\partial \mathbf{n}_i^P} - \frac{\partial f}{\partial \mathbf{n}_i^P}\right)\Big|_{e_{i,i+1}^P}.$$

Solving the linear system above and expanding leads to the solutions

$$K_{1,i}^P(f) = \frac{C_P}{18|\mathbf{e}_i^P|}\left(\mathbf{n}_i^P \cdot \left(\left(883\nabla f\big|_{v_i^P} - 258\nabla f\big|_{v_{i+1}^P}\right) + 6\left(25\nabla^2 f\big|_{v_i^P} + 18\nabla^2 f\big|_{v_{i+1}^P}\right)(\mathbf{e}_i^P)^\top\right)\right.$$
$$\left. + 5^4\left(2\frac{\partial f}{\partial \mathbf{n}_i^P}\Big|_{e_{i,i+1}^P} - 3\frac{\partial f}{\partial \mathbf{n}_i^P}\Big|_{e_{i,i}^P}\right)\right), \text{ and}$$
$$K_{3,i}^P(f) = \frac{C_P}{18|\mathbf{e}_i^P|}\left(\mathbf{n}_i^P \cdot \left(\left(883\nabla f\big|_{v_{i+1}^P} - 258\nabla f\big|_{v_i^P}\right) - 6\left(25\nabla^2 f\big|_{v_{i+1}^P} + 18\nabla^2 f\big|_{v_i^P}\right)(\mathbf{e}_i^P)^\top\right)\right.$$
$$\left. + 5^4\left(2\frac{\partial f}{\partial \mathbf{n}_i^P}\Big|_{e_{i,i}^P} - 3\frac{\partial f}{\partial \mathbf{n}_i^P}\Big|_{e_{i,i+1}^P}\right)\right).$$

Similarly, we must set

$$K_{2,i}^R(f) = \frac{C_R}{18|\mathbf{e}_{i-1}^R|}\left(\mathbf{n}_{i-1}^R \cdot \left(\left(883\nabla f\big|_{v_i^R} - 258\nabla f\big|_{v_{i-1}^R}\right) - 6\left(25\nabla^2 f\big|_{v_i^R} + 18\nabla^2 f\big|_{v_{i-1}^R}\right)(\mathbf{e}_{i-1}^R)^\top\right)\right.$$
$$\left. + 5^4\left(2\frac{\partial f}{\partial \mathbf{n}_{i-1}^R}\Big|_{e_{i-1,i-1}^R} - 3\frac{\partial f}{\partial \mathbf{n}_{i-1}^R}\Big|_{\mathbf{e}_{i-1,i}^R}\right)\right), \text{ and}$$
$$K_{4,i}^R(f) = \frac{C_R}{18|\mathbf{e}_{i-1}^R|}\left(\mathbf{n}_{i-1}^R \cdot \left(\left(883\nabla f\big|_{v_{i-1}^R} - 258\nabla f\big|_{v_i^R}\right) + 6\left(25\nabla^2 f\big|_{v_{i-1}^R} + 18\nabla^2 f\big|_{v_i^R}\right)(\mathbf{e}_{i-1}^R)^\top\right)\right.$$
$$\left. + 5^4\left(2\frac{\partial f}{\partial \mathbf{n}_{i-1}^R}\Big|_{e_{i-1,i}^R} - 3\frac{\partial f}{\partial \mathbf{n}_{i-1}^R}\Big|_{e_{i-1,i-1}^R}\right)\right).$$

Since the functions $\psi^P_{e,i}$ and $\psi^R_{e,i-1}$ are both valued zero on the shared edge, we know that $\psi_e(f)$ must be at least C^0 on the shared edge, but we need $\psi_e(f)$ to be C^1. We know that $\psi^P_{e,i}$ and $\psi^R_{e,i-1}$ share derivatives of 0 along the shared-edge direction $\mathbf{e}_i$, but we must ensure that the normal derivative values are the same at all points on the shared edge, not just at the points $v^P_i = v^R_i$, $v^P_{i+1} = v^R_{i-1}$, $e^P_{i,i} = e^R_{i-1,i}$ and $e^P_{i,i+1} = e^R_{i-1,i-1}$. In fact, if we take the normal derivatives of $\psi^P_{e,i}(f)$ and $\psi^R_{e,i-1}(f)$ on the shared edge, we retrieve the following:

$$\left.\frac{\partial \psi^P_{e,i}(f)}{\partial \mathbf{n}^P_i}\right|_{\mathbf{e}^P_i} = -\left(\phi^P_i \phi^P_{i+1}\right)^2 \left(K^P_{1,i}\phi^P_i + K^P_{3,i}\phi^P_{i+1}\right) \frac{|\mathbf{e}^P_i|}{2C_P}, \text{ and}$$

$$\left.\frac{\partial \psi^R_{e,i-1}(f)}{\partial \mathbf{n}^R_{i-1}}\right|_{\mathbf{e}^R_{i-1}} = -\left(\phi^R_i \phi^R_{i-1}\right)^2 \left(K^R_{2,i}\phi^R_i + K^R_{4,i}\phi^R_{i-1}\right) \frac{|\mathbf{e}^R_{i-1}|}{2C_R}.$$

We need these to sum to zero, and taking into account that $\phi^P_i = \phi^R_i$, $\phi^P_{i+1} = \phi^R_{i-1}$, and ${\mathbf{e}_i}^P = -{\mathbf{e}_{i-1}}^R$ we retrieve that

$$\left.\frac{\partial \psi^P_{e,i}(f)}{\partial \mathbf{n}^P_i}\right|_{\mathbf{e}^P_i} + \left.\frac{\partial \psi^R_{e,i-1}(f)}{\partial \mathbf{n}^R_{i-1}}\right|_{e^R_{i-1}} = |\mathbf{e}^P_i| \left(\phi^P_i \phi^P_{i+1}\right)^2 \left(\left(\frac{K^P_{1,i}}{2C_P} + \frac{K^R_{2,i}}{2C_R}\right)\phi^P_i + \left(\frac{K^P_{3,i}}{2C_P} + \frac{K^R_{4,i}}{2C_R}\right)\phi^P_{i+1}\right),$$

which will be zero exactly when

$$\frac{K^P_{1,i}}{C_P} = \frac{-K^R_{2,i}}{C_R} \text{ and } \frac{K^P_{3,i}}{C_P} = \frac{-K^R_{4,i}}{C_R}. \tag{22}$$

Since $\mathbf{n}^P_i = -\mathbf{n}^R_{i-1}$, ${\mathbf{e}_i}^P = -{\mathbf{e}_{i-1}}^R$, $e^P_{i,i} = e^R_{i-1,i}$, and $e^P_{i,i+1} = e^R_{i-1,i-1}$, this is easy to see from the definitions of the four coefficients that (22) holds.

Our goal for these edge splines was to increase our polynomial span, so we will define another interpolatory function $S_E(f)$ by

$$S_E(f) = S_I(f) + \sum_{e\in\mathcal{P}} \psi_e(f). \tag{23}$$

Restricted within a parallelogram P, it is easy to see that we still have more work to do: since $\psi^P_{e,i}(f)$ doesn't contain a factor of B^2 for any i, then the difference $x^3|_P - S_E(f)|_P$ cannot be zero, since the result in (19) contains terms with a factor of B^2. However, we are in good shape:

$$x^3\big|_P - S_E(x^3)\big|_P = x^3\big|_P - S_I(x^3)\big|_P - \sum_{e\in\mathcal{P}} \psi^P_{e,i}(x^3),$$

and a lengthy simplification shows that

$$\sum_{e\in\mathcal{P}} \psi^P_{e,i}(x^3) = 9B\sum_{j=1}^{4} \phi^2_j \left(\phi_{j+1} e^2_{j,x}\left(e_{j-1,x} + \frac{|\mathbf{e}_{j-1}|}{|\mathbf{e}_j|}\cos(\theta_j) e_{j,x}\right) - \phi_{j-1} e^2_{j-1,x}\left(e_{j,x} + \frac{|\mathbf{e}_j|}{|\mathbf{e}_{j-1}|}\cos(\theta_j) e_{j-1,x}\right)\right),$$

which we combine with the result in (19) to see that

$$x^3\big|_P - S_E(x^3)\big|_P = -\sum_{j=1}^{4} 12B^2 \phi_j (e_{j,x} - e_{j-1,x}) e_{j,x} e_{j-1,x}.$$

Now we have the values and gradients of our interpolant matching on all the edges of P, but there remain differences in some values on the interior. We will create one more class of spline, *face splines* to be constructed in the following subsection.

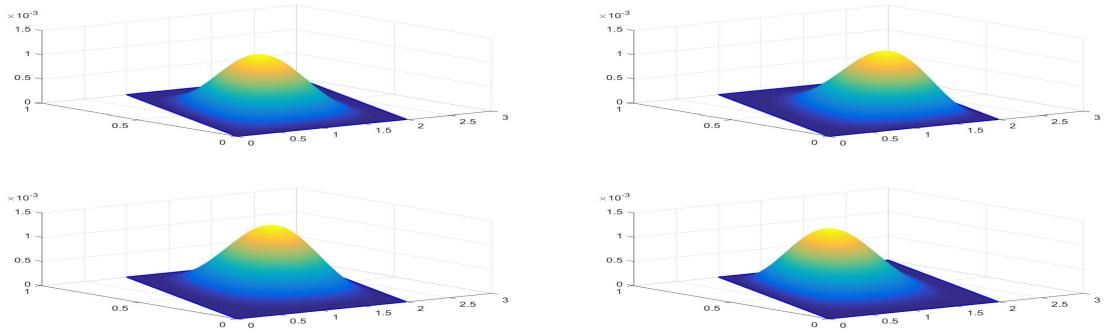

Figure 8: The plot of $\psi_{F,i}, i = 1, 2, 3, 4$

3.6 Face Splines

Face splines are those splines functions which are supported only within a quadrilateral. Within a single parallelogram P, we define the following functions for $i = 1, 2, 3, 4$:

$$\psi_{F,i}^P = \phi_i^3 \phi_{i+2}^2 = B^2 \phi_i.$$

Then the interpolatory face spline of a function f over P is defined by

$$\psi_F^P = \sum_{i=1}^{4} S_i^P(f) \psi_{F,i}^P \tag{24}$$

for some constants $S_i^P(f)$ depending on the function f. The graphs of these four functions $\psi_{F,i}^P, i = 1, 2, 3, 4$ supported over one parallelogram are shown in Fig. 8.

We'll determine the constants $S_i^P(f)$ using values of f at four points on the interior of P; we will choose the points which maximize the values of each function $\psi_{F,i}^P$. Simple calculus combined with some parallelogram geometry provides that, for each i, the point

$$p_i^P = \frac{1}{25}(9v_i^P + 6v_{i+1}^P + 6v_{i-1}^P + 4v_{i+2}^P) = \frac{3}{5}v_i^P + \frac{2}{5}v_{i+2}^P$$

is the one which maximizes $\psi_{F,i}^P$ for each i. A relatively simple evaluation gives the following values of $\psi_{F_i}^P$ at each point p_j^P:

$$\psi_{F,i}^P|_{p_i^P} = \frac{3^6 2^4}{5^{10}}; \psi_{F,i}^P|_{p_{i+1}^P} = \frac{3^5 2^5}{5^{10}}; \psi_{F,i}^P|_{p_{i-1}^P} = \frac{3^5 2^5}{5^{10}}; \psi_{F,i}^P|_{p_{i+2}^P} = \frac{3^4 2^6}{5^{10}}.$$

Then, for each i, we have

$$\psi_F^P|_{p_i^P} = \frac{3^4 2^4}{5^{10}}(9S_i^P(f) + 6(S_{i+1}^P(f) + S_{i-1}^P(f)) + 4S_{i+2}^P(f)).$$

We aim to construct a new interpolatory function $S_F(f)$ by

$$S_F(f) = S_E(f) + \sum_{P \in \mathcal{P}} \psi_F^P,$$

so for each P and $i = 1, 2, 3, 4$, we need $\psi_F^P\big|_{p_i^P} = (f - S_E(f))\big|_{p_i^P}$.

Then we can solve for the coefficients $S_i^P(f)$ by the following linear system:

$$\frac{3^4\ 2^4}{5^{10}} \begin{pmatrix} 9 & 6 & 4 & 6 \\ 6 & 9 & 6 & 4 \\ 4 & 6 & 9 & 6 \\ 6 & 4 & 6 & 9 \end{pmatrix} \begin{pmatrix} S_1^P(f) \\ S_2^P(f) \\ S_3^P(f) \\ S_4^P(f) \end{pmatrix} = \begin{pmatrix} (f - S_E(f))\big|_{p_1^P} \\ (f - S_E(f))\big|_{p_2^P} \\ (f - S_E(f))\big|_{p_3^P} \\ (f - S_E(f))\big|_{p_4^P} \end{pmatrix} \tag{25}$$

While it might be preferable to compute some closed form of $S_E(f)|_{p_i^P}$ (and, indeed, it can be done), the expression is perhaps best described as abominable. Instead, since the linear system above can be solved using only the values of $S_E(f)$, in practice it has been both easier and computationally faster to simply build $S_E(f)$ in full as an intermediate step in the construction of $S_F(f)$, and then evaluate $S_E(f)$ at the relevant points for each $P \in \mathcal{P}$.

3.7 Quasi-Interpolatory Operators based on Degree-5 Polygonal Splines

Let us explore how to use these vertex, edge, and face splines to construct quasi-interpolatory operators. Given a function f that we wish to interpolate, we recall $S_I(f)$ from (18), which is the interpolatory function satisfying

$$\begin{aligned} &S_I(f)(v) = f(v),\ D_x S_I(f)(v) = f_x(v),\ D_y S_I(f)(v) = f_y(v),\ D_{xx} S_I(f)(v) = f_{xx}(v), \\ &D_{xy} S_I(f)(v) = f_{xy}(v),\ D_{yy} S_I(f)(v) = f_{yy}(v), \end{aligned} \tag{26}$$

for all vertices $v \in \mathcal{P}$.

Next we define a new interpolant. Recall that over each parallelogram $P \in \mathcal{P}$, we have defined $\psi_e^P(f)$ for all edges $e \in P$ before. Now let

$$S_E(f)(\mathbf{x}) = S_I(f)(\mathbf{x}) + \sum_{e \in E} \psi_e(f)(\mathbf{x}) \tag{27}$$

Then the following theorem holds by construction:

Theorem 4 *For a sufficiently differentiable function f, we define $S_I(f)|_P = S^P(f), \forall P \in \mathcal{P}$ and $\psi_e(f)$ as above for each edge $e \in E$. Then the function $S_E(f)$ defined in (27) is in $C^1(\Omega)$, and satisfies the following five properties:*

$$\begin{aligned} &\textit{(i)} S_E(f)(v) = f(v), \qquad \textit{(ii)}\ \nabla S_E(f)(v) = \nabla f(v), \qquad \textit{(iii)}\ \nabla^2 S_E(f)(v) = \nabla^2 f(v), \\ &\textit{(iv)}\ \frac{\partial}{\partial n_e} S_E(f)(e_1) = \frac{\partial}{\partial n_e} f(e_1), \quad \textit{(v)}\ \frac{\partial}{\partial n_e} S_E(f)(e_2) = \frac{\partial}{\partial n_e} f(e_2), \end{aligned}$$

for all vertices v and edges e in $\mathcal{P}$, where n_e is the normal direction to e, and e_1 and e_2 are the points $\frac{2}{5}$ and $\frac{3}{5}$ of the way along the edge e.

Proof. (i), (ii), and (iii) follow by the properties of $S_I(f)$ and the fact that within any parallelogram P, for any value $i = 1, 2, 3, 4$, the functions $\psi_{e,i}^P$ have value, gradient, and Hessian of zero at each vertex $v \in P$, which implies that the same is true for each function $\psi_e(f)$ at all vertices.
(iv) and (v) follow from the construction of the edge splines $\psi_e(f)$. □

Since the face splines of P have no value, gradient, or Hessian on the edges of P, we do not need to be concerned with C^1 smoothness when analyzing them. We need only find how to use them for quasi-interpolation. We will use these to interpolate values at some points on the interior of each parallelogram. For a given parallelogram P, the function $\psi^P_{F,i}$ is maximized at the point $p_i = (9v_i + 6v_{i+1} + 4v_{i+2} + 6v_{i-1})/25$ for $i = 1, 2, 3, 4$; these will be the points at which we interpolate values. For a given function f, define the new interpolant over P by

$$S^P_5(f) = S_E(f)|_P + \sum_{i=1}^{4} S^P_i(f)\psi^P_{F,i},$$

so we need to determine the coefficients $S^P_i(f)$ such that $S^P_5(f)|_{p_i} = f|_{p_i}$ for $i = 1, 2, 3, 4$. We simply evaluate $S_E(f)$ at each point p_i and solve the linear system given by

$$\sum_{i=1}^{4} S^P_i(f)\psi_{P,i}(p_j) = f(p_j) - S_E(f)(p_j), j = 1, 2, 3, 4. \tag{28}$$

which has a unique solution $S^P_i(f), i = 1, 2, 3, 4$.

We now summarize the discussion above in the following theorem:

Theorem 5 *Given a sufficiently differentiable function f, compute $S_e(f)$ and solve the linear system given in (28) over each parallelogram $P \in \mathcal{P}$ for the coefficients $S^P_i(f), i = 1, 2, 3, 4$. Then the function*

$$S_5(f) := S_I(f) + \sum_{e\in E} \psi_e(f)(\mathbf{x}) + \sum_{P\in\mathcal{P}} \sum_{i=1}^{4} S^P_i(f)\psi_{P,i}, \tag{29}$$

satisfies all 5 properties listed in Theorem 4 along with the following interpolatory property that

$$S_5(f)(p^P_i) = f(p^P_i),\ i = 1, 2, 3, 4$$

for every $P \in \mathcal{P}$.

Proof. At each vertex in a given parallelogram P, the face splines $S^P_i(f)$ are valueless with gradient and Hessian 0. All the functions $S^P_i(f)$ also have value and gradient 0 along the edges, so satisfaction of the properties. Altogether, this means that addition of the face splines does not affect satisfaction of any of the 5 properties listed in Theorem 4. The additional interpolation property listed in this Theorem follows by construction of the face splines. □

Next we explain the approximation property of the quasi-interpolatory spline $S_5(f)$ in (29). First we can easily see that $S_5(f)$ is able to reproduce all polynomials of degree ≤ 5 by the constructions of these vertex splines as well as the edge splines and face splines.

Theorem 6 *Let Ψ_V be the collection of all the vertex splines $\psi_v, \psi_{x,v}, \psi_{y,v}, \psi_{x^2,v}, \psi_{xy,v}, \psi_{y^2,v}$ for each vertex v of $\mathcal{P}$. Let Ψ_E be the collection of all the edge splines $\psi_{e,1}$ and $\psi_{e,2}$ for edges e of $\mathcal{P}$. Let Ψ_P be the collection of all the parallelogram splines $\psi_{P,1}, \psi_{P,2}, \psi_{P,3}, \psi_{P,4}$ for parallelograms P of $\mathcal{P}$. Then $span(\Psi_V)\oplus span(\Psi_E)\oplus span(\Psi_P) \supseteq \Pi_5$, where Π_5 is the space of all bivariate polynomials of degree 5 or less. In particular, $S_5(p) = p$ for any polynomial $p \in \Pi_5$.*

Proof. We have already seen that $S_5(p) = p$ for all the standard polynomial basis functions p up to degree 2 - in fact, $S_I(p) = p$ for polynomials p up to degree 2. Using a computer algebra program (e.g.

Mathematica) will show that $S_5(p) = p$ for degree 3, 4, and 5 monomials, most easily achieved by the following scheme:

First, expand the degree-5 Wachspress polynomial expression of the monomial, limited to a single parallelogram P. Using xy^3 as an example degree-4 function, write

$$p = xy^3 = (x)(y)^3(1) = \left(\sum_{i=1}^{4} v_{i,x}\phi_i\right)\left(\sum_{i=1}^{4} v_{i,y}\phi_i\right)^3\left(\sum_{i=1}^{4}\phi_i\right).$$

Next, compute the symbolic expansion of the interpolant $S_5(p)|_P$. It is helpful to collect like terms at this point.

Finally, take the difference $(S_5(p)-p)|_P$, and again simplify and collect like terms. Each coefficient (depending on order of simplification and assumption application, likely a lengthy geometrically-linked term at this point) can be simplified to zero, so that $S_5(p) = p$ on every parallelogram P. □

3.8 Approximation Properties and Numerical Results

Let $\mathcal{P}$ be a collection of parallelograms and let $\mathcal{P}_k$ be the kth uniform refinement of $\mathcal{P}_{k-1}$ with $\mathcal{P}_0 = \mathcal{P}$. Then $\mathcal{P}_k$ is quasi-uniform in the sense that the ratio of the largest edge length over the smallest edge length is bounded. Also, the interior angles of $\mathcal{P}_k$ are bounded from above and from below in the sense that when $k \to \infty$, the smallest interior angle of $\mathcal{P}_k$ will not go to zero and the largest will not go to π. Define $\mathcal{S}_5(\mathcal{P})$ to be the span of all vertex splines we constructed in the previous subsections. That is, where V is the collection of all vertices in $\mathcal{P}$ and $\mathcal{E}$ is the collection of all edges of $\mathcal{P}$, we define

$$\mathcal{S}_5(\mathcal{P}) = \text{span}(\Psi_V) \oplus \text{span}(\Psi_E) \oplus \text{span}(\Psi_P), \tag{30}$$

and similarly define $\mathcal{S}_5(\mathcal{P}_k)$ as the analogous spline space over the kth refinement $\mathcal{P}_k$. For the interpolatory operator $S_I(f) \in \mathcal{S}_5(\mathcal{P})$, we let $S_{I,k}(f) \in \mathcal{S}_5(\mathcal{P}_k)$ be the interpolatory spline in $\mathcal{S}_5(\mathcal{P}_k)$.

One can show the following:

Theorem 7 *Let Ω be the union of all parallelograms in $\mathcal{P}$. For any $f \in C^5(\Omega)$, the quasi-interpolant $S_{I,k}(f) \in \mathcal{S}_5(\mathcal{P}_k)$ satisfies*

$$\|f - S_{I,k}(f)\|_{\infty,\Omega} \le C_1|f|_{3,\infty,\Omega}2^{-3k} + C_2|f|_{4,\infty,\Omega}2^{-4k} + C_3|f|_{5,\infty,\Omega}2^{-5k}, \tag{31}$$

where C_1, C_2, and C_3 are positive constants independent of f. Furthermore,

$$\|\nabla f - \nabla S_{I,k}(f)\|_{\infty,\Omega} \le C_1|f|_{3,\infty,\Omega}2^{-2k} + C_2|f|_{4,\infty,\Omega}2^{-3k} + C_3|f|_{5,\infty,\Omega}2^{-4k} \tag{32}$$

for all $f \in C^5(\Omega)$.

To prove the results above, we need a preparatory lemma.

Lemma 2 *Suppose that the partition $\mathcal{P}$ is quasi-uniform, that is, there exists a $\beta \ge 1$ such that the ratio of the longest edge length and shortest edge length of each parallelogram $P \in \mathcal{P}$ is bounded by β. Then the maximum norms of $\psi_v, \psi_{x,v}, \psi_{y,v}, \psi_{x^2,v}, \psi_{xy,v}, \psi_{y^2,v}$ have the following estimates:*

$$\begin{aligned}&\|\psi_v\|_{\infty,\mathcal{P}} \le C, \|\psi_{x,v}\|_{\infty,\mathcal{P}} \le C|\mathcal{P}|, \|\psi_{y,v}\|_{\infty,\mathcal{P}} \le C|\mathcal{P}|,\\ &\|\psi_{x^2,v}\|_{\infty,\mathcal{P}} \le C|\mathcal{P}|^2, \|\psi_{xy,v}\|_{\infty,\mathcal{P}} \le C|\mathcal{P}|^2, \|\psi_{y^2,v}\|_{\infty,\mathcal{P}} \le C|\mathcal{P}|^2\end{aligned} \tag{33}$$

for a positive constant C independent of the partition $\mathcal{P}$, where $|\mathcal{P}|$ stands for the size of $\mathcal{P}$ which is the largest edge length of $\mathcal{P}$. Similarly, we have

$$\|\nabla\psi_v\|_{\infty,\mathcal{P}} \le C_*/|\mathcal{P}|, \|\nabla\psi_{x,v}\|_{\infty,\mathcal{P}} \le C_*, \|\nabla\psi_{y,v}\|_{\infty,\mathcal{P}} \le C_*|\mathcal{P}|,$$
$$\|\nabla\psi_{x^2,v}\|_{\infty,\mathcal{P}} \le C_*|\mathcal{P}|^2, \|\nabla\psi_{xy,v}\|_{\infty,\mathcal{P}} \le C_*|\mathcal{P}|^2, \|\nabla\psi_{y^2,v}\|_{\infty,\mathcal{P}} \le C_*|\mathcal{P}|^2, \tag{34}$$

for a positive constant C_* dependent on the minimal angle at four corners of each parallelogram P for all $P \in \mathcal{P}$ and the quasi-uniformality $\gamma_{\mathcal{P}} = \max_{P\in\mathcal{P}} \dfrac{|P|}{\rho_P}$.

Proof. It is easy to see from the explicit representation that ψ_v is bounded in the maximum norm because all the GBC functions ϕ_i are bounded and the coefficients are fixed values which can be seen from (9). Similarly, from (10), we can see that the coefficients of $\psi_{x,v}$ contain $e_{i,x}$ or $e_{i,y}$ and other similar terms. It is easy to see that $|e_{i,x}| \le |P|$ and hence, $\|\psi_{x,v}\|_\infty \le C|P|$. Similar for the other terms to be estimated. This establishes (33).

Next we bound the gradients of the Wachspress coordinates. Fortunately, it has been shown in [15] that

$$\sup_{\mathbf{x}\in P} \sum_{j=1}^{n} ||\nabla\phi_j(\mathbf{x})||_2 \le \frac{4}{h_*}, \tag{35}$$

where h^* is the shortest perpendicular distance from any vertex of P to a non-incident edge of P (cf. [15] and [25]. It is easy to see that $|P|/h_*$ is dependent on the minimum value of the angles at four corners of P. So $\|\nabla\psi_v\|_{\infty,\Omega} = \|\nabla\psi_v\|_{\infty,P_\infty} = C\frac{4}{h_*} \le \frac{4C}{|P_\infty|}\frac{|P_\infty|}{h_*} \le C_*/|\mathcal{P}|$ as the partition $\mathcal{P}$ is assumed to be quasi-uniform, where C is the largest coefficient in absolute value in the formula (9). Similar for other terms and hence, we finish the proof for (34). □

Proof.[Proof of Theorem 7] Given the locality of each vertex spline and reproduction of all quadratic polynomials, we can use the same technique in [26] to establish the proof. Indeed, let $P_0 \in \mathcal{P}_k$ be a parallelogram such that $\|f - S_{I,k}(f)\|_{\infty,\Omega} = \|f - S_{I,k}(f)\|_{\infty,P_0}$ for a fixed integer $k \ge 1$. Let $(x_0, y_0) \in P_0$ be the center of P_0. We use the Taylor polynomial p_f of degree 2 of f at (x_0, y_0) with remainder $R_3(f)$ which involves the 3rd order derivatives of f. We recall the following formula for the exact remainder of the classical Taylor polynomial p_f of degree d:

$$\begin{aligned} R_{d+1}(f) &= f(x,y) - p_f(x,y) \\ &= (d+1) \sum_{\alpha+\beta=d+1} \frac{(x-u)^\alpha (y-v)^\beta}{\alpha!\beta!} \int_0^1 D_1^\alpha D_2^\beta f((x,y) + t(u-x, v-y)) t^d dt, \end{aligned} \tag{36}$$

where the differential operators D_1 and D_2 denote differentiation with respect to the first and second variables, respectively. Since $f = p_f + R_3(f)$,

$$\|f - S_{I,k}(f)\|_{\infty,P_0} \le \|p_f - S_{I,k}(p_f)\|_{\infty,P_0} + \|R_3(f) - S_{I,k}(R_3(f))\|_{\infty,P_0}.$$

By Theorem 6, we have $\|p_f - S_{I,k}(p_f)\|_{\infty,P_0} = 0$ and

$$\|f - S_{I,k}(f)\|_{\infty,P_0} \le \|R_3(f) - S_{I,k}(R_3(f))\|_{\infty,P_0} \le \|R_3(f)\|_{\infty,P_0} + \|S_{I,k}(R_3(f))\|_{\infty,P_0}.$$

It is easy to see $\|R_3(f)\|_{\infty,P_0} \le C|P_0|^3$ for a positive constant dependent only on f; in fact, the maximum norm of the 3rd derivatives of f over P_0 with the size $|P_0| \le |\mathcal{P}|/2^k$. The last term in the

above equation is divided into three sub-terms:

$$\begin{aligned}\|S_{I,k}(R_3(f))\|_{\infty,P_0} \leq & \|\sum_{v\in\mathcal{P}_k} R_3(f)(v)\psi_v\|_{\infty,P_0} + \|\sum_{v\in\mathcal{P}_k} R_3(f)_x(v)\psi_{x,v} + R_3(f)_y(v)\psi_{y,v}\|_{\infty,P_0} \\ & + \|\sum_{v\in\mathcal{P}_k} R_3(f)_{xx}(v)\psi_{x^2,v} + R_3(f)_{xy}(v)\psi_{xy,v} + R_3(f)_{yy}(v)\psi_{y^2,v}\|_{\infty,P_0}.\end{aligned}$$

Let us begin with the first term on the right-hand side of the inequality above. From the formula (36) for remainder $R_3(f)$ and the boundedness of ψ_v, we have $\|R_3(f)\psi_v\|_{\infty,P_0} \leq |R_3(f)(v)|\|\psi_v\|_\infty \leq C|P_0|^3 \leq C2^{-3k}$, where $C > 0$ stands for a positive constant (which may not be the same constant in each occurrence), and we have used one of the estimates in Lemma 2. For the second term on the right-hand side, we need to estimate $\|R_3(f)_x(v)\psi_{x,v}\|_\infty$. We have to use the product rule of derivatives to have $|R_3(f)_x(v)| \leq C|f|_{3,\infty}|P_0|^2 + C|f|_{4,\infty}|P_0|^3$ and hence,

$$\|R_3(f)_x(v)\psi_{x,v}\|_\infty \leq C|f|_{3,\infty}|P_0|^3 + C|f|_{4,\infty}|P_0|^4 = C|f|_{3,\infty}2^{-3k} + C|f|_{4,\infty}2^{-4k}.$$

Similar calculations for the other terms on the right-hand side of the inequality for $\|S_{I,k}(R_3(f))\|_{\infty,P_0}$ complete the proof of (31).

Next we estimate the derivative approximation: since $f = p_f + R_3(f)$, we have

$$\begin{aligned}\|\nabla f - \nabla S_{I,k}(f)\|_{\infty,P_0} &\leq \|\nabla p_f - \nabla S_{I,k}(p_f)\|_{\infty,P_0} + \|\nabla R_3(f) - \nabla S_{I,k}(R_3(f))\|_{\infty,P_0} \\ &\leq \|\nabla R_3(f)\|_{\infty,P_0} + \|\nabla S_{I,k}(R_3(f))\|_{\infty,P_0}.\end{aligned}$$

The first term on the right-hand side is easy:

$$\|\nabla R_3(f)\|_{\infty,P_0} \leq C|f|_{3,\infty}|P_0|^2 + C|f|_{4,\infty}|P_0|^3.$$

Now we note that $\|\nabla S_{I,k}(R_3(f)\|_{\infty,P_0}$ can be estimated exactly in the same fashion as above using Lemma 2 to obtain (32). □

For the approximation property in the L^2 norm, we can establish the following:

Theorem 8 *Suppose that $\mathcal{P}$ is fixed and let $\mathcal{P}_k, k \geq 1$ be the uniform refinements of $\mathcal{P}$. Then for any $u \in H^5(\Omega)$, there exists a polygonal spline $Q(u) \in \mathcal{S}_I(\mathcal{P}_k)$ such that*

$$\|u - Q(u)\|_{2,\Omega} \leq C|u|_{3,2,\Omega}2^{-3k} + C|u|_{4,2,\Omega}2^{-4k} + C|u|_{5,2,\Omega}2^{-5k} \tag{37}$$

and

$$|u - Q(u)|_{1,2,\Omega} \leq C|u|_{3,2,\Omega}2^{-2k} + C|u|_{4,2,\Omega}2^{-3k} + C|u|_{5,2,\Omega}2^{-4k} \tag{38}$$

for a positive constant C independent of u, but may be dependent on the quasi-uniformality $\gamma_{\mathcal{P}}$.

Proof. We shall use averaged Taylor polynomials. Let $B := B(u_0, v_0, \rho) := \{(x, y) : (x - u_0)^2 + (y - v_0)^2 \leq \rho^2\}$ be a disk in $\mathbb{R}^2$ of radius ρ with center (u_0, v_0). Let

$$g_B(u, v) := \begin{cases} ce^{-\rho^2/(\rho^2-(u-u_0)^2-(v-v_0)^2)}, & (u, v) \in B(u_0, v_0, \rho), \\ 0, & otherwise, \end{cases} \tag{39}$$

where c is chosen so that $\int_B g_B(u, v)dudv = 1$. Given an integrable function $f \in L_1(B(x, y, \rho))$, let

$$F_{d,B}f(x, y) := \sum_{0\leq i+j\leq d} \frac{(-1)^{i+j}}{i!j!} \int_{B(u_0,v_0,\rho)} f(u, v)D_u^i D_v^j \left[(x - u)^i(y - v)^j g_B(u, v)\right] dudv \tag{40}$$

which is called the averaged Taylor polynomial of degree d relative to B associated with f. It is known from Theorem 1.7 in [26] that

$$\|f - F_{d,B}f\|_{2,\Omega} \leq C|\Omega|^{d+1}|f|_{d+1,2,\Omega}, \tag{41}$$

for a positive constant C independent of f and Ω, where Ω containing $B(u_0, v_0, \rho)$.

For each $P \in \mathcal{P}$, let $\mathbf{p}$ be the center of P and $g_P(u, v)$ be the kernel function as defined in (39) with $(u_0, v_0) = \mathbf{p}$ and ρ_P is the largest radius such that the disk $B(\mathbf{p}, \rho_P) \subset P$. We shall use $F_{f,P}$ to denote the averaged Taylor polynomial of degree 2 relative to $B(\mathbf{p}, \rho_P)$ associated with f. Then

$$\begin{aligned}
\|f - S_{I,k}(f)\|_{2,\Omega}^2 &= \sum_{P\in\mathcal{P}} \|f - S_{I,k}(f)\|_{2,P}^2 = \sum_{P\in\mathcal{P}} \|f - F_{f,P} + F_{f,P} - S_{I,k}(F_{f,P}) + S_{I,k}(F_{f,P} - f)\|_{2,P}^2 \\
&\leq 2\sum_{P\in\mathcal{P}} \|f - F_{f,P}\|_{2,P}^2 + \|S_{I,k}(F_{f,P} - f)\|_{2,P}^2 \\
&\leq 2C\sum_{P\in\mathcal{P}} |P|^{2(2+1)}|f|_{3,2,P}^2 + \|S_{I,k}(F_{f,P} - f)\|_{2,P}^2
\end{aligned} \tag{42}$$

where we have used (41). We now estimate the last term $\|S_{I,k}(F_{f,P} - f)\|_{2,P}^2$ for each $P \in \mathcal{P}$. Let us recall the exact remainder of the averaged Taylor polynomial of f from [26].

$$\begin{aligned}
R_{d+1} = f(x, y) - F_{f,P}(x, y) &= \int_{B(u_0,v_0,\rho)} \big[f(x, y) - T_{d,(u,v)}f(x, y)\big] g_B(u, v)dudv \\
&= \sum_{\alpha+\beta=d+1} \frac{d+1}{\alpha!\beta!} \int_{B(\mathbf{p},\rho_P)} \int_0^1 g_B(u, v)(x - u)^\alpha (y - v)^\beta \\
&\quad \times D_1^\alpha D_2^\beta f((x, y) + t(u - x, v - y))t^d dtdudv,
\end{aligned} \tag{43}$$

From (18), $S_{I,k}(R_3(f))$ is given by letting $h = R_3(f)$,

$$S_{I,k}(h) = \sum_{v\in\mathcal{P}} h(v)\psi_{v,k} + h_x(v)\psi_{x,v,k} + h_y(v)\psi_{y,v,k} + h_{xx}(v)\psi_{x^2,v,k} + h_{xy}(v)\psi_{xy,v,k} + h_{yy}(v)\psi_{y^2,v,k}. \tag{44}$$

We first find the L^2 norm of $h(\mathbf{v})\psi_{\mathbf{v},k}$ over P of $\mathcal{P}$ with $\mathbf{v} \in P$. Clearly, $\|\psi_{\mathbf{v},k}\|_{2,P} \leq C|P|$ by using Lemma 2. Let us take a close look at $R_3(f)(\mathbf{v})$. Mainly, we look at one of the terms in the summation of R_3 in (43):

$$\int_{B(\mathbf{p},\rho_P)} \int_0^1 \Big| g_B(u, v)(v_1 - u)^\alpha (v_2 - v)^\beta D_1^\alpha D_2^\beta f((v_1, v_2) + t(u - v_1, v - v_2)) \Big| t^d dtdudv,$$

where $\mathbf{v} = (v_1, v_2)$. Letting LHS be the term above, it follows that

$$\begin{aligned}
LHS &\leq |P|^{\alpha+\beta}\|g_B\|_\infty \int_{B(\mathbf{p},\rho_P)} \int_0^1 |D_1^\alpha D_2^\beta f((v_1, v_2) + t(u - v_1, v - v_2))|t^d dtdudv \\
&\leq |P|^{\alpha+\beta}\frac{K_1}{\rho_P^2} \int_0^1 t^{d-2} \int_{t(B(\mathbf{p},\rho_P)-\mathbf{v})+\mathbf{v}} |D_1^\alpha D_2^\beta f(w_1, w_2)|dw_1dw_2dt \\
&\leq |P|^{d+1}\frac{K_1}{\rho_P^2} \left| \int_P |D_1^\alpha D_2^\beta f(w_1, w_2)|dw_1dw_2 \right|^{1/2} |P| \leq K_1|f|_{d+1,2,P}|P|^{d+2}/\rho_P^2,
\end{aligned}$$

by using Cauchy-Schwarz inequality since $d \geq 2$, where we have used the estimate $\|g_B\|_\infty \leq K_1/\rho_P^2$ (cf. [26]) and the substitution $(w_1, w_2) = (v_1, v_2) + t(u - v_1, v - v_2)$ which leads to a new integral

domain $t(B(\mathbf{p},\rho_P)-\mathbf{v})+\mathbf{v}$ which is a subset of P. Letting $K_{\mathcal{P}} \geq |P|^2/\rho_P^2$ be the quasi-uniform constant of partition $\mathcal{P}$, we have $LHS \leq K_1 K_{\mathcal{P}} |f|_{d+1,2,P}|P|^d = K_1 K_{\mathcal{P}}|f|_{3,2,P}|P|^2$. It follows that the first term in the summation on the right-hand side of (44) can be estimated by

$$\|R_3(f)(\mathbf{v})\psi_{v,k}\|_{2,P} \leq |R_3(f)(\mathbf{v})|C|P| \leq C|P| \sum_{\alpha+\beta=3} \frac{3!}{\alpha!\beta!} K_1 K_{\mathcal{P}}|f|_{3,2,P}|P|^2 = C_1|f|_{3,2,P}|P|^3$$

for a positive constant C_1. Next for the term involving $D_x R_3(f)(\mathbf{v})$ and $D_y R_3(f)(\mathbf{v})$, we have to apply the product rule of derivatives inside the integral and hence, we will use the same argument as above to have

$$|D_x R_3(f)(\mathbf{v})| \leq C_2|f|_{3,2,P}|P| + C_3|f|_{4,2,P}|P|^2.$$

Since $\|\psi_{x,v,k}\|_{2,\Omega} \leq C|P|^2$ by using Lemma 2, we obtain

$$\|D_x R_3(f)(\mathbf{v})\psi_{x,v,k}\|_{2,P} \leq |D_x R_3(f)|C|P|^2 C_2|f|_{3,2,P}|P|^3 + C_3|f|_{4,2,P}|P|^4.$$

Similar for the terms involving second derivatives of $R_3(f)$. Adding all terms together, we have $\|S_{I,k}(R_3(f))\|_{2,P}^2 \leq C(|f|_{3,2,P}^2|P|^6 + |f|_{4,2,P}^2|P|^8 + |f|_{4,2,P}^2|P|^{10})$. Summing over all $P \in \mathcal{P}$, taking the square root, we complete the desired estimate (37) with a constant C dependent on $K_{\mathcal{P}}$.

Similarly, we can prove (38) by using the above approach. The detail is left to the interested reader. □

If one uses the whole space $\mathcal{S}_5(\mathcal{P})$, the approximation power is, of course, better than using $\mathcal{S}_I(\mathcal{P})$ only. We can do so by using the constructed quasi-interpolatory spline given in Theorem 5. That is, given a set of scattered data on an unknown function f, i.e. data locations and function values, we approximate f by $S_5(f)$ described below. In this situation, we need to estimate these coefficients in (29), e.g. function values $u(\mathbf{v}_i)$ and first order and second order derivatives at $\mathbf{v}_i$ in order to use the quasi-interpolatory operator S_5. To do so, we can use a two-stage method described in [34]. For the data set $\mathcal{D} = \{(x_i, y_i, u(x_i, y_i)), i = 1, \cdots, N\}$, we assume that $(x_i, y_i) \in \Omega$ for a bounded domain Ω for all $i = 1, \cdots, N$. We can choose a partition $\mathcal{P}$ consisting of parallelograms to contain the region Ω of interest so that all data locations are within these parallelograms. Note that Ω may be just the union of all parallelograms. For each vertex $\mathbf{v}$ of $\mathcal{P}$, we use the given data values nearby $\mathbf{v}$ to estimate $f(\mathbf{v}), \nabla f(\mathbf{v}), \nabla^2 f(\mathbf{v})$, (e.g. by using the least-squares best-fit quadratic polynomial). Similarly, we can approximate $f(\mathbf{v}_{P,i}), i = 1, \cdots, 4$ by using the best quadratic polynomial fit over the data values over each parallelogram P, or over all points within all the parallelograms sharing e. In this way, we obtained the needed first and second derivatives at all vertices as well as the two locations inside each edge and four locations inside each parallelogram in $\mathcal{P}$. We then use the formula in (29). Similar to the proof above, we can establish

Theorem 9 *Suppose that $\mathcal{P}$ is fixed and let $\mathcal{P}_k, k \geq 1$ be the uniform refinements of $\mathcal{P}$. Then for any $u \in H^8(\Omega)$, there exists a polygonal spline $Q(u) \in \mathcal{S}_5(\mathcal{P}_k)$ such that*

$$\|u - Q(u)\|_{2,\Omega} \leq C_1|u|_{6,2,\Omega}2^{-6k} + C_2|u|_{7,2,\Omega}2^{-7k} + C_3|u|_{8,2,\Omega}2^{-8k} \tag{45}$$

for positive constants C_1, C_2, C_3 which are independent of u, but may be dependent the boundary of Ω if Ω is nonconvex.

In the end of this section, we present numerical evidence on the quasi-interpolatory splines constructed in this section to approximate some testing functions. We'll use one of the parallelogram tilings shown in Figure 1 along with its uniform refinements to show the order of convergence, which is consistent with the result in Theorem 7.

Example 1 *In this example, we report the number of quadrilaterals in the partition for each refinement, along with the mesh size h, which we have defined as the largest diameter of any parallelogram in the partition. We report the root mean square error* $\|u - S_I(u)\|_{RMS}$ *computed over* 500×500 *points on interior of the partition, along with the convergence rate in terms of h; since we expect* L^2 *convergence of* $O(h^3)$*, we should expect a rate equal to 3. We first use three trigonometric functions to test the convergence of our quasi-interpolants.* $u_1 = \sin(x)\sin(y)$*,* $u_2 = \sin(\pi x)\sin(\pi y)$*, and* $u_3 = \sin(2\pi x)\sin(2\pi y)$*: Let* S_u *be the quasi-interpolatory spline defined in (18) for function u.*

Table 1: The convergence over two refinements for u_1, u_2, u_3

# Quads	h	$\|\|u_1 - S_{u_1}\|\|_{RMS}$	rate	$\|\|u_2 - S_{u_2}\|\|_{RMS}$	rate	$\|\|u_3 - S_{u_3}\|\|_{RMS}$	rate
5	2.24e+00	1.45e-03	0.00	2.02e-01	0.00	1.22e+00	0.00
20	1.12e+00	2.01e-04	2.86	6.24e-03	5.02	2.02e-01	2.60
80	5.59e-01	2.49e-05	3.01	8.18e-04	2.93	6.24e-03	5.02

Next we repeat the same experiments for functions which are more difficult to approximate. Consider test functions $u_4 = \sin(\pi(x^2 + y^2))$*,* $u_5 = (10 + x + y)^{-1}$*, and* $u_6 = (1 + x^2 + y^2)^{-1}$*.*

Table 2: The convergence over two refinements for more difficult functions u_4, u_5 and u_6

# Quads	mesh	$\|\|u_4 - S_{u_4}\|\|_{RMS}$	rate	$\|\|u_5 - S_{u_5}\|\|_{RMS}$	rate	$\|\|u_6 - S_{u_6}\|\|_{RMS}$	rate
5	2.24e+00	1.82e+00	0.00	2.11e-06	0.00	5.57e-03	0.00
20	1.12e+00	4.66e-01	1.96	2.60e-07	3.02	5.98e-04	3.22
80	5.59e-01	2.88e-02	4.01	3.24e-08	3.00	7.65e-05	2.97

Example 2 *Next we present tables of numerical experimental results based on the quasi-interpolatory operator* S_5*. We display the numerical errors of the quasi-interpolants in Tables 3 of three testing functions:* $u_1(x, y) = \sin(x)\sin(y)$*,* $u_2(x, y) = \sin(\pi x)\sin(\pi y)$*, and* $u_3(x, y) = \sin(2\pi x)\sin(2\pi y)$*. We measure the errors* $E_F(u)$ *of the quasi-interpolants constructed over the partition in the root-mean square errors which are computed based on* 200×200 *equally-spaced points which are inside the domain.*

Table 3: C^1 polygonal spline quasi-interpolation S_5 of the functions $u_1(x, y) = \sin(x)\sin(y)$, $u_2(x, y) = \sin(\pi x)\sin(\pi y)$, $u_3(x, y) = \sin(2\pi x)\sin(2\pi y)$

# Quads	h	$E_F(u_1)$	rate	$E_F(u_2)$	rate	$E_F(u_3)$	rate
6	2.06e+00	1.89e-05	0.00	1.31e-02	0.00	2.51e-01	0.00
24	1.03e+00	3.07e-07	5.94	3.07e-04	5.41	1.44e-02	4.13
96	5.15e-01	4.86e-09	5.98	4.93e-06	5.96	2.87e-04	5.64
384	2.58e-01	7.68e-11	5.98	7.88e-08	5.97	4.84e-06	5.89

Notice that, for functions which oscillate more quickly, we require a finer mesh before a correct convergence rate can be observed. In the cases of u_1 *and* u_2*, we see convergence immediately, but in the case of* u_3*, we need the partition refined an additional time before seeing the appropriate convergence rate using the full quasi-interpolant* $S_5(u_3)$*.*

4 Construction of Vertex Splines over Convex Quadrilaterals

It is known that any polygon can be partitioned into a collection of convex quadrilaterals, since any polygonal region can be triangulated, and any triangle can be partitioned by convex quadrilaterals. Hence, the polygonal splines built in this section are useful for general regions. Let Ω be a polygon and $\mathcal{P}$ be a partition of Ω which consists of convex quadrilaterals. Of note, since we are not restricted to parallelograms, the splines we are building will generally be rational functions, not polynomials, and the derivatives will be much more involved both in the geometric constants involved and in the degree of simplification possible.

We'll proceed in the same order, first making a basis function analogous to ψ_v within a given quadrilateral Q with $v_{i,Q} = v$, using the template (6). We can determine the J coefficients readily; K_0 is also not difficult to determine, although it is more complicated since we do not have the luxury of working within the geometry of a parallelogram:

$$\begin{aligned}\psi_i = \phi_i^2\Bigg(&\phi_i^3 + 5\phi_i^2(\phi_{i+1} + \phi_{i-1} + 10\phi_i(\phi_{i+1}^2 + \phi_{i-1}^2)\\ &+ \phi_{i+2}\left(\left(5 + 20\frac{C_{i+1}C_{i-1}}{C_iC_{i+2}}\right)\phi_i^2 + \phi_i(K_1\phi_{i+1} + K_2\phi_{i-1}) + K_3\phi_{i+1}^2 + K_4\phi_{i-1}^2\right)\\ &+ \phi_{i+2}^2(S_0\phi_i + S_1\phi_{i+1} + S_2\phi_{i-1} + S_3\phi_{i+2})\Bigg).\end{aligned}$$

As in the parallelogram case, we can now take normal derivatives on the edges to determine smoothness conditions. Considering a quadrilateral R which shares the edge $\mathbf{e}_{i,Q} = \mathbf{e}_{i-1,R}$, we will want $\left(\frac{\partial\psi_{i,Q}}{\partial\mathbf{n}_{i,Q}} + \frac{\partial\psi_{i,R}}{\partial\mathbf{n}_{i-1,R}}\right)\Big|_{\mathbf{e}_{i,Q}} = 0.$

With substantial work, we can simplify this sum to the following mess:

$$\begin{aligned}&\phi_{i,Q}^2\phi_{i+1,Q}^2\Bigg(\phi_{i,Q}^2\Bigg(-30\left(\frac{|\mathbf{e}_{i-1,Q}|\cos(\theta_{i,Q})}{2C_{i,Q}} + \frac{|\mathbf{e}_{i,R}|\cos(\theta_{i,R})}{2C_{i,R}}\right)\\ &\qquad + |\mathbf{e}_{i,Q}|\left(30\left(\frac{C_{i-1,Q}}{2A_{i+2,Q}C_{i,Q}} + \frac{C_{i+1,R}}{2A_{i+1,R}C_{i,R}}\right)\right.\\ &\qquad\qquad \left.+(20 - K_{1,Q})\frac{C_{i+2,Q}}{2A_{i+2,Q}C_{i+1,Q}} + (20 - K_{2,R})\frac{C_{i+2,R}}{2A_{i+1,R}C_{i-1,R}}\right)\Bigg)\\ &+ \phi_{i,P}\phi_{i+1,P}\Bigg(30\left(\frac{|\mathbf{e}_{i+1,Q}|\cos(\theta_{i+1,Q})}{2C_{i+1,Q}} - \frac{|\mathbf{e}_{i-1,Q}|\cos(\theta_{i,Q})}{2C_{i,Q}}\right.\\ &\qquad \left.+\frac{|\mathbf{e}_{i+2,R}|\cos(\theta_{i-1,R})}{2C_{i-1,R}} - \frac{|\mathbf{e}_{i,R}|\cos(\theta_{i,R})}{2C_{i,R}}\right)\\ &\qquad + |\mathbf{e}_{i,Q}|\left((50 - K_{1,Q} - K_{3,Q})\frac{C_{i+2,Q}}{2A_{i+2,Q}C_{i+1,Q}}\right.\\ &\qquad\qquad \left.+(50 - K_{2,R} - K_{4,R})\frac{C_{i+2,R}}{2A_{i+1,R}C_{i-1,R}}\right)\Bigg)\\ &+ \phi_{i+1,P}^2\left(30\left(\frac{|\mathbf{e}_{i+1,P}|\cos(\theta_{i+1,Q})}{2C_{i+1,Q}} + \frac{|\mathbf{e}_{i+2,R}|\cos(\theta_{i-1,R})}{2C_{i-1,R}}\right)\right.\\ &\qquad \left.-|\mathbf{e}_{i,Q}|\left(K_{3,Q}\frac{C_{i+2,Q}}{2A_{i+2,Q}C_{i+1,Q}} + K_{4,R}\frac{C_{i+2,R}}{2A_{i+2,R}C_{i-1,R}}\right)\right)\Bigg)\end{aligned}$$

Notice first that this is a rational function, and that the "coefficients" on each Wachspress monomial are in fact rational functions themselves, with the linear area functions A appearing in denominators.

If we wish for this sum to be zero, we'll need all of the coefficients on the Wachspress monomials to independently resolve to zero.

Focus on the terms divisible by $\phi_{i,Q}^4 \phi_{i+1,Q}^2$. Notice that the K terms are multiplied by the terms which contain linear denominators, but the terms on the first line are totally constant, and don't necessarily resolve to 0; in fact, they simplify to $\dfrac{-30}{|\mathbf{e}_{i,Q}|}(\cot(\theta_{i,Q}) + \cot(\theta_{i,R}))$. Therefore, if we have any hope of making this term resolve to zero, we'll either need to make the K terms themselves be non-constant linear functions in order to be able to interact with this first line, or we'll need this first line itself to be zero. Of course, we want these K terms to be constant, so we'll need this first line to resolve to zero. Since Q and R are convex, this is only possible when $\theta_{i,Q} + \theta_{i,R} = \pi$, which would imply that $\mathbf{e}_{i-1,Q}$ and $\mathbf{e}_{i,R}$ are collinear; this amounts to a geometric restriction beyond convexity. In fact, this is how we land at the parallelogram partition requirement in degree 5: we dodge this issue by forcing $A_{i+2,Q}|_{\mathbf{e}_{i,Q}}$ and $A_{i+1,R}|_{\mathbf{e}_{i-1,R}}$ to be constant by making opposite edges of Q and R parallel, which leads to the requirement that all the quadrilaterals must be parallelograms.

To avoid such a restriction, we can increase the degree of our Wachspress functions. A similar attempt in degree 6 will reach the same step and require similar restrictions, again suggesting a restriction to parallelograms, but increasing to degree 7 will do the trick.

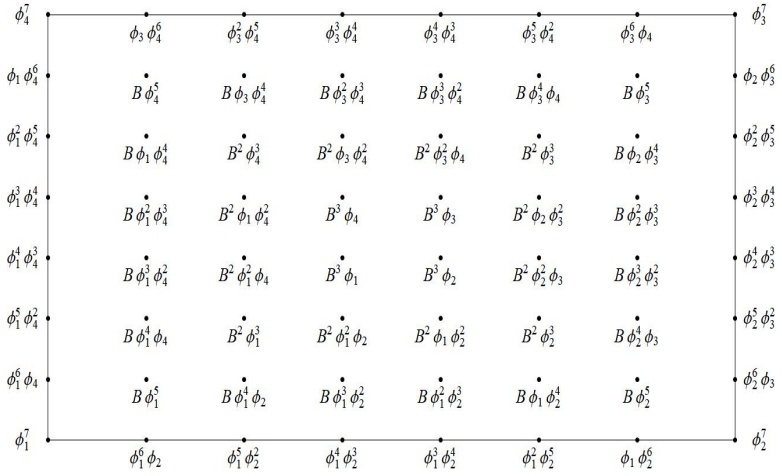

Figure 9: The monomials of Wachspress GBCs over a quadriteral

For each vertex $v \in \mathcal{P}$, let Ω_v be the collection of all quadrilaterals sharing the vertex v as before. As in the previous section we shall restrict our attention to a single quadrilateral Q in Ω_v first. Let us present the monomials of Wachspress GBCs of degree 7 in Figure 9. Let us consider nodal basis functions first as in the previous section.

We seek a general template as we found in (6); in the degree-7 case, a lengthy calculation and

simplification leads to

$$\begin{aligned}\psi_i^{(7),Q} = \phi_i^2\big(&J_{0,i}\phi_i^5 + \phi_i^4(J_{1,i}\phi_{i+1} + J_{2,i}\phi_{i-1}) + \phi_i^3(J_{3,i}\phi_{i+1}^2 + J_{4,i}\phi_{i-1}^2)\\ &+ \phi_i^2(J_{5,i}\phi_{i+1}^3 + J_{6,i}\phi_{i-1}^3) + \phi_i\left(J_{7,i}\phi_{i+1}^4 + J_{8,i}\phi_{i-1}^4\right) + J_{9,i}\phi_{i+1}^5 + J_{10,i}\phi_{i-1}^5\\ &+ \phi_{i+2}\big(K_{0,i}\phi_i^4 + \phi_i^3(K_{1,i}\phi_{i+1} + K_{2,i}\phi_{i-1}) + \phi_i^2(K_{3,i}\phi_{i+1}^2 + K_{4,i}\phi_{i-1}^2)\\ &\quad + \phi_i(K_{5,i}\phi_{i+1}^3 + K_{6,i}\phi_{i-1}^3) + K_{7,i}\phi_{i+1}^4 + K_{8,i}\phi_{i-1}^4\big)\\ &+ \phi_{i+2}^2\big(S_{0,i}\phi_i^3 + \phi_i^2(S_{1,i}\phi_{i+1} + S_{2,i}\phi_{i-1}) + \phi_i(S_{3,i}\phi_{i+1}^2 + S_{4,i}\phi_{i-1}^2) + S_{5,i}\phi_{i+1}^3 + S_{6,i}\phi_{i-1}^3\big)\\ &+ \phi_{i+2}^3\big(L_{0,i}\phi_i^2 + \phi_i(L_{1,i}\phi_{i+1} + L_{2,i}\phi_{i-1}) + L_{3,i}\phi_{i+1}^2 + L_{4,i}\phi_{i-1}^2\big)\\ &+ \phi_{i+2}^4\big(N_{0,i}\phi_i + N_{1,i}\phi_{i+1} + N_{2,i}\phi_{i-1} + N_{3,i}\phi_{i+2}\big)\big).\end{aligned} \tag{46}$$

4.1 Nodal Basis Functions $\psi_v^{(7)}$

We shall construct in the same order as in the degree 5 case, starting first with a spline to interpolate function values at vertices. Write $\psi_v^{(7)}\big|_Q = \psi_i^{(7),Q}$, where $v = v_i$ in Q and we have added a degree index in the superscript of the functions to distinguish.

We want to satisfy the same properties from the degree-5 case in the previous section:

Property 1. $\psi_v^{(7)}(w) = \delta_{v,w}$ for $w \in V$; Property 2. $\operatorname{supp}(\psi_v^{(7)}) \subseteq \Omega_v$;

Property 3. $\psi_v^{(7)} \in C^1(\Omega)$; Property 4. $\sum \psi_v^{(7)} = 1$;

Property 5. $\psi_v^{(7)}$ is piecewise-defined, with a non-zero piece for each quadrilateral in Ω_v;

Property 6. $\nabla\psi_v^{(7)}|_{w\in V} = 0$; and Property 7. $\nabla^2\psi_v^{(7)}|_{v\in V} = 0$.

Restricting attention to $\psi_i^{(7),Q}$, the factor of ϕ_i^2 enforces a zero first derivative at all vertices in Q except possibly v_i, but the second derivatives at v_{i+1} and v_{i-1} depend on $J_{9,i}$ and $J_{10,i}$, respectively. Therefore we preemptively set these to 0.

It is also worth noting that all the S, L, and N coefficients are more or less free with respect to the conditions we are interested in, as these affect neither values nor C^1-smoothness anywhere on the boundary of Q. To ease the burden here, we'll set all these as zero except for $S_{0,i}$, $S_{1,i}$, $S_{2,i}$, and $L_{0,i}$. We retrieve the following simplified template:

$$\begin{aligned}\psi_i^{(7),Q} = \phi_i^2\big(&J_{0,i}\phi_i^5 + \phi_i^4(J_{1,i}\phi_{i+1} + J_{2,i}\phi_{i-1}) + \phi_i^3(J_{3,i}\phi_{i+1}^2 + J_{4,i}\phi_{i-1}^2)\\ &+ \phi_i^2(J_{5,i}\phi_{i+1}^3 + J_{6,i}\phi_{i-1}^3) + \phi_i\left(J_{7,i}\phi_{i+1}^4 + J_{8,i}\phi_{i-1}^4\right)\\ &+ \phi_{i+2}\big(K_{0,i}\phi_i^4 + \phi_i^3(K_{1,i}\phi_{i+1} + K_{2,i}\phi_{i-1}) + \phi_i^2(K_{3,i}\phi_{i+1}^2 + K_{4,i}\phi_{i-1}^2)\\ &\quad + \phi_i(K_{5,i}\phi_{i+1}^3 + K_{6,i}\phi_{i-1}^3) + K_{7,i}\phi_{i+1}^4 + K_{8,i}\phi_{i-1}^4\big)\\ &+ \phi_{i+2}^2\big(S_{0,i}\phi_i^3 + \phi_i^2(S_{1,i}\phi_{i+1} + S_{2,i}\phi_{i-1})\big) + L_{0,i}\phi_{i+2}^3\phi_i^2\big).\end{aligned} \tag{47}$$

Property 1 above clearly implies that $J_{0,i} = 1$. Property 6 is automatically enforced at all vertices except v_i by the factor of ϕ_i^2; at v_i, it is easier to consider the derivatives in the edge directions at each vertex. Since Wachspress coordinates are linear on edges, this is easy. Rewrite $\psi_i^{(7),Q} = \phi_i^2 F$, where F is the degree-5 Wachspress function in parentheses in (47), and we retrieve

$$\begin{aligned}\left.\frac{\partial\psi_i^{(7),Q}}{\partial\tilde{\mathbf{e}}_i}\right|_{v_i} &= \left.\left(2\phi_i\frac{\partial\phi_i}{\partial\tilde{\mathbf{e}}_i}F + \phi_i^2\frac{\partial F}{\partial\tilde{\mathbf{e}}_i}\right)\right|_{v_i}\\ &= \left.\left(2\frac{\partial\phi_i}{\partial\tilde{\mathbf{e}}_i} + \left(5\phi_i^4\frac{\partial\phi_i}{\partial\tilde{\mathbf{e}}_i} + \phi_i^4\left(J_{1,i}\frac{\partial\phi_{i+1}}{\partial\tilde{\mathbf{e}}_i} + J_{2,i}\frac{\partial\phi_{i-1}}{\partial\tilde{\mathbf{e}}_i}\right)\right)\right)\right|_{v_i} = \frac{J_{1,i} - 7}{|\mathbf{e}_i|},\end{aligned}$$

which is 0 when $J_{1,i} = 7$. A similar calculation in the $\tilde{\mathbf{e}}_{i-1}$ direction gives us $J_{2,i} = 7$.

Since we removed the coefficients $J_{9,i}$ and $J_{10,i}$, we only have to worry about Property 7 at v_i. Taking the second derivative in either edge direction is straightforward:

$$\begin{aligned}\left.\frac{\partial^2 \psi_i^{(7),Q}}{\partial \tilde{\mathbf{e}}_i{}^2}\right|_{v_i} &= \left(2\left(\frac{\partial \phi_i}{\partial \tilde{\mathbf{e}}_i}\right)^2 F + 2\phi_i \frac{\partial^2 \phi_i}{\partial \tilde{\mathbf{e}}_i{}^2} F + 4\phi_i \frac{\partial \phi_i}{\partial \tilde{\mathbf{e}}_i}\frac{\partial F}{\partial \tilde{\mathbf{e}}_i} + \phi_i^2 \frac{\partial^2 F}{\partial \tilde{\mathbf{e}}_i{}^2}\right)\Bigg|_{v_i} \\ &= \left(2\frac{1}{|\mathbf{e}_i|^2}(1) + 2(1)(0)(1) + 4(1)\frac{-1}{|\mathbf{e}_i|}\frac{2}{|\mathbf{e}_i|} + (1)^2\frac{2J_{3,i} - 36}{|\mathbf{e}_i|^2}\right) = \frac{1}{|\mathbf{e}_i|^2}(2J_{3,i} - 42),\end{aligned}$$

which is 0 when $J_{3,i} = 21$. A similar calculation in the $\tilde{\mathbf{e}}_{i-1}$ direction gives us $J_{4,i} = 21$.

We still must deal with the issue of the mixed-direction second derivative at v_i. For this, we will need to use the following, which can be computed from the definition of Wachspress coordinates:

$$\left.\frac{\partial^2 \phi_i}{\partial \tilde{\mathbf{e}}_i \partial \tilde{\mathbf{e}}_{i-1}}\right|_{v_i} = \frac{-C_{i+2}^2}{|\mathbf{e}_i||\mathbf{e}_{i-1}|C_{i+1}C_{i-1}}, \qquad \left.\frac{\partial^2 \phi_{i+1}}{\partial \tilde{\mathbf{e}}_i \partial \tilde{\mathbf{e}}_{i-1}}\right|_{v_i} = \frac{C_{i+2}}{|\mathbf{e}_i||\mathbf{e}_{i-1}|C_{i+1}},$$
$$\left.\frac{\partial^2 \phi_{i-1}}{\partial \tilde{\mathbf{e}}_i \partial \tilde{\mathbf{e}}_{i-1}}\right|_{v_i} = \frac{C_{i+2}}{|\mathbf{e}_i||\mathbf{e}_{i-1}|C_{i-1}}, \qquad \left.\frac{\partial^2 \phi_{i+2}}{\partial \tilde{\mathbf{e}}_i \partial \tilde{\mathbf{e}}_{i-1}}\right|_{v_i} = \frac{-C_i C_{i+2}}{|\mathbf{e}_i||\mathbf{e}_{i-1}|C_{i+1}C_{i-1}}.$$

Taking the mixed-direction second derivative of $\psi_i^{(7),Q}$ in the $\mathbf{e}_i$ and $\mathbf{e}_{i-1}$ directions at v_i (and performing substantial simplification) leads to the following:

$$\begin{aligned}\left.\frac{\partial^2 \psi_i^{(7),Q}}{\partial \tilde{\mathbf{e}}_i \tilde{\mathbf{e}}_{i-1}}\right|_{v_i} &= 7\left(\frac{\partial^2 \phi_i}{\partial \tilde{\mathbf{e}}_i \partial \tilde{\mathbf{e}}_{i-1}} + \frac{\partial^2 \phi_{i+1}}{\partial \tilde{\mathbf{e}}_i \partial \tilde{\mathbf{e}}_{i-1}} + \frac{\partial^2 \phi_{i-1}}{\partial \tilde{\mathbf{e}}_i \partial \tilde{\mathbf{e}}_{i-1}}\right) \\ &\quad + 42\left(\frac{\partial \phi_i}{\partial \tilde{\mathbf{e}}_i}\frac{\partial \phi_i}{\partial \tilde{\mathbf{e}}_{i-1}} + \frac{\partial \phi_i}{\partial \tilde{\mathbf{e}}_i}\frac{\partial \phi_{i-1}}{\partial \tilde{\mathbf{e}}_{i-1}} + \frac{\partial \phi_i}{\partial \tilde{\mathbf{e}}_{i-1}}\frac{\partial \phi_{i+1}}{\partial \tilde{\mathbf{e}}_i}\right) + K_{0,i}\frac{\partial^2 \phi_{i+2}}{\partial \tilde{\mathbf{e}}_i \partial \tilde{\mathbf{e}}_{i-1}} \\ &= \frac{1}{|\mathbf{e}_i||\mathbf{e}_{i-1}|}\left(42 + \frac{C_i C_{i+2}}{C_{i+1}C_{i-1}}(7 - K_{0,i})\right),\end{aligned}$$

which is 0 when $K_{0,i} = 7 + 42\dfrac{C_{i+1}C_{i-1}}{C_i C_{i+2}}$.

We are still missing the $J_{k,i}$ coefficients for $k = 5, 6, 7, 8$, and intuitively these should be easier to determine, so we turn our attention there. If we consider Property 4 on an edge, say $\mathbf{e}_i$, we can retrieve the following:

$$\begin{aligned}\left(1 - \sum_{j=1}^{4} \psi_i^{(7),Q}\right)\Bigg|_{\mathbf{e}_i} &= \left((\phi_i + \phi_{i+1})^7 - \left(\psi_i^{(7),Q} + \psi_i^{(7),Q}\right)\right)|_{\mathbf{e}_i} \\ &= (35 - (J_{5,i} + J_{8,i+1}))\phi_i^4 \phi_{i+1}^3 + (35 - (J_{7,i} + J_{6,i+1}))\phi_i^3 \phi_{i+1}^4.\end{aligned}$$

We make two assumptions at this point: first, that $J_{k,i} = J_{k,j}$ for any fixed k, since all other J values have been constants; second, that $J_{5,i} = J_{6,i}$ and similarly that $J_{7,i} = J_{8,i}$ for each i. Then this gives us that $J_{7,i} = 35 - J_{5,i}$, which leaves only one remaining degree of freedom which we unfortunately cannot resolve just yet. We can, however, solve for the remaining K coefficients in terms of $J_{5,i}$, which will lead us to the solution.

To find the K coefficients, we must take outward normal derivatives along the edges, and we are serendipitously able to enforce that $\left.\dfrac{\partial \psi_i^{(7),Q}}{\partial \mathbf{n}_i}\right|_{\mathbf{e}_i} = \left.\dfrac{\partial \psi_i^{(7),Q}}{\partial \mathbf{n}_{i-1}}\right|_{\mathbf{e}_{i-1}} = 0$ as we did in the degree-5 case.

The outward normal derivatives are exceptionally long and arduous to retrieve and simplify; for the sake of brevity, we will show the expression of the outward normal derivative on the edge $\mathbf{e}_i$:

$$\begin{aligned}
\left.\frac{\partial \psi_i^{(7),Q}}{\partial \mathbf{n}_i}\right|_{\mathbf{e}_i} &= \frac{1}{2A_{i+2}}\Bigg(\phi_i^6\phi_{i+1}^2\Bigg((105|\mathbf{e}_i| + (3J_{5,i}-105)|\mathbf{e}_{i-1}|\cos(\theta_i))\frac{C_{i-1}}{C_i} + (42-K_{1,i})|\mathbf{e}_i|\frac{C_{i+2}}{C_{i+1}}\Bigg) \\
&+ \phi_i^5\phi_{i+1}^3\Bigg((147-K_{1,i}-K_{3,i})|\mathbf{e}_i|\frac{C_{i+2}}{C_{i+1}} + (7J_{5,i}|\mathbf{e}_i| + (140-8J_{5,i})|\mathbf{e}_{i-1}|\cos(\theta_i))\frac{C_{i-1}}{C_i} \\
&\quad +(3J_{5,i}-105)|\mathbf{e}_{i-1}|\cos(\theta_i)\frac{C_{i+2}}{C_i} + (105-3J_{5,i})|\mathbf{e}_{i+1}|\cos(\theta_{i+1})\frac{C_{i-1}}{C_{i+1}}\Bigg) \\
&+ \phi_i^4\phi_{i+1}^4\Bigg(((7J_{5,i}-K_{3,i}-K_{5,i})|\mathbf{e}_i| + (105-3J_{5,i})|\mathbf{e}_{i+1}|\cos(\theta_{i+1}))\frac{C_{i+2}}{C_{i+1}} \\
&\quad + ((245-7J_{5,i})|\mathbf{e}_i| + (3J_{5,i}-105)|\mathbf{e}_{i-1}|\cos(\theta_i))\frac{C_{i-1}}{C_i} \\
&\quad +(140-8J_{5,i})|e_{i-1}|\cos(\theta_i)\frac{C_{i+2}}{C_i} + (8J_{5,i}-140)|\mathbf{e}_{i+1}|\cos(\theta_{i+1})\frac{C_{i-1}}{C_{i+1}}\Bigg) \\
&+ \phi_i^3\phi_{i+1}^5\Bigg(((245-7J_{5,i}-K_{5,i}-K_{7,i})|\mathbf{e}_i| + (8J_{5,i}-140)|\mathbf{e}_{i+1}|\cos(\theta_{i+1}))\frac{C_{i+2}}{C_{i+1}} \\
&\quad +(3J_{5,i}-105)|\mathbf{e}_{i-1}|\cos(\theta_i)\frac{C_{i+2}}{C_i} + (105-3J_{5,i})|\mathbf{e}_{i+1}|\cos(\theta_{i+1})\frac{C_{i-1}}{C_{i+1}}\Bigg) \\
&+\phi_i^2\phi_{i+1}^6\Bigg((-K_{7,i}|\mathbf{e}_i| + (105-3J_{5,i})|\mathbf{e}_{i+1}|\cos(\theta_{i+1}))\frac{C_{i+2}}{C_{i+1}}\Bigg)\Bigg). \qquad (48)
\end{aligned}$$

Moving from bottom to top, we can choose the following choices of K coefficients (in terms of $J_{5,i}$) to set each term zero one at a time:

$$\begin{aligned}
K_{7,i} &= (105-3J_{5,i})\frac{|\mathbf{e}_{i+1}|}{|\mathbf{e}_i|}|\cos(\theta_{i+1}); \\
K_{5,i} &= 245-7J_{5,i} + \left(11J_{5,i}-245+(105-3J_{5,i}\frac{C_{i-1}}{C_{i+2}}\right)\frac{|\mathbf{e}_{i+1}|}{|\mathbf{e}_i|}\cos(\theta_{i+1}) \\
&\quad + (3J_{5,i}-105)\frac{|\mathbf{e}_{i-1}|}{|\mathbf{e}_i|}\frac{C_{i+1}}{C_i}\cos(\theta_i); \\
K_{3,i} &= 14J_{5,i}-245 + \left(350-14J_{5,i}+(11J_{5,i}-245)\frac{C_{i-1}}{C_{i+2}}\right)\frac{|\mathbf{e}_{i+1}|}{|\mathbf{e}_i|}\cos(\theta_{i+1}) \\
&\quad + \left(245-11J_{5,i}+(140-4J_{5,i})\frac{C_{i-1}}{C_{i+2}}\right)\frac{C_{i+1}}{C_i}\frac{|\mathbf{e}_{i-1}|}{|\mathbf{e}_i|}\cos(\theta_i); \\
K_{1,i} &= 392-14J_{5,i} + \left(14J_{5,i}-350+(350-14J_{5,i})\frac{C_{i-1}}{C_{i+2}}\right)\frac{|\mathbf{e}_{i+1}|}{|\mathbf{e}_i|}\cos(\theta_{i+1}) \\
&\quad + \left(14J_{5,i}-350+3J_{5,i}\frac{C_{i-1}}{C_{i+2}}\right)\frac{C_{i+1}}{C_i}\frac{|\mathbf{e}_{i-1}|}{|\mathbf{e}_i|}\cos(\theta_i).
\end{aligned}$$

With these choices, the normal derivative in (48) simplifies to

$$\begin{aligned}
\left.\frac{\partial \psi_i^{(7),Q}}{\partial \mathbf{n}_i}\right|_{\mathbf{e}_i} &= \frac{\phi_i^6\phi_{i+1}^2}{2A_{i+2}}(350-14J_{5,i})\Bigg((|\mathbf{e}_i| - |\mathbf{e}_{i-1}|\cos(\theta_i))\frac{C_{i-1}}{C_i} - |\mathbf{e}_{i+1}|\cos(\theta_{i+1})\frac{C_{i-1}}{C_{i+1}} \\
&\quad -(|\mathbf{e}_i| - |\mathbf{e}_{i+1}|\cos(\theta_{i+1}))\frac{C_{i+2}}{C_{i+1}} + |\mathbf{e}_{i-1}|\cos(\theta_i)\frac{C_{i+2}}{C_i}\Bigg),
\end{aligned}$$

which is zero when $J_{5,i} = 25$. Then we deduce the following:

$$J_{7,i} = 10; K_{1,i} = 42 + 15\left(7 - 2\frac{|\mathbf{e}_{i-1}|}{|\mathbf{e}_i|}\cos(\theta_i)\right)\frac{C_{i-1}C_{i+1}}{C_iC_{i+2}};$$
$$K_{3,i} = 5\left(21 + \left(14 - 6\frac{|\mathbf{e}_{i-1}|}{|\mathbf{e}_i|}\cos(\theta_i)\right)\frac{C_{i-1}C_{i+1}}{C_iC_{i+2}} + 6\left(\frac{|\mathbf{e}_{i+1}|}{|\mathbf{e}_i|}\frac{C_{i-1}}{C_{i+2}}\cos(\theta_{i+1}) - \frac{|\mathbf{e}_{i-1}|}{|\mathbf{e}_i|}\frac{C_{i+1}}{C_i}\cos(\theta_i)\right)\right);$$
$$K_{5,i} = 10\left(7 - 3\left(\frac{|\mathbf{e}_{i-1}|}{|\mathbf{e}_i|}\frac{C_{i+1}}{C_i}\cos(\theta_i) - \left(1 + \frac{C_{i-1}}{C_{i+2}}\right)\frac{|\mathbf{e}_{i+1}|}{|\mathbf{e}_i|}\cos(\theta_{i+1})\right)\right);$$
$$K_{7,i} = 30\frac{|\mathbf{e}_{i+1}|}{|\mathbf{e}_i|}\cos(\theta_{i+1}).$$

A similar analysis on edge e_{i-1} provides us with the remaining J and K coefficients:

$$J_{6,i} = 25; J_{8,i} = 10;$$
$$K_{2,i} = 42 + 15\left(7 - 2\frac{|\mathbf{e}_i|}{|\mathbf{e}_{i-1}|}\cos(\theta_i)\right)\frac{C_{i-1}C_{i+1}}{C_iC_{i+2}};$$
$$K_{4,i} = 5\left(21 + \left(14 - 6\frac{|\mathbf{e}_i|}{|\mathbf{e}_{i-1}|}\cos(\theta_i)\right)\frac{C_{i-1}C_{i+1}}{C_iC_{i+2}} + 6\left(\frac{|\mathbf{e}_{i+2}|}{|\mathbf{e}_{i-1}|}\frac{C_{i+1}}{C_{i+2}}\cos(\theta_{i-1}) - \frac{|\mathbf{e}_i|}{|\mathbf{e}_{i-1}|}\frac{C_{i-1}}{C_i}\cos(\theta_i)\right)\right);$$
$$K_{6,i} = 10\left(7 - 3\left(\frac{|\mathbf{e}_i|}{|\mathbf{e}_{i-1}|}\frac{C_{i-1}}{C_i}\cos(\theta_i) - \left(1 + \frac{C_{i+1}}{C_{i+2}}\right)\frac{|\mathbf{e}_{i+2}|}{|\mathbf{e}_{i-1}|}\cos(\theta_{i-1})\right)\right);$$
$$K_{8,i} = 30\frac{|\mathbf{e}_{i+2}|}{|\mathbf{e}_{i-1}|}\cos(\theta_{i-1}).$$

At this point, the only coefficients which are left to be determined are $S_{0,i}, S_{1,i}, S_{2,i}$, and $L_{0,i}$. These can be determined these using Property 4, with the usual method of writing $1 = \left(\sum_{j+1}^{4}\phi_i\right)^7$ and collecting like terms in the subtraction. The details are lengthy and are not illuminating; we merely report the deduced values of the coefficients:

$$S_{0,i} = 3\left(7 + 10\frac{C_{i+1}C_{i-1}}{C_iC_{i+2}}\left(7 + 5\frac{C_{i+1}C_{i-1}}{C_iC_{i+2}}\right)\right);$$
$$S_{1,i} = S_{2,i} = 105\left(1 + 2\frac{C_{i+1}C_{i-1}}{C_iC_{i+2}}\left(2 + \frac{C_{i+1}C_{i-1}}{C_iC_{i+2}}\right)\right);$$
$$L_{0,i} = 35\left(1 + 2\frac{C_{i+1}C_{i-1}}{C_iC_{i+2}}\left(6 + \frac{C_{i+1}C_{i-1}}{C_iC_{i+2}}\left(9 + 2\frac{C_{i+1}C_{i-1}}{C_iC_{i+2}}\right)\right)\right).$$

The final expression of $\psi_i^{(7),Q}$, then, is the following:

$$
\begin{aligned}
\psi_i^{(7),Q} = \phi_i^2\Bigg(& \phi_i^5 + 7\phi_i^4(\phi_{i+1}+\phi_{i-1}) + 21\phi_i^3(\phi_{i+1}^2+\phi_{i-1}^2) \\
& + 25\phi_i^2(\phi_{i+1}^3+\phi_{i-1}^3) + 10\phi_i\left(\phi_{i+1}^4+\phi_{i-1}^4\right) \\
& + \phi_{i+2}\Bigg(\left(7+42\frac{C_{i+1}C_{i-1}}{C_iC_{i+2}}\right)\phi_i^4 + \phi_i^3\Bigg(\left(42+15\left(7-2\frac{|\mathbf{e}_{i-1}|}{|\mathbf{e}_i|}\cos(\theta_i)\right)\frac{C_{i+1}C_{i-1}}{C_iC_{i+2}}\right)\phi_{i+1} \\
& \qquad + \left(42+15\left(7-2\frac{|\mathbf{e}_i|}{|\mathbf{e}_{i-1}|}\cos(\theta_i)\right)\frac{C_{i+1}C_{i-1}}{C_iC_{i+2}}\right)\phi_{i-1}\Bigg) \\
& \quad + 5\phi_i^2\Bigg(\Bigg(21+\left(14-6\frac{|\mathbf{e}_{i-1}|}{|\mathbf{e}_i|}\cos(\theta_i)\right)\frac{C_{i-1}C_{i+1}}{C_iC_{i+2}} \\
& \qquad\qquad + 6\left(\frac{|\mathbf{e}_{i+1}|}{|\mathbf{e}_i|}\frac{C_{i-1}}{C_{i+2}}\cos(\theta_{i+1}) - \frac{|\mathbf{e}_{i-1}|}{|\mathbf{e}_i|}\frac{C_{i+1}}{C_i}\cos(\theta_i)\right)\Bigg)\phi_{i+1}^2 \\
& \qquad + \Bigg(21+\left(14-6\frac{|\mathbf{e}_i|}{|\mathbf{e}_{i-1}|}\cos(\theta_i)\right)\frac{C_{i+1}C_{i-1}}{C_iC_{i+2}} \\
& \qquad\qquad + 6\left(\frac{|\mathbf{e}_{i+2}|}{|\mathbf{e}_{i-1}|}\frac{C_{i+1}}{C_{i+2}}\cos(\theta_{i-1}) - \frac{|\mathbf{e}_i|}{|\mathbf{e}_{i-1}|}\frac{C_{i-1}}{C_i}\cos(\theta_i)\right)\Bigg)\phi_{i-1}^2\Bigg) \\
& \quad + 10\phi_i\Bigg(\left(7-3\left(\frac{|\mathbf{e}_{i-1}|}{|\mathbf{e}_i|}\frac{C_{i+1}}{C_i}\cos(\theta_i) - \left(1+\frac{C_{i-1}}{C_{i+2}}\right)\frac{|\mathbf{e}_{i+1}|}{|\mathbf{e}_i|}\cos(\theta_{i+1})\right)\right)\phi_{i+1}^3 \\
& \qquad + \left(7-3\left(\frac{|\mathbf{e}_i|}{|\mathbf{e}_{i-1}|}\frac{C_{i-1}}{C_i}\cos(\theta_i) - \left(1+\frac{C_{i+1}}{C_{i+2}}\right)\frac{|\mathbf{e}_{i+2}|}{|\mathbf{e}_{i-1}|}\cos(\theta_{i-1})\right)\right)\phi_{i-1}^3\Bigg) \\
& \quad + 30\left(\frac{|\mathbf{e}_{i+1}|}{|\mathbf{e}_i|}\cos(\theta_{i+1})\phi_{i+1}^4 + \frac{|\mathbf{e}_{i+2}|}{|\mathbf{e}_{i-1}|}\cos(\theta_{i-1})\phi_{i-1}^4\right)\Bigg) \\
& + 3\phi_{i+2}^2\Bigg(\left(7+10\frac{C_{i+1}C_{i-1}}{C_iC_{i+2}}\left(7+5\frac{C_{i+1}C_{i-1}}{C_iC_{i+2}}\right)\right)\phi_i^3 \\
& \quad + 35\left(1+2\frac{C_{i+1}C_{i-1}}{C_iC_{i+2}}\left(2+\frac{C_{i+1}C_{i-1}}{C_iC_{i+2}}\right)\right)\phi_i^2\left(\phi_{i+1}+\phi_{i-1}\right)\Bigg) \\
& + 35\left(1+2\frac{C_{i+1}C_{i-1}}{C_iC_{i+2}}\left(6+\frac{C_{i+1}C_{i-1}}{C_iC_{i+2}}\left(9+2\frac{C_{i+1}C_{i-1}}{C_iC_{i+2}}\right)\right)\right)\phi_{i+2}^3\phi_i^2\Bigg).
\end{aligned}
$$

Similar to Theorem 1, we have by construction the following:

Theorem 10 *Let Ω be any polygonal region in $\mathbb{R}^2$, and let $\mathcal{P}$ be a partition of Ω by quadrilaterals. For every vertex v in the partition $\mathcal{P}$, define a polygonal spline $\psi_v^{(7)}$ over Ω_v by*

$$
\psi_v^{(7)}(\mathbf{x}) := \begin{cases} \psi_i^{(7),Q}(\mathbf{x}) & \mathbf{x}\in P\subseteq\Omega_v;\ v=v_{i,P} \\ 0 & \mathbf{x}\notin\Omega_v, \end{cases}
$$

where $\psi_i^{(7),Q}$ is the function in (47). Then $\psi_v^{(7)}\in C^1(\Omega)$ and satisfies the following properties:

(1) $\psi_v^{(7)}(w)=\delta_{v,w}$ for any vertex w of $\mathcal{P}$; (2) $\nabla\psi_v^{(7)}(w)=0$ for any vertex w of $\mathcal{P}$;
(3) $\nabla^2\psi_v^{(7)}(w)=0$ for any vertex w of $\mathcal{P}$; and (4) $\displaystyle\sum_{v\in\mathcal{P}}\psi_v^{(7)}=1$.

The proof is based on the construction similar to the proof of Theorem 1. We thus omit the detail or see [27]. Figure 10 shows an unstructured quadrilateral partition and the plot of a function $\psi_v^{(7)}$ over this partition.

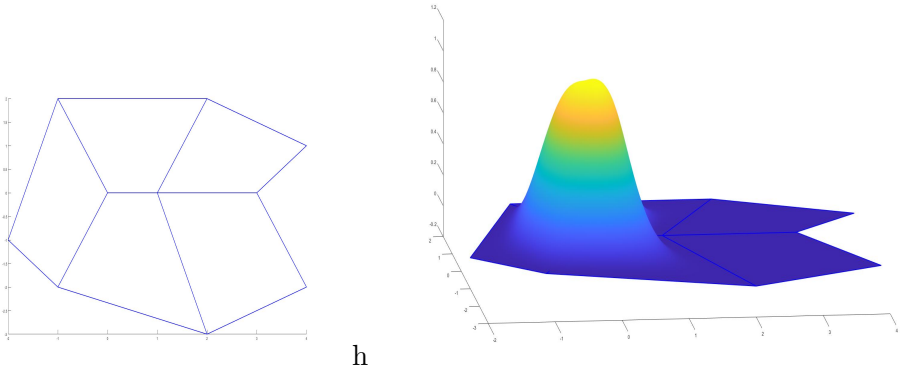

h

Figure 10: An unstructured quadrilateral partition and the plot of a function $\psi_v^{(7)}$

Similar to the construction above, we can build gradient interpolatory functions $\psi_{x,v}^{(7)}, \psi_{y,v}^{(7)} \in C^1(\Omega)$ and they satisfy the following properties:

1. $\psi_{x,v}^{(7)}(w) = \psi_{y,v}^{(7)}(w) = 0$ for any vertex w of $\mathcal{P}$;
2. $\nabla\psi_{x,v}^{(7)}(w) = \langle \delta_{v,w}, 0\rangle$ and $\nabla\psi_{y,v}^{(7)}(w) = \langle 0, \delta_{v,w}\rangle$ for any vertex w of $\mathcal{P}$;
3. $\nabla^2\psi_{x^2,v}^{(7)}(w) = \nabla^2\psi_{y,v}^{(7)}(w) = 0$ for any vertex w of $\mathcal{P}$; and
4. $\sum\limits_{v\in\mathcal{P}} v_x\psi_v^{(7)} + \psi_{x,v}^{(7)} = x$ and $\sum\limits_{v\in\mathcal{P}} v_y\psi_v^{(7)} + \psi_{y,v}^{(7)} = y$.

There is not much additional value to be had from repeating the same flavor of calculations as in the previous section; we use nearly the same techniques applied to these properties instead. For this reason, we simply present the final expression of the functions.

Figure 11 shows the plot of the functions $\psi_{x,v}^{(7)}$ and $\psi_{y,v}^{(7)}$ over the partition shown in Figure 10.

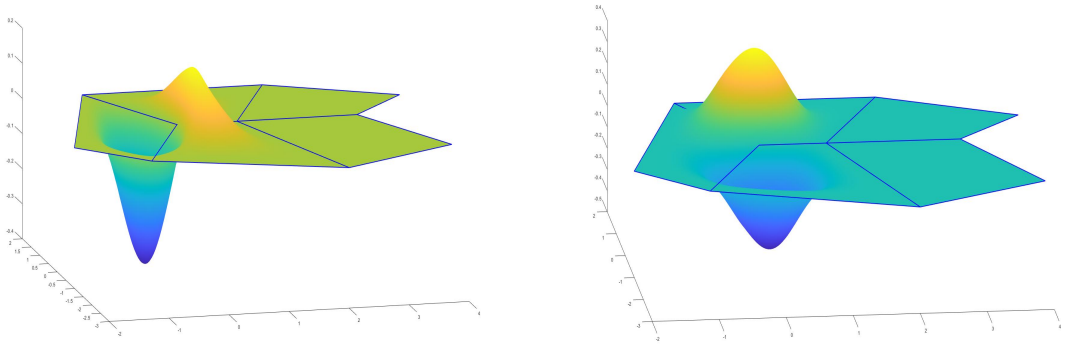

Figure 11: Plots of degree-7 gradient-adjustment basis splines

Below is the expression of $\psi^{(7),Q}_{x,i}$:

$$
\begin{aligned}
\psi^{(7),Q}_{x,i} = \phi_i^2\Bigg(&\phi_i^4(e_{i,x}\phi_{i+1} - e_{i-1,x}\phi_{i-1}) + 6\phi_i^3(e_{i,x}\phi_{i+1}^2 - e_{i-1,x}\phi_{i-1}^2) + 5\phi_i^2(e_{i,x}\phi_{i+1}^3 - e_{i-1,x}\phi_{i-1}^3)\\
&+ \phi_{i+2}\Bigg(\Bigg(\Bigg(\Bigg(1+6\frac{C_{i+1}}{C_{i+2}}\Bigg)\frac{C_{i-1}}{C_i}e_{i,x} - \Bigg(1+6\frac{C_{i-1}}{C_{i+2}}\Bigg)\frac{C_{i+1}}{C_i}e_{i-1,x}\Bigg)\phi_i^4\\
&\quad + 3\phi_i^3\Bigg(\Bigg(2\Bigg(e_{i,x} - \frac{C_{i+1}}{C_i}e_{i-1,x} + \frac{C_{i-1}}{C_{i+2}}e_{i+1,x}\Bigg)\\
&\qquad + \frac{C_{i+1}C_{i-1}}{C_iC_{i+2}}\Bigg(\Bigg(12 - 10\frac{|\mathbf{e}_{i-1}|}{|\mathbf{e}_i|}\cos(\theta_i)\Bigg)e_{i,x} - 3e_{i-1,x}\Bigg)\Bigg)\phi_{i+1}\\
&\qquad - \Bigg(2\Bigg(e_{i-1,x} - \frac{C_{i-1}}{C_i}e_{i,x} + \frac{C_{i+1}}{C_{i+2}}e_{i+2,x}\Bigg)\\
&\qquad\quad + \frac{C_{i+1}C_{i-1}}{C_iC_{i+2}}\Bigg(\Bigg(12 - 10\frac{|\mathbf{e}_i|}{|\mathbf{e}_{i-1}|}\cos(\theta_i)\Bigg)e_{i-1,x} - 3e_{i,x}\Bigg)\Bigg)\phi_{i-1}\Bigg)\\
&\quad + 5\phi_i^2\Bigg(\Bigg(7e_{i,x} + \Bigg(1-4\frac{C_{i-1}}{C_{i+2}}\Bigg)e_{i+1,x} - \frac{C_{i+1}}{C_i}\Bigg(2e_{i-1,x} + 6\frac{|\mathbf{e}_{i-1}|}{|\mathbf{e}_i|}\cos(\theta_i)e_{i,x}\Bigg)\\
&\qquad - 6\frac{C_{i+1}C_{i-1}}{C_iC_{i+2}}\Bigg(e_{i-1,x} + \frac{|\mathbf{e}_{i-1}|}{|\mathbf{e}_i|}\cos(\theta_i)e_{i-1,x}\Bigg)\Bigg)\phi_{i+1}^2\\
&\qquad - \Bigg(7e_{i-1,x} + \Bigg(1-4\frac{C_{i+1}}{C_{i+2}}\Bigg)e_{i+2,x} - \frac{C_{i-1}}{C_i}\Bigg(2e_{i,x} + 6\frac{|\mathbf{e}_i|}{|\mathbf{e}_{i-1}|}\cos(\theta_i)e_{i-1,x}\Bigg)\\
&\qquad - 6\frac{C_{i+1}C_{i-1}}{C_iC_{i+2}}\Bigg(e_{i,x} + \frac{|\mathbf{e}_i|}{|\mathbf{e}_{i-1}|}\cos(\theta_i)e_{i-1,x}\Bigg)\Bigg)\phi_{i-1}^2\Bigg)\\
&\quad - 10\phi_i\Bigg(\Bigg(2e_{i+1,x} + 3\frac{C_{i+1}}{C_i}\Bigg(e_{i-1,x} + \frac{|\mathbf{e}_{i-1}|}{|\mathbf{e}_i|}\cos(\theta_i)e_{i,x}\Bigg)\Bigg)\phi_{i+1}^3\\
&\qquad - \Bigg(2e_{i+2,x} + 3\frac{C_{i-1}}{C_i}\Bigg(e_{i,x} + \frac{|\mathbf{e}_i|}{|\mathbf{e}_{i-1}|}\cos(\theta_i)e_{i-1,x}\Bigg)\Bigg)\phi_{i-1}^3\Bigg)\Bigg)\\
&+ 3\phi_{i+2}^2\Bigg(2\Bigg(\Bigg(1+5\frac{C_{i+1}C_{i-1}}{C_iC_{i+2}}\Bigg)(e_{i,x} + e_{i+1,x})\\
&\qquad + 5\frac{C_{i+1}C_{i-1}}{C_iC_{i+2}}\Bigg(1+2\frac{C_{i+1}C_{i-1}}{C_iC_{i+2}}\Bigg)(e_{i,x} - e_{i-1,x})\Bigg)\phi_i^3\\
&\quad + 5\phi_i^2\Bigg(\Bigg(\Bigg(1+2\frac{C_{i+1}C_{i-1}}{C_iC_{i+2}}\Bigg)(3e_{i,x} + 2e_{i+1,x})\\
&\qquad + 2\frac{C_{i+1}C_{i-1}}{C_iC_{i+2}}\Bigg(1+\frac{C_{i+1}C_{i-1}}{C_iC_{i+2}}\Bigg)(3e_{i,x} - 2e_{i-1,x})\Bigg)\phi_{i+1}\\
&\qquad - \Bigg(\Bigg(1+2\frac{C_{i+1}C_{i-1}}{C_iC_{i+2}}\Bigg)(3e_{i-1,x} + 2e_{i+2,x})\\
&\qquad\quad + 2\frac{C_{i+1}C_{i-1}}{C_iC_{i+2}}\Bigg(1+\frac{C_{i+1}C_{i-1}}{C_iC_{i+2}}\Bigg)(3e_{i-1,x} - 2e_{i,x})\Bigg)\phi_{i-1}\Bigg)\Bigg)\\
&\quad 15\Bigg(\Bigg(1+2\frac{C_{i+1}C_{i-1}}{C_iC_{i+2}}\Bigg(4+3\frac{C_{i+1}C_{i-1}}{C_iC_{i+2}}\Bigg)\Bigg)(e_{i,x} + e_{i+1,x})\\
&\qquad + 4\frac{C_{i+1}C_{i-1}}{C_iC_{i+2}}\Bigg(1+\frac{C_{i+1}C_{i-1}}{C_iC_{i+2}}\Bigg(3+\frac{C_{i+1}C_{i-1}}{C_iC_{i+2}}\Bigg)\Bigg)(e_{i,x} - e_{i-1,x})\Bigg)\phi_{i+2}^3\phi_i^2\Bigg)
\end{aligned}
$$

The expression of $\psi^{(7),Q}_{y,i}$ can be retrieved by replacing every x with y, and we can define the vertex

splines $\psi^{(7)}_{x,v}$ and $\psi^{(7)}_{y,v}$ piecewise in Ω_v as usual.

Finally, we present vertex splines $\psi^{(7)}_{x^2,v}$, $\psi^{(7)}_{y^2,v}$, and $\psi^{(7)}_{xy,v}$. These functions have 0 for function values and 0 for the values of first order derivatives. Their Hessians have cardinal interpolatory properties similar to the one in the previous section. As before, there is not much insight to be gained from the computations of these functions, as it is almost exactly the same as in the previous section. The overall flavor and repertoire of techniques are nearly identical, merely applied to a different set of constraints.

The expression of these functions will not fit on a single page, but we use the same template as before in (47) and present the coefficients. For $\psi^{(7),Q}_{xy,i}$, the coefficients are:

$$
\begin{aligned}
&J_{0,i} = J_{1,i} = J_{2,i} = J_{7,i} = J_{8,i} = 0; J_{3,i} = e_{i,x}e_{i,y}; J_{4,i} = e_{i-1,x}e_{i-1,y}; J_{5,i} = -5e_{i,x}e_{i,y};\\
&J_{6,i} = -5e_{i-1,x}e_{i-1,y}; K_{0,i} = -\frac{C_{i+1}C_{i-1}}{C_iC_{i+2}}(e_{i,x}e_{i-1,y} + e_{i,y}e_{i-1,x});\\
&K_{1,i} = \frac{C_{i-1}}{C_{i+2}}(e_{i,x}e_{i+1,y} + e_{i,y}e_{i+1,x}) - \frac{C_{i+1}}{C_i}(e_{i,x}e_{i-1,y} + e_{i,y}e_{i-1,x})\\
&\qquad + \frac{C_{i+1}C_{i-1}}{C_iC_{i+2}}\left(\left(7 - 30\frac{|\mathbf{e}_{i-1}|}{|\mathbf{e}_i|}\cos(\theta_i)\right)e_{i,x}e_{i,y} - 4(e_{i,x}e_{i-1,y} + e_{i,y}e_{i-1,x})\right);\\
&K_{2,i} = \frac{C_{i+1}}{C_{i+2}}(e_{i-1,x}e_{i+2,y} + e_{i-1,y}e_{i+2,x}) - \frac{C_{i-1}}{C_i}(e_{i,x}e_{i-1,y} + e_{i,y}e_{i-1,x})\\
&\qquad + \frac{C_{i+1}C_{i-1}}{C_iC_{i+2}}\left(\left(7 - 30\frac{|\mathbf{e}_i|}{|\mathbf{e}_{i-1}|}\cos(\theta_i)\right)e_{i-1,x}e_{i-1,y} - 4(e_{i,x}e_{i-1,y} + e_{i,y}e_{i-1,x})\right);\\
&K_{3,i} = 7e_{i,x}e_{i,y} + (e_{i,x}e_{i+1,y} + e_{i,y}e_{i+1,x}) + 22\frac{C_{i-1}}{C_{i+2}}\frac{|\mathbf{e}_{i+1}|}{|\mathbf{e}_i|}\cos(\theta_{i+1})e_{i,x}e_{i,y}\\
&\qquad - \frac{C_{i+1}}{C_i}\left(4(e_{i,x}e_{i-1,y} + e_{i,y}e_{i-1,x}) + 30\frac{|\mathbf{e}_{i-1}|}{|\mathbf{e}_i|}\cos(\theta_i)e_{i,x}e_{i,y}\right)\\
&\qquad - 42\frac{C_{i+1}C_{i-1}}{C_iC_{i+2}}\left(1 - \frac{|\mathbf{e}_{i-1}|}{|\mathbf{e}_i|}\cos(\theta_i)\right)e_{i,x}e_{i,y};\\
&K_{4,i} = 7e_{i-1,x}e_{i-1,y} + (e_{i-1,x}e_{i+2,y} + e_{i-1,y}e_{i+2,x}) + 22\frac{C_{i+1}}{C_{i+2}}\frac{|\mathbf{e}_{i+2}|}{|\mathbf{e}_{i-1}|}\cos(\theta_{i-1})e_{i-1,x}e_{i-1,y}\\
&\qquad - \frac{C_{i-1}}{C_i}\left(4(e_{i,x}e_{i-1,y} + e_{i,y}e_{i-1,x}) + 30\frac{|\mathbf{e}_i|}{|e_{i-1}|}\cos(\theta_i)e_{i-1,x}e_{i-1,y}\right)\\
&\qquad - 42\frac{C_{i+1}C_{i-1}}{C_iC_{i+2}}\left(1 - \frac{|\mathbf{e}_i|}{|e_{i-1}|}\cos(\theta_i)\right)e_{i-1,x}e_{i-1,y};\\
&K_{5,i} = -20\frac{|\mathbf{e}_{i+1}|}{|\mathbf{e}_i|}\cos(\theta_{i+1})e_{i,x}e_{i,y}; K_{6,i} = -20\frac{|\mathbf{e}_{i+2}|}{|\mathbf{e}_{i-1}|}\cos(\theta_{i-1})e_{i-1,x}e_{i-1,y};\\
&K_{7,i} = K_{8,i} = 0;\\
&S_{0,i} = (e_{i,x} + e_{i+1,x})(e_{i,y} + e_{i+1,y}) + 5\frac{C_{i+1}C_{i-1}}{C_iC_{i+2}}\Bigg((e_{i,x} - e_{i-1,x})(e_{i,y} + e_{i+1,y})\\
&\qquad + (e_{i,y} - e_{i-1,y})(e_{i,x} + e_{i+1,x}) - (e_{i,x}e_{i-1,y} + e_{i,y}e_{i-1,x})\\
&\qquad + 2\frac{C_{i+1}C_{i-1}}{C_iC_{i+2}}\Big((e_{i,x} - e_{i-1,x})(e_{i,y} - e_{i-1,y}) - (e_{i,x}e_{i-1,y} + e_{i,y}e_{i-1,x})\Big)\Bigg);
\end{aligned}
$$

$$
\begin{aligned}
S_{1,i} = 5\Bigg(&3e_{i-1,x}e_{i-1,y} + e_{i+2,x}e_{i+2,y} + 2(e_{i,x}e_{i+1,y} + e_{i,y}e_{i+1,x}) \\
&+ 2\frac{C_{i+1}C_{i-1}}{C_iC_{i+2}}\Bigg(2(3e_{i,x}e_{i,y} + e_{i,x}(e_{i+1,y} - e_{i-1,y}) + e_{i,y}(e_{i+1,x} - e_{i-1,x})) \\
&\quad - (e_{i-1,x}(e_{i,y} + e_{i+1,y} + e_{i-1,y}(e_{i,x} + e_{i+1,x})) \\
&\quad + \frac{C_{i+1}C_{i-1}}{C_iC_{i+2}}(e_{i-1,x}e_{i-1,y} + 3(e_{i,x}e_{i,y} - (e_{i,x}e_{i-1,y} + e_{i,y}e_{i-1,x})))\Bigg)\Bigg); \\
S_{2,i} = 5\Bigg(&3e_{i-1,x}e_{i-1,y} + e_{i+2,x}e_{i+2,y} + 2(e_{i-1,x}e_{i+2,y} - e_{i-1,y}e_{i+2,x}) \\
&+ 2\frac{C_{i+1}C_{i-1}}{C_iC_{i+2}}\Bigg(2(3e_{i-1,x}e_{i-1,y} + e_{i-1,x}(e_{i+2,y} - e_{i,y}) + e_{i-1,y}(e_{i+2,x} - e_{i,x})) \\
&\quad - (e_{i,x}(e_{i-1,y} + e_{i+2,y}) + e_{i,y}(e_{i-1,x} + e_{i+2,x})) \\
&\quad + \frac{C_{i+1}C_{i-1}}{C_iC_{i+2}}(e_{i,x}e_{i,y} + 3(e_{i-1,x}e_{i-1,y} - (e_{i,x}e_{i-1,y} + e_{i,y}e_{i-1,x})))\Bigg)\Bigg); \\
L_{0,i} = 5\Bigg(&(e_{i,x} + e_{i+1,x})(e_{i,y} + e_{i+1,y}) + 2\frac{C_{i+1}C_{i-1}}{C_iC_{i+2}}\Bigg(6e_{i,x}e_{i,y} + 2e_{i+1,x}e_{i+1,y} \\
&+ 4(e_{i,x}e_{i+1,y} + e_{i,y}e_{i+1,x}) - (e_{i-1,x}(3e_{i,y} + 2e_{i+1,y}) + e_{i-1,y}(3e_{i,x} + e_{i+1,x})) \\
&\frac{C_{i+1}C_{i-1}}{C_iC_{i+2}}\Bigg(3(3e_{i,x}e_{i,y} + e_{i-1,x}e_{i-1,y} + (e_{i,x}e_{i+1,y} + e_{i,y}e_{i+1,x}) \\
&\quad - (e_{i-1,x}(3e_{i,y} + e_{i+1,y}) + e_{i-1,y}(3e_{i,x} + e_{i+1,x}))) \\
&+ \frac{C_{i+1}C_{i-1}}{C_iC_{i+2}}(2(e_{i,x}e_{i,y} + e_{i-1,x}e_{i-1,y}) - 3(e_{i,x}e_{i-1,y} + e_{i,y}e_{i-1,x}))\Bigg)\Bigg)\Bigg).
\end{aligned}
$$

From these, we can retrieve the corresponding coefficients for $\psi^{(7),Q}_{x^2,i}$ (or $\psi^{(7),Q}_{y^2,i}$) by replacing each y by x (or each x by y) and dividing by 2. We only show the graph of these functions in Figure 12 while leaving the details to [27].

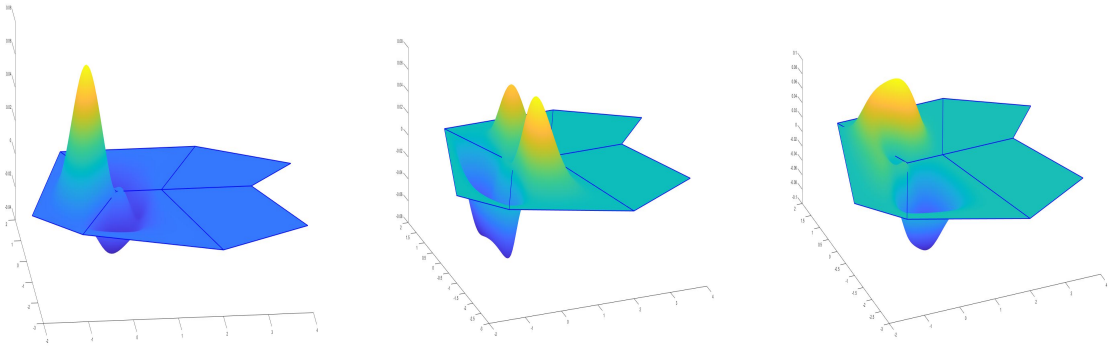

Figure 12: Plots of degree-7 Hessian-adjustment basis splines

With these vertex spline functions ready, we can formulate an interpolatory scheme. Given a function f, we let $Q_I(f)$ be the interpolatory spline which satisfies the following interpolatory conditions:

$$
\begin{aligned}
&Q_I(f)(v) = f(v),\ D_xQ_I(f)(v) = f_x(v),\ D_yQ_I(f)(v) = f_y(v),\ D_{xx}Q_I(f)(v) = f_{xx}(v), \\
&D_{xy}Q_I(f)(v) = f_{xy}(v),\ D_{yy}Q_I(f)(v) = f_{yy}(v),
\end{aligned} \tag{49}
$$

for all vertex $v \in \mathcal{P}$. In fact, based on the discussion above, Q_I can be constructed by

$$Q_I(f) = \sum_{v\in\mathcal{P}} f(v)\psi_v^{(7)} + f_x(v)\psi_{x,v}^{(7)} + f_y(v)\psi_{y,v}^{(7)} + f_{xx}(v)\psi_{x^2,v}^{(7)} + f_{xy}(v)\psi_{xy,v}^{(7)} + f_{yy}(v)\psi_{y^2,v}^{(7)}. \tag{50}$$

We summarize the discussion above to conclude the following:

Theorem 11 *Suppose that $f \in C^2(\Omega)$ and $\mathcal{P}$ be a partition of polynomial domain Ω consisting of convex quadrilaterals. Define $Q_I(f)$ as in (50). Then $Q_I(f)$ reproduces all polynomial functions of degree 2. That is, if $f \in \Pi_2$, the space of all quadratic polynomials, then $Q_I(f) = f$.*

Proof. Due to the interpolatory properties of the vertex splines $\psi_v^{(7)}, \psi_{x,v}^{(7)}, \psi_{y,v}^{(7)}, \psi_{x^2,v}^{(7)}, \psi_{xy,v}^{(7)}, \psi_{y^2,v}^{(7)}$, Q_I will interpolate f as described above. □

In addition, the construction of edge and face splines are similar to the setting of parallelograms. We leave the detail to the interested reader. The quasi-interpolatory operators can be constructed and their approximation order can be studied similarly to the previous section. Again we omit these discussions. We shall pay attention to a real life application of C^1 vertex splines to be discussed in the next section.

5 Applications

In this section, we present a few examples to explain how to use our smooth polygonal splines for constructing surfaces. In particular, our approach enables us to construct C^1 smooth surfaces over a partition of convex quadrilaterals which may contain several extraordinary points(EP). See our construction of suitcase corners and surfaces around the body of a bunny. MATLAB codes for these surface constructions will be sent upon request.

Example 3 *Our first example is to construct a set of functions which have GBC-like properties: For a quadrilateral partition, we simply use the contour plot to show ψ_v, $\psi_{x,v}, \psi_{y,v}$ for each vertex $v = (v_x, v_y) \in \mathcal{P}$. These functions satisfy the following properties:*

$$\begin{aligned} \sum_{v\in\mathcal{P}} \psi_v(x,y) &= 1, \quad (x,y) \in \mathcal{P} \\ \sum_{v\in\mathcal{P}} \psi_v(x,y)(x_v,y_v) + \sum_{v\in\mathcal{P}} (\psi_{x,v},\psi_{y,v}) &= (x,y), (x,y) \in \mathcal{P}. \end{aligned} \tag{51}$$

These are like the properties of standard GBC functions. Consider a polygon Ω with 10 sides and divide it into a quadrilateral partition by adding one interior vertex v_{11}. Let us plot the contours of ψ_v for all 11 vertices. There are also functions $\psi_{x,v}$, $\psi_{y,v}$, $\psi_{x^2,v}, \psi_{xy,v}$ and $\psi_{y^2,v}$ for each vertex, along with 2 edge splines per edge (so 30 edge splines) and a face spline per quadrilateral (5), for a total of 101 smooth interpolatory basis polygonal splines over this partition.

However, these functions are significantly different from the standard GBC functions. First of all, the surface of each ψ_v is only C^1 inside the polygon Ω which is divided into a collection of quadrilaterals. Secondly, over the boundary edges of Ω, they are not piecewise linear due to our construction. In order to make them to be piecewise linear over the boundary, one has to add edge splines. Thirdly, they are locally supported. That is, if we modify one vertex of Ω, the surface will not change globally. They have a desired property of locality (cf. [38]). As mentioned above, $\psi_{x^iy^j,v}, i+j \le 2, v \in \Omega$ can be used to modify the surface locally. These give a computer designer more handles to control a surface. The MATLAB codes can be found at the first author's web page.

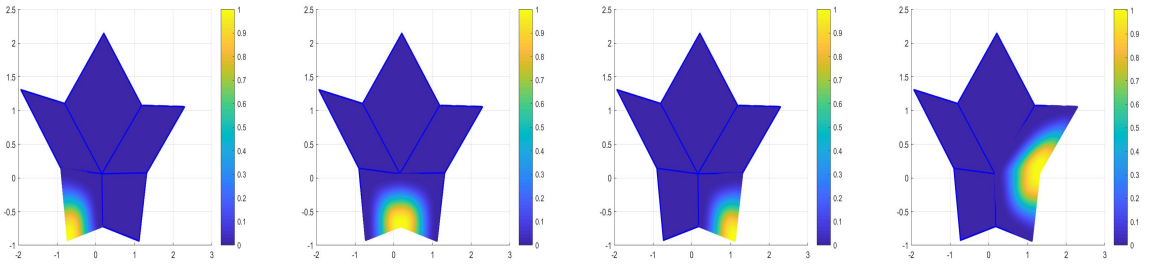

Figure 13: Contours of ψ_v's

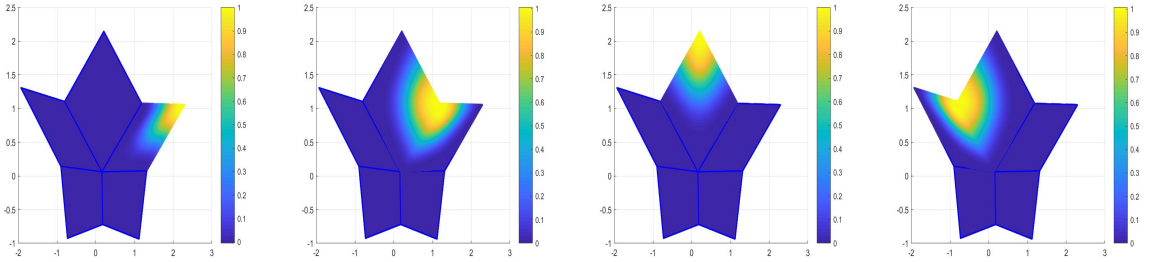

Figure 14: Contours of more ψ_v's

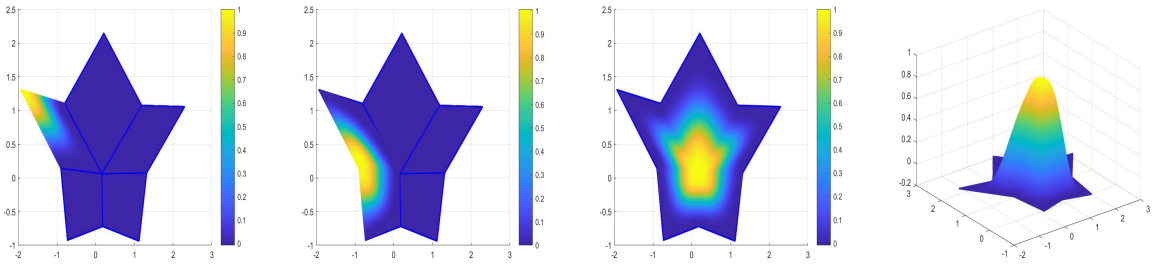

Figure 15: Contours of ψ_v's and one 3D graph of ψ_v supported inside Ω

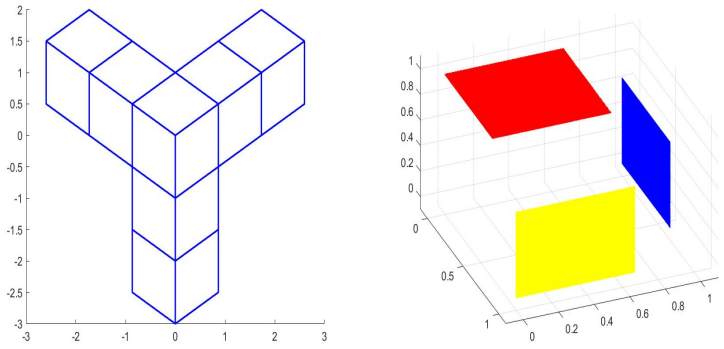

Figure 16: A Y-quadriangulation and three planar surface patches

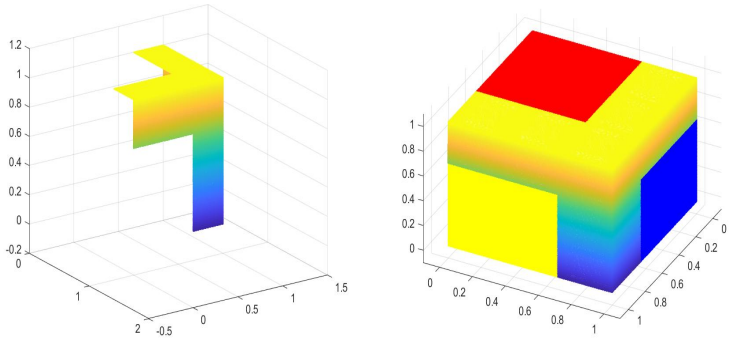

Figure 17: C^1 connecting surface and the suitcase corner

Example 4 (Construction of Suitcase Corners) *One possible application of our construction of C^1 vertex splines over quadrilateral partition is to attack the difficulty of piecing tensor product B-spline surfaces together at an extraordinary point. The most simple case is to construct a smooth suitcase corner based on three given surface patches, e.g. planar surfaces (red, yellow and blue) shown on the right of Figure 16. We construct a mending surface S defined over Y-shaped domain partitioned as shown on the left of Figure 17. Join S with three given planar surfaces to form a desired suitcase corner. To see that the surface S connecting three planar surfaces in C^1 fashion and the suitcase corner is indeed C^1, we present a few different views in Figure 18.*

Our construction procedure is to define three functions $(X(u,v), Y(u,v), Z(u,v))$ over the Y-shaped domain by using the formula S_I discussed before. More precisely, consider $X(u,v)$ first. The values of X at the five vertices on the top rim of the domain are the values of the red planar surface. These determine the coefficients of vertex spline ψ_v for five vertices v on the top rim of the domain. Since the gradients and Hessian of the red planar surface are zero, we do not need to use $\psi_{v,x}, \psi_{v,y}, \psi_{v,xx}, ...,$. Similar for the vertices on the left and right sides of Y-shaped domain. The values at the 10 vertices inside the Y-shaped quadrangulation are defined according to the locations of the physical frame of the corner. In the same fashion, we construct $Y(u,v)$ and $Z(u,v)$. These generate the surface on the left of Figure 17.

When the given surface patches are not necessary planar surfaces, we use gradients and second order

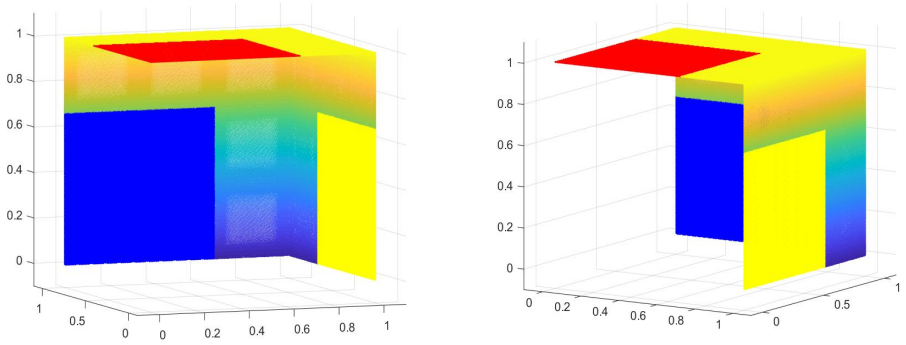

Figure 18: C^1 surface connecting three planar surfaces in two different views

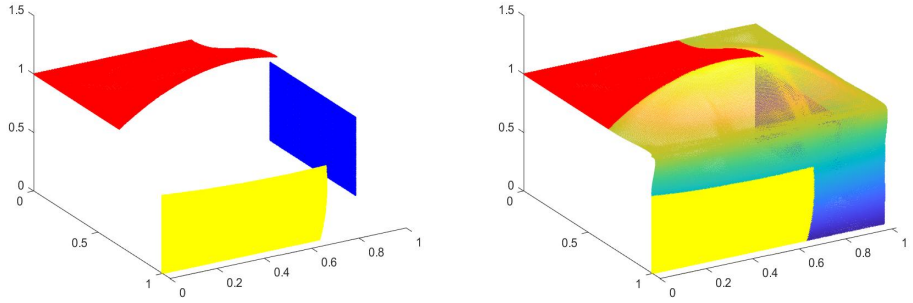

Figure 19: Three given surface patches (left) and one mending surface patch S matching with three given surface patches (right)

derivatives at the vertices of Y-shaped domain as well as edge and face splines. That is, the construction requires to use the gradient functions $\psi_{x,v}$ and $\psi_{y,v}$ and etc.. On the left graph of Figure 19, we are given three surface patches. We construct a mending surface S, the left graph of Figure 19 over the Y-shaped domain consists of three given surface patches, one is a planar surface (blue), one is a large wavy surface(red), and one is a median wavy surface(yellow). The C^1 suitcase corner surface is shown on the right of Figure 19 as well as in Figure 20 for two different views.

Example 5 *Finally, we present an example to show how to use C^1 vertex splines using degree 7 Wachspress coordinates for surface construction. Consider a quadrilateral partition of the surface of a bunny (see Figure 21). We cut a part of the surface as indicated in red on the surface of the bunny. The projection of this patch to the x-y plane is a general quadrilateral partition $\mathcal{P}$ with vertices $\mathcal{V}$. We used our C^1 vertex splines of degree 7 to construct a fitting surface due to the fact that the quadrilateral partition is a general one. We use the heights (the z-components) of the vertices in $\mathcal{V}$ as the function values and estimate the first order and second order derivatives at each vertex in $\mathcal{V}$ from the given bunny set to construct a C^1 interpolatory surface as shown on the right of Figure 21. This method can be useful to handle bounded smooth manifolds. Indeed, as a smooth manifold M is bounded, there exists an atlas of finitely many charts $(S_i, \phi_i), i = 1, \cdots, n$ such that $\cup_{i=1}^n S_i = M$ and ϕ_i is a smooth function such that $D_i = \phi_i^{-1}(S_i)$ is a planar domain. The quadrilateral partition of*

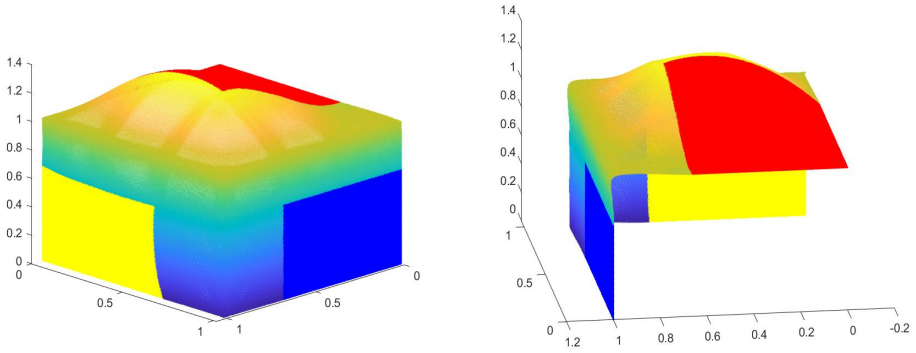

Figure 20: C^1 suitcase corner in two different view

M restricted to S_i induces a quadrilateral partition on D_i. We use the derivative information of ϕ_i at each vertex on D_i to construct C^1 interpolatory surface using our C^1 spline $\Psi_v, \Psi_{v,x}, \cdots, \Psi_{v,xy}$ to form a surface. In practice, we do not have ϕ_i, but we can estimate the values and derivatives at the vertices of quadrilateral partition on S_i. In this way, we can construct C^1 surface based on any given quadrilateral partition with and without extraordinary points. See Figures 23 and 24 for two fitting surfaces which form a smooth fitting patch. One can see that they fit the back of the bunny nicely.

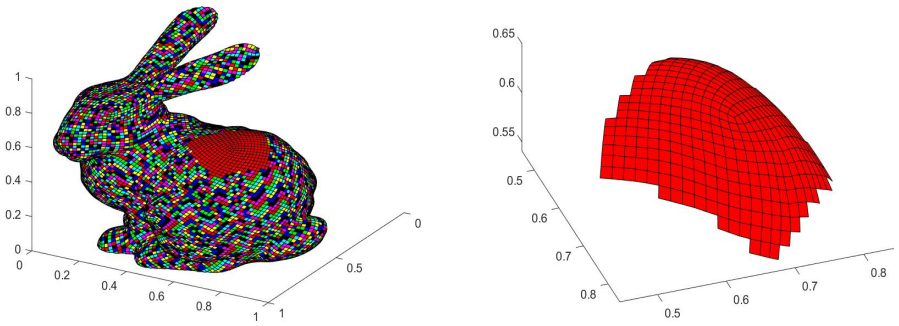

Figure 21: a bunny (left) and a space quadrilateral patch (right)

6 Possible Extensions and Open Problems

We list a few possible extensions and open research problems.

- 1. It is of interest to construct C^1 vertex splines over pentagons. What degree of polynomials of Wachspress GBC functions is necessary to achieve C^1 smoothness? More generally, how can one construct C^1 vertex splines over a polygon of size n for $n \geq 5$?
- 2. It is of interest to study how to construct C^2 vertex splines over quadrilateral (or other) partitions.

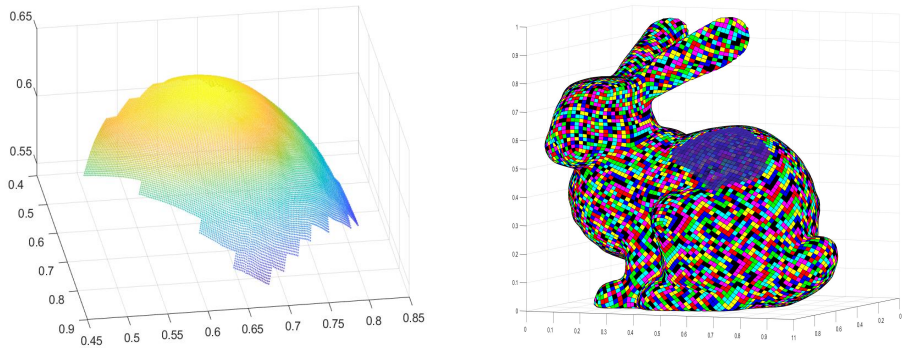

Figure 22: a C^1 surface and the bunny with a smooth patch

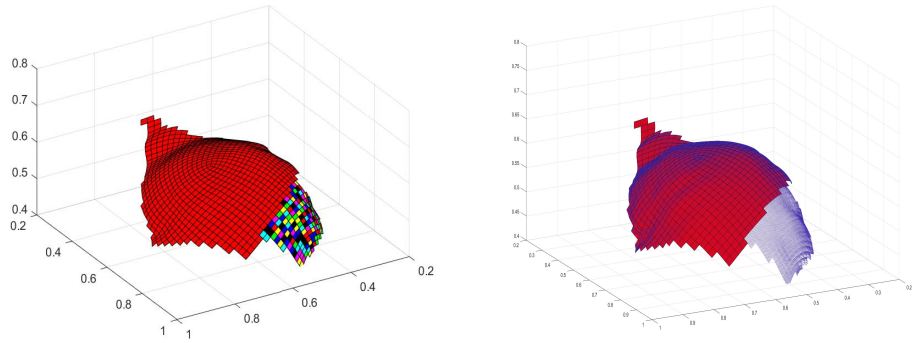

Figure 23: Two connected patches from the back of a bunny and two C^1 vertex spline surfaces

- 3. It is of interest to know if one can construct C^1 vertex splines based on GBC functions other than Wachspress coordinates. To extend the construction in this paper, one would need to know the first and second derivatives of other GBC functions.
- 4. Another interesting research problem to tackle would be to extend our construction into the 3D setting, e.g. construct C^1 vertex splines over some class of hexahedral partitions or other polyhedrons.

All these problems are left to the interested reader. MATHEMATICA codes used in this paper may be requested by emailing to the authors.

Acknowledgment

The first author would like to thank the National Science Foundation for the support (grant #DMS 1521537) to the research contained in this paper.

References

[1] G. Awanou, M. -J. Lai, and P. Wenston. The multivariate spline method for scattered data fitting and numerical solution of ptial differential equations. In Wavelets and splines: Athens 2005, pages 24–74. Nashboro Press, Brentwood, TN, 2006.

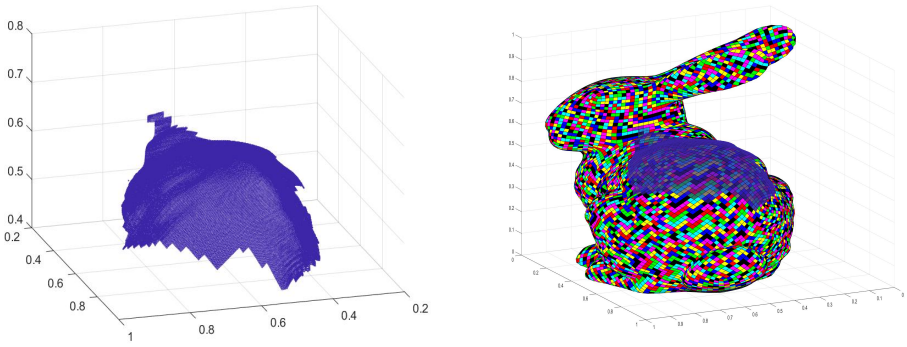

Figure 24: Two C^1 vertex spline surfaces (shown in Figure 23) form a smooth one surface patch (left) and the bunny with a smooth patch (right)

[2] L. Beirao da Veiga, K. Lipnikov, and G. Manzini, Arbitrary-order nodal mimetic discretizations of elliptic problems on polygonal meshes. SIAM Journal on Numerical Analysis, 49(5):1737–1760, 2011.

[3] L. Beirão da Veiga, F. Brezzi, A. Cangiani, G. Manzini, L. D. Marini, and A. Russo. Basic principles of virtual element methods. Math. Models Methods Appl. Sci., 23(1):199–214, 2013.

[4] L.Beirão da Veiga, G. Manzini. A virtual element method with arbitrary regularity. IMA J. Numer. Anal., 34(2): 759–781, 2014.

[5] M. Bercovier and T. Matskewich, Smooth Bézier Surfaces over Unstructured Quadrilateral Meshes, Springer Verlag, 2017.

[6] C. de Boor, K. Höllig, Approximation power of smooth bivariate PP functions, Mathematische Zeitschrift, 197 (1988), pp. 343–363.

[7] S. C. Brenner and L. R. Scott, The mathematical theory of finite element methods, Springer Verlag, New York, 1994.

[8] S. C. Brenner and L.-Y. Sung. C^0 interior penalty methods for fourth order elliptic boundary value problems on polygonal domains. Journal of Scientific Computing, 22(1-3):83118, 2005.

[9] E. Catmull and J. Clark, Recursively generated B-spline surfaces on arbitrary topological meshes, Comput. Aided Des., 10 (September 1978), pp. 350–355.

[10] Chui, C. K. and Lai, M. -J., On Bivariate Vertex Splines, Multivariate Approximation Theory III, Birkhauser, (1985) edited by W. Schempp and K. Zeller, pp. 84–115.

[11] P. G. Ciarlet, The Finite Element Method for Elliptic Problems, North–Holland, 1978.

[12] L. Evans, Partial Differential Equations, American Math. Society, Providence, 1998.

[13] M. Floater, Generalized barycentric coordinates and applications, Acta Numerica, 24 (2015), 161–214.

[14] M. Floater and M. -J. Lai, Polygonal spline spaces and the numerical solution of the Poisson equation, SIAM Journal on Numerical Analysis, (2016) pp. 797–824.

[15] M. S. Floater, A. Gillette and N. Sukumar, Gradient bounds for Wachspress coordinates on polytopes, SIAM J. Numer. Anal. 52, 515–532.

[16] Jan Grošelj, Mario Kapl, Marjeta Knez, Thomas Takacs, Vito Vitrih, A super-smooth C^1 spline space over mixed triangle and quadrilateral meshes, arXiv:2003.14138v1, 2020.

[17] J.A. Gregory, J. Zhou, Irregular C^2 surface construction using bi-polynomial rectangular patches, Computer Aided Geometric Design 16 (1999) 423–435.

[18] M. Kapl, G. Sangalli, T. Takacs, Isogeometric analysis with C^1 functions on unstructured quadrilateral meshes, arXiv:1812.09088v1, 2018.

[19] M. Kapl, G. Sangalli, T. Takacs, A family of C^1 quadrilateral finite elements, RICAM-Report 2020-20.

[20] M. Kapl, V. Vitrih. Space of C^2-smooth geometrically continuous isogeometric functions on planar multi-patch geometries: Dimension and numerical experiments. Comput. Math. Appl. 71 (2017): 2319–2338.

[21] R. Kenyon, Tiling a polygon with parallelograms. Algorithmica 9 (1993), no. 4, 382–397.

[22] K. Karciauskas and J. Peters, Biquintic G^2 surfaces via functionals, Comput. Aided Geom. Design 33 (2015), 17–29.

[23] K. Karciauskas and J. Peters, Biquintic G^2 surfaces, in The Mathematics of Surfaces XIV, Institute of Mathematics and Its Applications (September 2013), G. Mullineux, Robert J. Cripps, M.A. Sabin (Eds.), pp. 213–236.

[24] M. -J., Lai, On Construction of Bivariate and Triavariate Vertex Splines, Ph.D. Dissertation, Dept. of Mathematics, Texas AM University, (1989).

[25] M. -J., Lai, and Lanterman, J., A polygonal spline method for general 2nd order elliptic equations and its applications, in Approximation Theory XV: San Antonio, 2016, Springer Verlag, (2017) edited by G. Fasshauer and L. L. Schumaker, pp. 119–154.

[26] M. -J. Lai and L. L. Schumaker, *Spline Functions over Triangulations*, Cambridge University Press, 2007.

[27] James Lanterman, A Generalization of Bivariate Splines Over Polygonal Partitions and Applications, Ph.D. Dissertation, the University of Georgia, May, 2018.

[28] G. Manzini, A. Russo, N. Sukumar. New perspectives on polygonal and polyhedral finite element methods. Math. Models Methods Appl. Sci., 24(8): 1665–1699, 2014.

[29] M. Meyer, H. Lee, A. Barr, M. Desbrun. Generalized barycentric coordinates on irregular polygons. Journal of Graphics Tools, 7 (2002): 13–22.

[30] L. Mu, J. Wang, X. Ye. Weak Galerkin finite element methods on polytopal meshes. International J. of Num. Anal. and Modeling, 12(1): 31–53, 2015.

[31] L. Mu, J. Wang, Y. Wang, and X. Ye. A Computational Study of the Weak Galerkin Method for Second-order Elliptic Equations, Numerical Algorithms, 63(2013): 753–777.

[32] T. Nguyen and J. Peters, Refinable C^1 spline elements for irregular quad layout, Comput. Aided Geom. Design 43 (2016), 123–130.

[33] A. Rand, A. Gillette, C. Bajaj. Quadratic serendipity finite elements on polygons using generalized barycentric coordinates. Math. of computation, 83(290): 2691–2716, 2014.

[34] Larry L. Schumaker, Two-stage spline methods for fitting surfaces. Approximation theory (Proc. Internat. Colloq., Inst. Angew. Math. Univ. Bonn, Bonn, 1976), pp. 378–389. Springer, Berlin, 1976.

[35] L. L. Schumaker, Spline Functions: Computational Methods, SIAM Publication, 2015.

[36] I. Smears and E. Süli, Discontinuous Galerkin finite element approximation of nondivergence form elliptic equations with Cordés coefficients, SIAM J Numer. Anal., Vol. 51, No. 4, 2013, pp. 2088–2106.

[37] E. L. Wachspress, A Rational Finite Element Basis, Math. Sci. Eng. 114, Academic, New York, 1975.

[38] J. Zhang, B. Deng, Z. Liu, G. Patané, S. Bouaziz, J. Hormann, and L. Liu, Local Barycentric Coordinates, SIGGRAPH, Asia, 2014.